Studies of pain mechanisms on a rat osteoarthritis model of the ankle joint

Valérie Bourassa

Department of Pharmacology and Therapeutics

Integrated Program in Neuroscience

SPRING 2024

A thesis submitted to McGill University in partial requirement of the degree of Doctor of Philosophy

TABLE OF CONTENTS

TABLE OF FIGURES

LIST OF ABBREVIATIONS

ABC	Avidin-biotin complex
ACLT	Anterior cruciate ligament transection
ANOVA	Analysis of variance
ANS	Autonomic nervous system
ATF3	Activating transcription factor 3 or Cyclic AMP-dependent transcription factor
B.C.E	Before Common Era
BDNF	Brain-derived neurotrophic factor
BMD	Bone mineral density
CaBP	calcium-binding protein
CCI	Chronic constriction injury
CFA	Complete Freund's Adjuvant
CGRP	Calcitonin gene-related peptide
CNS	Central nervous system
CTb	Cholera toxin subunit B
DAB	Diaminobenzidine
DAPI	4′,6-diamidino-2-phenylindole

DMM	Destabilization of the medial meniscus
DRt	Dorsal reticular nucleus
DRG	Dorsal root ganglia
ECM	Extracellular matrix
EDTA	Ethylenediaminetetraacetic acid
GFAP	Glial fibrillary acidic protein
HPC	Heat/Pinch/Cold
IASP	International Association for the Study of Pain
Iba1	Ionized calcium binding adaptor molecule 1
IB4	Isolectin B4
IgG	Immunoglobulin G
IHC	Immunohistochemistry
IL	Interleukin
i.p.	Intraperitoneally
-ir	Immunoreactive
i.t.	Intrathecally
KCC2	Potassium-chloride co-transporter 2
LI-V	Laminae I through V

MIA	Mono-iodoacetate
MMP	Matrix metalloproteinase
MMT	Medial-meniscal tear
MRI	Magnetic resonance imaging
NA	Noreadrenaline
NF200	Neurofilament 200
NGF	Nerve growth factor
NK1-r	Neurokinin-1 receptor
NP	Neuropathic pain
NS	Nociceptive-specific
NSAIDS	Non-steroidal anti-inflammatory drugs
NT3	Neurotrophin 3
OA	Osteoarthritis
OARSI	Osteoarthritis Research Society International
OVX	Ovariectomy
PAG	Periaqueductal gray matter
PB	Phosphate buffer
PBS	Phosphate buffer saline

PBS+T	Phosphate buffer saline containing 0.02% Triton X-100
PBN	Parabrachial nucleus
PFA	Paraformaldehyde
PGP 9.5	Protein gene product 9.5
PMM	Partial medial meniscectomy
PNS	Peripheral nervous system
PSNL	Partial sciatic nerve ligation
PV	Parvalbumin
RA	Rheumatoid arthritis
Scgn	Secretagogin
SEM	Standard error of the mean
SNI	Spared nerve injury
SNL	Spinal nerve ligation
SNS	Sympathetic nervous system
SP	Substance P
TGF-β	Transforming growth factor-β
TNF-α	Tumor necrosis factor-α
TrkA	Tyrosine receptor kinase A

TrkB	Tyrosine receptor kinase B
TrkC	Tyrosine receptor kinase C
TRPM2	Transient receptor potential cation channel subfamily M (melastatin) member 2
TRPM8	Transient receptor potential cation channel subfamily M (melastatin) member 8
TRPV1	Transient receptor potential cation channel subfamily V member 1
VLM	Caudal medullary ventrolateral reticular formation
VMAT-2	Vesicular mono-amine transporter 2
WDR	Wide dynamic range
μCT	Microtomography

ABSTRACT

Osteoarthritis (OA), the degenerative and most common form of arthritis, is a complex disease of the whole joint and affects over 4 million Canadian adults. To this day, there is no satisfactory method of relieving osteoarthritic pain and, although chronic pain is the most reported complaint of the disease, our understanding of its driving mechanisms remains limited. Studies in this thesis were devised with the objective of contributing to understanding of the mechanism of pain in OA.

Studies investigating changes of innervation of bone have been few and sparse in the literature, mostly due to the complexity and poor success of performing histological labellings on decalcified bone tissue. As a result, there has been a lack of understanding of mechanisms contributing to pain in diseases such as arthritis, osteoporosis, and low back pain. In this thesis, we developed a robust methodology for labelling nerve fibers in bone in various animal models of OA, osteoporosis, and bone fracture.

In this thesis, we provide a multi-facetted time-course study of relevant changes in a mono-iodoacetate (MIA) model of OA in the rat ankle joint. We showed a correlation between pain-related behavior and pathological changes, including cartilage and bone degeneration, sprouting of sensory and sympathetic nerves in the bone and synovium, and increased density and activation of glial cells in the dorsal horn. There are many clinical and pre-clinical lines of evidence suggesting a neuropathic component to OA pain, including the occurrence of microgliosis in the spinal cord and modulation of nociceptors by sympathetic afferents. However, putative for a neuropathic pain-like component to OA is the possible contribution of primary afferent damage following joint degeneration. We have shown expression of Activating Transcription Factor 3

(ATF3), a marker of neuronal stress, principally in large-diameter cell bodies that also colocalize with parvalbumin (PV), a marker of proprioceptors. This suggests that myelinated afferents innervating the articular joint in OA pain are mostly affected following joint degeneration, which drives interest in understanding the contribution of lamina III-V that receives input from these fibers, in the persistence of OA pain.

The internalization of the receptor for substance P, the neurokinin-1 receptor (NK1-r) on lamina I projection neurons of the spinal dorsal horn has been used as a marker of nociceptive responses. Lamina I is an important centre for the modulation and forwarding to the brain of pain-related information. Therefore, changes in the properties of lamina I projection neurons may be important for pain. Previous work from our lab has shown increased expression of NK1-r on lamina I pyramidal neurons in both neuropathic pain and inflammatory arthritis models. In this thesis, we showed similar morphological changes and internalization of the receptor on NK1-r positive neurons, in a rat ankle joint model of osteoarthritis (OA) following movement of the affected joint in lamina I.

This work combines many studies of important changes occurring in OA in the peripheral and central nervous systems, identifying various contributing mechanisms to chronic and irreversible pain in the disease, including a neuropathic pain-like component. Such studies have important implications in the development of more suitable therapeutic strategies by identifying potential targets.

RÉSUMÉ

L'arthrose, la forme d'arthrite dégénérative la plus courante, est une maladie complexe de l'ensemble de l'articulation et touche plus de 3 millions d'adultes canadiens. À ce jour, il n'existe pas de méthode satisfaisante pour soulager la douleur arthrosique et, bien que la douleur chronique soit la plainte la plus rapportée de la maladie, notre compréhension de ses mécanismes reste limitée.

Les études portant sur les changements d'innervation de l'os sont peu nombreuses et plutôt rares dans la littérature, principalement en raison de la complexité et du faible succès de la réalisation de marquages histologiques sur du tissu osseux décalcifié. En conséquence, le domaine de la douleur a souffert d'un manque de compréhension des mécanismes contribuant à la douleur dans des maladies telles que l'arthrite, l'ostéoporose et les lombalgies. Dans ce travail de thèse, nous avons développé une méthodologie robuste pour marquer les fibres nerveuses dans l'os dans divers modèles animaux d'arthrose, d'ostéoporose et de fracture osseuse.

Nous avons fourni une évolution temporelle à multiples facettes des changements pertinents dans un modèle mono-iodoacetate (MIA) de l'arthrose dans l'articulation de la cheville du rat et avons montré une corrélation entre le comportement lié à la douleur et les changements pathologiques, y compris la dégénération du cartilage et des os, l'hyper-innervation par des fibres sensorielles et sympathiques dans l'os et la membrane synoviale, et une augmentation de la densité et de l'activation des cellules gliales dans la corne dorsale. Il existe de nombreuses lignes de preuves cliniques et précliniques suggérant une composante neuropathique à la douleur arthrosique, y compris la survenue d'une microgliose dans la moelle épinière et la modulation des nocicepteurs par les nerfs sympathiques. Cependant, la contribution possible d'une lésion afférente

primaire à la suite d'une dégénération articulaire peut être considérée comme une composante de type douleur neuropathique dans l'arthrose. Nous avons montré l'expression de ATF3, un marqueur du stress neuronal, principalement dans les corps cellulaires de grand diamètre qui colocalisent également avec la parvalbumine (PV), un marqueur des propriocepteurs. Cela suggère que les mécanorécepteurs myélinisés innervant la jointure, qui sont majoritairement des propriocepteurs, sont principalement affectés à la suite d'une dégénération articulaire, ce qui suscite l'intérêt de comprendre la contribution de la couche III-V de la corne dorsale qui reçoit l'apport de ces fibres, dans la persistance de la douleur arthrosique.

L'internalisation du récepteur de la substance P, le récepteur de la neurokinine-1 (NK1-r) sur les neurones de projection de la couche I de la corne dorsale spinale a été utilisée comme marqueur des réponses nociceptives. La couche I est un centre important pour la modulation et la transmission au cerveau des informations liées à la douleur. Par conséquent, les changements dans les propriétés des neurones de projection de la couche I peuvent être importants pour la douleur. Des travaux antérieurs de notre laboratoire ont montré une expression accrue de NK1-r sur les neurones pyramidaux de la couche I dans les modèles de douleur neuropathique et d'arthrite inflammatoire. Dans cette thèse, nous avons montré des changements morphologiques similaires, ainsi que l'internalisation du récepteur NK1 dans la couche I de la corne dorsale suite au mouvement de la jointure.

Ce travail rassemble de nombreuses études sur les changements importants se produisant dans l'arthrose dans les systèmes nerveux périphérique et central, identifiant divers mécanismes contribuant à la douleur chronique et irréversible dans la maladie, y compris une composante de type douleur neuropathique. De telles études ont des implications importantes dans le

développement de stratégies thérapeutiques plus efficaces avec l'identification de cibles pharmacologiques potentielles.

ACKNOWLEDGEMENTS

I am profoundly grateful to acknowledge the invaluable support and guidance that have carried me through this arduous journey of research and discovery. The path I embarked upon was undeniably rocky, riddled with challenges, uncertainties, and self-doubt, yet it was illuminated by the untiring kindness and patience of my remarkable peers, mentors, friends and family members. Their devoted encouragement and belief in my potential served as inspiration, pushing me forward even in moments of distress. I am indebted to their selfless commitment, their open doors, and their willingness to lend a helping hand whenever I faltered. With their collective wisdom and boundless generosity, I have not only crossed the hurdles of this journey but have also emerged stronger, more resilient, and deeply appreciative of the power of kindness and understanding in the pursuit of knowledge.

I am deeply appreciative to my supervisor, Dr. Alfredo Ribeiro-da-Silva, whose unwavering patience, understanding, and genuine consideration for the person behind the student have been a constant source of inspiration and support. Through their expert guidance and teaching, I have had the privilege to develop proficiency in the field of microscopy, a skillset that I carried with me and shared with the newer generations of graduate students.

I would like to extend my heartfelt appreciation to Manon St-Louis, who illuminated each day I spent in the lab with her warmth, and positivity. Her presence was a constant source of encouragement and brightness that enriched my research experience beyond measure.

I am thankful to my colleagues who have played a pivotal role in my scientific journey. Dr. Noosha Yousefpour, Haley Deamond, Dr. Morgan Foret, Dr. Samantha Locke, Hannah Derue, Dr. Claire Magnussen, Dr. Miyako Suzuki, and Dr. Sophie Pawlowski have been instrumental in

shaping my growth, offering their expertise and insights. Their collective contributions have been invaluable, and I extend my heartfelt gratitude for their support and friendships.

I am immensely thankful to my advisory committee members, Dr. Laura S. Stone and Dr. Ji Zhang, for their invaluable guidance that has been instrumental in shaping the trajectory of my research journey. I am also grateful that these discussions have yielded opportunities for collaboration. Additionally, I extend my heartfelt appreciation to my advisor, Dr. Dusica Maysinger, for her support and persistence in helping me broaden my knowledge and understanding of pharmacology.

I extend my heartfelt appreciation to the members of the Department of Pharmacology and Therapeutics, the IPN, and the Alan Edwards Centre for the Research on Pain. Thank you for bringing together the community with engaging events and conferences.

I wish to thank the Louise and Alan Edwards Foundation for funding my research for three and a half years. This thesis would not have been possible without them.

I also wish to express my deep gratitude to the teaching opportunities that I eagerly pursued at TPULSE (Tomlinson Project in University-Level Science Education), as a teaching assistant in the Biology Department, at TLS (Teaching and Learning Services), and at OSE (Office of Science Education). Engaging with these teaching roles allowed me to gain a profound sense of scientific agency that extended beyond the confines of my own research. The privilege of nurturing and shaping the minds of aspiring students brought an immeasurable sense of purpose and fulfillment. Through these experiences, I came to realize that honing teaching and learning skills is not only beneficial for educators but is equally transformative for scientists. The ability to convey complex ideas effectively, to inspire curiosity, and to foster a collaborative learning environment not only

enhances one's teaching competencies but also refines their scientific communication and critical thinking abilities. I want to mention here my past and present pedagogy colleagues who have made such a great positive impression and impact on my teaching and learning philosophy, but who also have become dear friends: Dr. Armin Yazdani, Dr. Cassidy Vandershee, Dr. Chris Bailey, Helen Martin, Hilary Sweatman, Victoria Glynn, Brenden Moeun, Kira Smith, Rebecca Brosseau, Jonathan Brassard, Nathalie Jreidini, Dr. Mohammed Elkhodiry Aboelella, Dr. Mercedes Garcia-Holguera, Dr. Veronique Brulé, Dr. Tamara Western, Dr. Maria Orjuela-Laverde, Dr. Wagner De Souza Silva, Dr. Alex Liepins, Dr. David N. Harpp, and Dr. Marcy Slapcoff.

In memory of my dear friend Dan Petrescu, whose tragic passing in a plane crash on October 3rd, 2021, left an indelible void in my life, and in the lives of those in the McGill teaching and learning community who had the privilege to work with him. Dan was not only an exceptional individual but also a dedicated scholar. His unwavering commitment to teaching and learning and his passion for research were a testament to his character. Dan received his Ph.D. degree posthumously a few months after his passing. As I reach the culmination of my own academic journey, I dedicate this work to Dan, a brilliant mind, and a cherished friend, who continues to inspire and guide me, even in his absence.

Finally, I want to thank my parents, Carole and Yvan, whose presence and support have been the foundation of my journey. Their love for their daughters has carried me through every step, and I am immensely fortunate to have been guided by their strength. To my sister, Julie, a constant source of inspiration with her creativity, hard work, and resolute character, I extend my sincere admiration. As she continues her own Ph.D. journey in molecular medicine at the University of Ottawa, I wish her every success. A special mention goes to my partner, Javier,

whose love and support remained dedicated even through the challenges of geographical distance (and pandemics).

CONTRIBUTION TO ORIGINAL KNOWLEDGE

The works presented in this thesis provide valuable tools for the study of pain mechanisms in osteoarthritis, including a robust methodology for the detection of innervation in decalcified bone tissue, and a multi-facetted characterization of a MIA model of osteoarthritis in the rat ankle joint. More importantly, the results presented here provides strong pre-clinical evidence of a neuropathic pain component in OA, and alteration in the central nervous system (CNS) that contribute to the pain state. The findings presented here resulted in the following 3 manuscripts and a chapter of preliminary data:

Manuscript 1:

Bourassa, Valerie; Suzuki-Narita, Miyako; S. Stone, Laura; Ribeiro-da-Silva, Alfredo. An optimization of DAB-based immunohistochemistry detection of nerve fibers in rat and mouse decalcified bone. 2024. To be submitted to *Bone.*

Manuscript 2:

Bourassa, Valerie; Deamond, Haley; Yousefpour, Noosha, Mary-Ann; Ribeiro-da-Silva, Alfredo. Pain-related behavior is associated with increased joint innervation and ipsilateral dorsal horn gliosis in a rat model of osteoarthritis. **Pain Reports**. 5 (2020) e846.

Manuscript 3:

Bourassa, Valerie; Yousefpour, Noosha; Doyle, Kito; Derue, Hannah; Ribeiro-da-Silva, Alfredo. ATF3 immuno-reactivity and decrease density of proprioceptive primary afferents are associated with pain-related behavior in a rat model of osteoarthritis. 2024, In preparation.

CONTRIBUTION OF AUTHORS

The following statements describe the responsibilities of all the authors of the above co-authored manuscripts:

Dr. A. Ribeiro-da-Silva: Principal investigator of all the projects, overseeing the experimental plans, and editing of the manuscripts.

V. Bourassa: Designed, planned, and executed all projects in this thesis (except those mentioned below), analyzed the data, prepared the figures, and wrote all first versions of the manuscripts.

Dr. N. Yousefpour: Intellectual influence and invaluable critic of experimental design on manuscripts 2 and 3.

H. Deamond: Performed intrathecal injection of minocycline and fluocitrate and assisted with tissue extraction (manuscript 2).

K. Doyle: Assisted with tissue extraction, performed NF200 labelling and quantification in bone tissue and contributed to writing (manuscript 3).

H. Derue: Assisted with tissue extraction (manuscript 3)

Dr. M. Suzuki-Narita: Provided tissue from osteoporosis and tibia fracture mouse models, performed CGRP labelling on bone tissue (manuscript 1).

Dr. M-A. Fitzcharles: Analyzed bone images (manuscript 2).

Dr. L. S. Stone: Provided tissue from osteoporosis and tibia fracture mouse models, manuscript editing (manuscript 1).

CHAPTER 1

General Introduction

1.1 The burden of arthritis

Whether it is the person who can no longer tuck the sheets under their mattress when they make their bed, or the athlete who was so close to go "pro" before a life-changing injury, or the grandmother who struggles to finish her knitted sweater, most people know of someone who suffers from severe joint pain. Make no mistake, although some of the examples mentioned above may appear as endearing quirks or have been accepted has an inevitable path of life, joint pain can be debilitating and have many physical, psychological, and social impacts on a person's life. An estimated 6 million Canadians are affected by arthritis, which represents 1 in 5 adults, 2 out of 3 patients being women [16]. Our current health care system spends $33 billion annually in the sole effort of managing and alleviating symptoms of arthritis. Due to our rapidly aging population, these numbers are expected to rise to 9 million arthritis patients and at least $67 billion of health care costs by 2040, causing an increasingly alarming financial and clinical burden on our society [16].

Despite the important societal implications of arthritis, our understanding of the underlying mechanisms, including mechanisms related to pain associated with the disease, remains limited. Clues to the etiology of various forms of arthritis as well as insight into research advances can be informed by historical perspectives on the disease [54]. Unfortunately, by this process, robustly acquired misconceptions in the medical community relating to causes and mechanisms of arthritis can also hinder progress in treatment advances. This is particularly true for osteoarthritis (OA), the most common form of arthritis, which will be the focus of this thesis.

1.2 Arthritis through the arts and ages

The word arthritis comes from the Greek "arthro" meaning joint and "itis" meaning inflammation. Amongst the first disease to ever be recognized as a medical entity is gout arthritis, first described by the Egyptians in 2560 B.C.E [188]. Hippocrates also described the condition as the "unwalkable disease" that he associated with joint disability [6]. Interestingly at that time, gout was thought to be a "disease of lifestyle", and its various forms were classified based on the socio-economic status of the person affected [154]. The term "rheumatism" followed in 1591 when the French physician Guillaume de Baillou coined the term referring to the condition associated with joint soreness, stiffness, pain and inflammation [95]. Unlike rheumatism, gout was associated with rich foods and excessive consumption of alcohol; in fact an issue of the London Times dating to the year 1900 reads "The common cold is well named – but the gout seems instantly to raise the patient's social status" [37]). It was only in the 1800's that this notion was challenged with evidence of hereditary traits [67]. Today, the condition known as gout refers solely to the disease associated with the accumulation of small crystals of a chemical called uric acid that form in the joints [185].

It is surprising to see how late came the descriptions of arthritis in the medical literature when depictions in other media can be found centuries, if not millennia, earlier. In fact, many diseases were first depicted in art form before they were even defined clinically, or symptoms were identified. Trisomy 21, for example, was first described in the medical literature by J. Langdon Down in 1866 in very gross terms [51], and was attributed to the chromosome 21 in 1959 [109]. However, realism paintings dating back to the Renaissance show children with clear features associated with Trisomy 21 (ex: *Virgin with Child* by Andrea Mantegna (1490)) [208] with the earliest representation linked to a clay figurine dated 5000 B.C.E [47]. Similarly, representations of arthritic features can be found in many paintings of the Renaissance, including *The Donators*

by Jan Gossaert (1525-30), and *Portrait of Albrecht Durer* by Albrecht Durer Jnr (1490) [43; 234]. This is mainly caused by a surging interest in realisms and humanism which created a desire for artists of that time to study the anatomy of the human body in order to produce life-like art [108]. Of course, stylistic signatures may have pushed artists to deviate from the true anatomy, which highlights the importance of corroborating evaluations of portraits on which arthritis is depicted, as well as analyses of primary documents recording symptoms of arthritis; this process is called medico-artistic diagnosis [107].

Michelangelo Buonarroti is best known for being one of the most documented artists of the Renaissance, with famous works including *David* and the ceiling of the Sistine Chapel. However, what is less known about Michelangelo is that he faced health issues later in life that challenged his abilities in practicing humanism and realisms in his art. He wrote in his letters that "no one has mastery before he is at the end of his art and his life" as he complained to his nephew of "cruel pain" in his hands and symptoms they then associated with the general condition called "gout" [82]. Although no investigation was performed on Michelangelo's remains after his death to confirm pathologies, scholars turned to portraits of Michelangelo to analyze his afflictions. Of note were *Portrait of Michelangelo Buonarroti* by Jacopino del Conte (Figure 1A), and *Portrait of Michelangelo Buonarroti* by Pompeo di Giulio Caccini (Figure 1B). Both these portraits showed deformations on Michelangelo's hands, but with no-to-little signs of inflammation (Figure1C-D). More precisely, the trapezius-metacarpal joints and the metacarpo-phalangeal and interphalangeal joints of the thumb and index finger show advanced degeneration. Combined, these findings are believed to be associated with osteoarthritis [107].

Chapter 1 Figure 1: Arthritis in Portraits of Michelangelo Buonarroti.

A) by Jacopino del Conte (c.1535), oil on panel from the Casa Buonarroti Museum, Florence, Italy; B) by Pompeo di Giulio Caccini (c.1595), oil on wood from the Casa Buonarroti Museum, Florence, Italy. C-D) Magnifications of hands from A) and B).

The medical and art literature paint a rich history of the origin of diseases that we now categorize as arthritis. In the last few centuries, many advances in research and medicine have allowed for the differentiation between arthritis types. Not only do these advances affect how we treat and manage the disease in patients, but it also informs how we conceptualize the disease mechanism, which in turn drives research interests. In the next section, we will discuss recent advances and provide an overview of the modern understanding of some of the most common forms of arthritis.

1.3 Types of arthritis

Many rheumatoid disorders are categorized as arthritis due to their common musculoskeletal pain; in fact, over 100 conditions fall into the category of arthritis, including rheumatoid arthritis (RA), fibromyalgia, and OA [16]. For the purpose of the work presented here, we will further expand on RA and OA, which are represented in Figure 1.2.

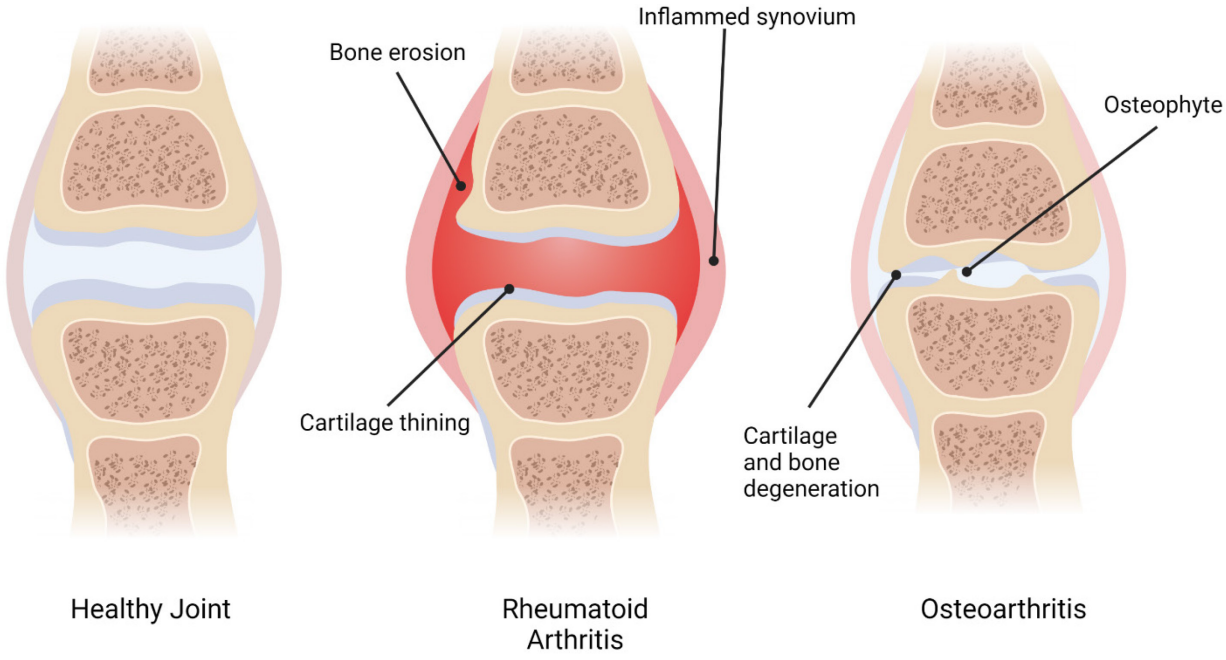

Chapter 1 Figure 2: Schematic representation of the healthy and arthritic synovial joints.

The RA joint is associated with important inflammation, as well as erosion of cartilage. The OA joint is associated with joint space narrowing caused by cartilage and bone degeneration, with a less prominent inflammatory component. Original image created with BioRender.

1.3.1 Rheumatoid arthritis

RA is the most common form of inflammatory arthritis, and the second most common form of arthritis. It is estimated that 1 in 100 Canadians adults suffer from RA, which represents 300 000 Canadians [16].

The first description of RA in modern medicine came from Augustin Jacob Landré-Beauvais in the year 1800, who described distinct symptoms from gout and rheumatism, that we now recognise as RA (cited by [9]). RA is a chronic relapsing autoimmune disease, that usually affects multiple diarthrodial, or synovial, joints. Like other autoimmune disorders, women are more likely to develop RA, by a three to one ratio [14; 36]. Central to the pathophysiology of RA is an inflamed synovium. However, the direction of subsequent damage is disputed: invasion of synovial tissue within the joint cavity, a structure called the pannus, can result in degradation of the cartilage, subchondral bone, and surrounding tissues, but evidence also shows inflammatory infiltrates from the bone marrow that can result in the aforementioned damage [212]. Nonetheless, the progression of the disease can be insidious in many patients, but 70% of patients will have radiographic evidence of degeneration of articular cartilage and bone within 2 years [131; 133]. The etiology of the disease is still murky, but appears to be multifactorial, with genetic, epigenetic and environmental factors. Analysis of RA studies involving monozygotic and dizygotic twins conclude that approximatively 60% of a population's predisposition for RA can be accounted by genetics [8; 123; 201].

1.3.2 Osteoarthritis

More than 4 million Canadian adults suffer from OA, the most common form of arthritis. This represents 1 in 7 Canadian adults [16]. The main risk factors include age, obesity, and traumatic injury. Patients most often complain of stiffness, joint instability, and chronic pain [58].

The first description of osteoarthritis in the medical literature came from William Heberden during the 18th century where he described cases of joint disease which he defined as being distinct from rheumatism and gout [97]. This "nodosity" of the joints, or joints resembling the bulky shape of knots likely due to the formation of osteophytes, was coined as the Heberden nodes. It is believed that the term "osteoarthritis" was first used in the mid-1850's by Richard von Volkmann who is regarded as the father of orthopaedic surgery, and who maintained that OA lesions were very distinct from the ones observed in RA [238]. Unfortunately, a competing school of thought completely eclipsed Volkmann's arguments, and the medical community continued to interpret OA as a certain grade of the RA disease [116; 158]. It is only in 1955 that R.M. Stecher connected Heberden nodes to osteoarthritis, and postulated that OA was a purely mechanical disease caused by injury or "wear-and-tear" on the joints [210]. What Heberden, Volkmann and Stecher all agreed on is that, contrary to RA, OA lacked the predominant inflammation component in the joints.

The term "osteoarthritis", which is still used to describe the condition even in modern day, is a misnomer as "osteo" which means bone and "arthro" which means joint are still defined with "itis" which means inflammation. Nonetheless, current literature now suggests that the real story behind OA pathological onset is far more complex. In fact, the Osteoarthritis Research Society International (OARSI) now describes this degenerative disease as follows:

> "Osteoarthritis is a disorder involving movable joints characterized by cell stress and extracellular matrix degradation initiated by micro- and macro-injury that activates maladaptive repair responses including pro-inflammatory pathways of innate immunity. The disease manifests first as a molecular derangement (abnormal joint tissue metabolism) followed by anatomic, and/or physiologic derangements (characterized by cartilage

degradation, bone remodeling, osteophyte formation, joint inflammation and loss of normal joint function), that can culminate in illness:" [102].

It is only recently that we started conceptualizing OA as a disease that goes beyond the articular cartilage. In addition to degeneration of the cartilage and joint space narrowing, we now acknowledge the importance of the whole joint, including changes occurring in the subchondral bone, the synovium, synovial fluid, and supporting ligaments [127]. In fact, OA is characterized by bone remodelling, the formation of osteophytes, lesions in the bone marrow, and in some case, ligament and meniscal tears [44; 49; 75; 165]. Changes occurring in each of those structures in the diseased state will be discussed in section 1.7.

Similar to RA, the pathogenesis of OA is still poorly understood. However, the transforming growth factor-β (TGF-β), Wnt3a, Indian hedgehog, signalling molecules such as Smad3, β-catenin and HIF-2α, and the transcription factor Runx2 all have been implicated in OA development and progression in genetic mouse models [32; 86; 96; 113; 179; 244; 245; 254]. As such, the genetic predisposition of OA is widely accepted in the literature [59; 118; 207], and lately research has been targeting the genes and signalling pathways of these molecules [138; 183; 190; 195; 231].

1.4 Pain

For 40 % of patients living with arthritis, which represents over 2.4 million Canadians, the pain associated with the condition is so severe that it limits their daily activities, mobility and ability to work [16]. It is of no contest now that chronic pain associated with OA is not solely a symptom, but a disease of its own. In the next few sections, we will review the past and present views on

pain-related transduction and transmission, which led to our current understanding of the pain state.

1.4.1 Pain through the ages

Descartes' Principles of Philosophy, published in 1644, had a section on pain in phantom limbs. He deduced that pain was felt in the brain rather than the phantom limb [46]. He was the first to claim that activation of the phantom limb's nerves created sensations as if the phantom limb was still intact. Then, in “L’Homme”, Descartes presented a model of pain in the shape of a child sticking his foot in a fire [45]. Descartes felt that as the fire approached the boy's foot, the pain caused a fine thread to be pulled up the boy's leg and to the brain through the shortest route. This model is perhaps the most known early conceptualization of pain and has inspired many more complex subsequent insights of the pain circuitry. The term “nociception” came much later in 1910 when Charles Sherrington, the renowned English neurophysiologist, used the Latin roots *nocere* (meaning “to harm”) to describe pain as the “physical adjunct of protective reflexes”. What Descartes and Sherrington had in common were their insightful deduction on the evolutionary purpose of pain; to teach the body to avoid future and probable injuries. This is commonly known as acute pain: pain that is relatively short-lasting and directly associated with an injury. However, we now know that pain can manifest itself if a much more complex long-lasting form and of mysterious origin.

1.4.2 Classification of pain

The International Association for the Study of Pain (IASP) defines chronic primary pain as pain that: “1) persists or recurs for longer than 3 months, 2) is associated with significant emotional distress (e.g., anxiety, anger, frustration, or depressed mood) and/or significant

functional disability (interference in activities of daily life and participation in social roles), and 3) the symptoms are not better accounted for by another diagnosis" [148]. Physiologically, it is believed that various events can lead to the onset and maintenance of chronic pain, and distinct terminology is used to differentiate between underlying initiating mechanisms. However, as we will explore in more detail in the following chapters of this thesis, chronic pain mechanisms are very complex with countless contributing mediators.

Nociceptive pain is a medical term that describes pain caused by physical or potential damage to the body. For example, many people will relate to having suffered a sports injury, or having undergone a dental surgery to remove wisdom teeth. Nociceptive pain occurs when nociceptive nerve fibres are activated by inflammation, chemicals, or physical events, such as a superficial paper cut on the finger, or stubbing your small toe over a piece of furniture. Thankfully, nociceptive pain tends to resolve quickly.

Nociplastic pain refers to "pain that arises from altered nociception despite no clear evidence of actual or threatened tissue damage causing the activation of peripheral nociceptors or evidence for disease or lesion of the somatosensory system causing the pain" (cited by [151]). This is a relatively new definition and aims to replace the well known concept of central sensitization as diagnostic term in the clinical context [152; 240].

IASP defines neuropathic pain as pain caused by a lesion or disease of the somatosensory nervous system [186]. Neuropathic pain in the context of OA is strongly suspected in patients, although the mechanisms in OA are poorly described to this day [48], and will be a major focus of this body of work. Interestingly, the notion of a neurogenic lesion originating outside of the joint was linked to OA by Garrod Jnr and John Spender in the late 19th century [50].

1.5 Somatosensory nervous system

The somatosensory nervous system is responsible for the perception of modalities such as touch, temperature, movement, and pain [91; 145]. These different types of perception experiences are first detected and transmitted by primary afferents through specialized sensory receptors. These receptors can be located in their peripheral terminals, or in some cases on the target organ itself. When primary afferents are activated by a sensory stimulus of adequate intensity, an action potential is generated and relayed to the neurons of the dorsal horn of the spinal cord. In the spinal cord, the sensory inputs are then processed and integrated to be relayed in their turn to higher centers of the brain. The perception of sensory stimulus as we know it is attributed to the somatosensory cortex [229]. We now know that centers of the central nervous system are also responsible for modulating sensory inputs, including the modulation of nociceptive stimuli that contribute to the pain experience [27; 56; 99; 136]. In this section, we will review the organization of the peripheral and central nervous systems, with emphasis on structures and circuitry known to contribute to chronic pain in OA.

1.5.1 Peripheral nervous system

There is a lot of power in classifying concepts; classification allows to share and conceptualize our understanding, and to model new ideas [80]. It is no surprise then that much effort has been put towards classifying different types of fibers responsible for sensory transduction and transmission. For example, Lawson & Waddell believed in two morphological types of neurons (large light and small dark neurons) [106]. Primary afferents have also been distinguished by target organ, conduction velocity, receptive fields, localization of neuropeptides,

sensory modality and more [4; 222]. Yet, there seems to be more to learn to fully account for the reported functional heterogeneity of primary afferents. In fact, gene expression profiles of DRGs point to 18 molecularly and functionally distinct classes of neurons that include modality-specific and polymodal primary afferents [224; 250]. Here, we will refer to primary afferents based on the type of stimulus that each transduce: nociceptive, thermoreceptor, mechanoreceptive and proprioceptive afferents. These neurons are pseudo-unipolar and possess two axonal branches: one that innervates the target organ in the periphery, and one that projects to the spinal dorsal horn. Their cell body is located in the dorsal root ganglia (DRG), where primary afferents receive support from glia (Schwann cells and satellite cells). Myelinating Schwann cells wrap around large caliber axons to provide electrical insulation that leads to rapid signal transmission. Non-myelinated Schwann cells also exist and are generally associated with slow-transmitting small caliber axons [3].

1.5.1.1 Nociceptors

Charles Sherrington was the first to describe a specialized set of neurons that transmit painful stimuli [196; 198]. Different fiber populations of nociceptors are distinguished according to certain parameters: the presence or absence of myelination, axonal diameter, and responsiveness to several types of noxious stimuli. Nociceptor populations have previously been described and categorized in Aδ and C fibers [162]. Aδ nociceptors are thinly myelinated and are responsible for transmitting thermal and mechanical fast pain: there are, however, a subset of Aδ fibers that are non-nociceptive and respond to low-threshold mechanical stimuli. Aδ fibers terminate in lamina I (LI) of the spinal cord, although they may also be found in lamina V [111]. On the other hand, C fibers are unmyelinated and slow conducting. They have been found to be activated by noxious mechanical, thermal, and chemical stimuli. Nociceptive C fibers can be of two natures: peptidergic and non-

peptidergic. Peptidergic nociceptors carry neuropeptides in dense core vesicles within the neuron. Such peptides include substance P (SP), and calcitonin gene-related peptide (CGRP). They project to LI and LII, although projections into LV exist [171]. Peptidergic C fibers are particularly important for understanding underlying mechanisms of OA pain since they are found, along with autonomic fibers, in all sections of normal joint tissue (ligaments, tendons, periosteum, and synovium) [125].

1.5.1.2 Thermoreceptors

Thermoreceptors detect change in temperatures on the skin. They have been categorized as C or Aδ fibers with free nerve endings embedded in the skin. In the dorsal horn, thermoreceptors project to LI, the most superficial layer. Interestingly, different ranges of temperature changes are detected by different thermoreceptors: low-threshold thermoreceptors detect innocuous changes in temperature, while high threshold thermoreceptors detect nociceptive changes in temperature. In addition, cold-sensing and warmth-sensing thermoreceptors can be distinguished.

Low-threshold cold-sensing thermoreceptor (around 15˚C) are generally Aδ fibers (although cold-specific C fibers exist), and express the putative cold-sensor transient receptor potential cation channel subfamily M (melastatin) member 8 (TRPM8) [18; 40; 132]. On the other hand, the description of cold-sensing high-threshold thermoreceptor has been challenging due to the activation of non-cold-sensing nociceptors likely due to tissue damage [202].

C fibers have been linked to low-threshold (30 - 45˚C) and high-threshold (> 45˚C) warmth-sensing thermoreceptors [184]. Non-peptidergic C fibers are marked by expression of Mrgpra3 or somatostatin (and are named, NP2, and NP3 types of neurons, respectively) and are responsible for non-noxious warmth sensation [224]. NP3 neurons are also specifically marked by the transient receptor potential cation channel subfamily M member 2 (TRPM2) [217], although

NP3 neurons may also be implicated in noxious heat sensation [142]. Furthermore, the transient receptor potential cation channel subfamily V member 1 (TRPV1) is known for its role in transducing heat hypersensitivity, and can be found in all peptidergic nociceptors [94].

1.5.1.3 Mechanoreceptors

Mechanoreceptors are responsible for transducing touch. Mechanoreceptors can be thickly-myelinated Aβ, thinly-myelinated Aδ fibers, and C fibers that terminate in LII-III of the spinal dorsal horn [222]. In the events that all these mechanoreceptors would be activated simultaneously, axons with thickest myelination, and therefore the fastest conduction velocity, would relay stimuli from the periphery first. There exists low-thresholds mechanoreceptors (LTMRs) and high-thresholds mechanoreceptors (HTMRs). In the skin, Aβ, Aδ and C LTMRs are responsible for transducing innocuous mechanical stimuli [4]. HTMRs, however, are nociceptors that respond to painful mechanical force. They are marked by mechanosensitive ion channels such as Piezo 2 [239].

1.5.1.4 Proprioceptors

In our everyday lives, we depend on feedback from our moving bodies to properly respond to the environment around us. Proprioceptors are responsible for sensing body position in space, as well as balance. Charles Sherrington was also responsible for coining the word “proprioception” to describe the conscious sensation of the position of limbs and joints in space [197]. Today, we also know of similar sensory neurons that detect stretch of internal organs, such as distension of arteries, lungs and the gut [167]. Proprioceptors are myelinated fibers that have been further classified into 3 types: types Ia and Ib proprioceptive afferents that innervate muscle spindles of muscles and Golgi tendons organs of muscles respectively, and type II that is responsible for sensing static positioning. Proprioceptors are marked by the presence of TrkC, the preferential

receptor of the neurotrophin NT-3, and parvalbumin (PV) in the DRG and terminate in deeper layers of the spinal cord [124; 224].

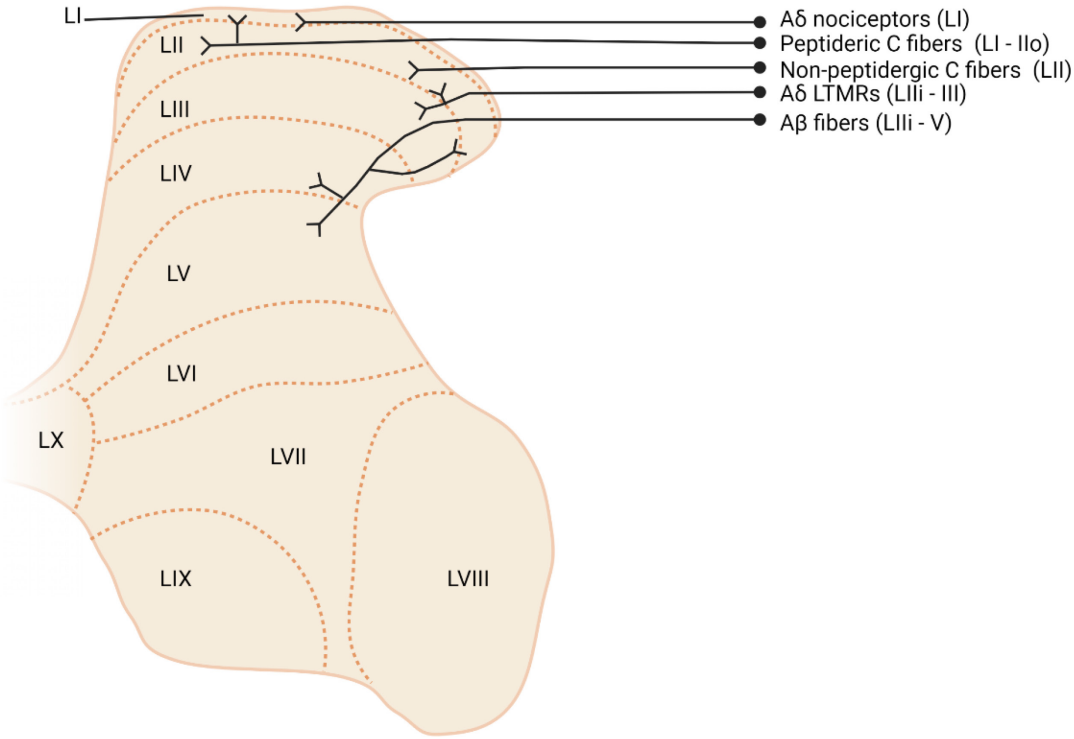

Chapter 1 Figure 3: Schematic representation of the central termination patterns of different classes of primary afferents.

The spinal gray matter is divided into 10 sections, called laminae, where different types of primary afferents terminate. These primary afferents are categorized as Aβ, Aδ and C fibers. Original image created with BioRender.

1.5.2 Central nervous system

Primary afferents relay signals to the spinal cord dorsal horn, and each primary afferent type has a characteristic distribution in one or more laminae of the dorsal horn. Bror Rexed first classified the cat spinal cord in 6 distinctive cytoarchitecture laminae in 1952 [170], which has since been updated and adapted to other species [25; 140; 168]. The central organization of different classes of primary afferents are represented in Figure 1.3.

1.5.2.1 The dorsal horn

The two most superficial layers of the dorsal horn, lamina I and the outer part of lamina II, along with deeper laminae III-V, represent the centers of the spinal cord predominantly involved in the pain circuitry. There, primary afferents form synapses with second order neurons, which represent mostly interneurons, but also projection neurons that relay nociceptive inputs to higher centers in the CNS including the lateral thalamus, the periaqueductal gray matter (PAG), cuneiform nucleus, caudal medullary ventrolateral reticular formation (VLM), the dorsal reticular nucleus (DRt), the nucleus tractus solitarius, and the parabrachial nucleus (PBN) [13].

What is most important, is that evidence shows a strong association between the morphological type of a lamina I projection neuron and its functional properties in primates [81]. Lamina I projection neurons have been categorized into three distinct populations based on their morphological characteristics (Figure 4): fusiform, multipolar, and pyramidal [247; 248; 251; 252]. Intracellular physiological investigations have facilitated the correlation between morphological and physiological attributes. Fusiform neurons were identified as nociceptive-specific (NS) and exhibited responses to noxious heat and pinch stimuli; multipolar neurons were either NS or responded to noxious heat, pinch, and both noxious and innocuous cold (HPC). In contrast, pyramidal neurons were non-nociceptive and responded solely to innocuous cooling

(COOL) [81]. Consistent with their responsiveness to noxious stimuli, the majority of fusiform and pyramidal neurons were found to be immunoreactive for the primary substance P (SP) receptor, the neurokinin-1 receptor (NK1-r). Conversely, in alignment with their lack of response to noxious stimuli, most pyramidal neurons were not immunoreactive to NK-1r [12; 247; 248].

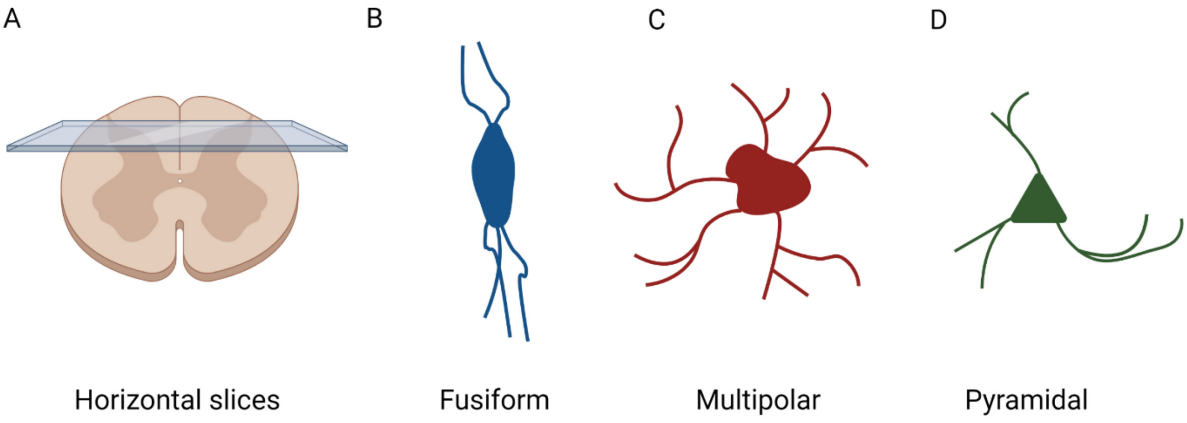

Chapter 1 Figure 4: Morphological classification of projection neurons in lamina I.

A) Projections neurons can be best identified using horizontal slices, as compared to other planes of view. B) Fusiform projection neuron. C) Multipolar projection neuron. D) Pyramidal projection neuron. Original image created with BioRender.

For a short time, the NK1-r was one of the most promising analgesic targets to reach clinical trials; however, antagonists failed to show pain alleviation, as evidenced by the clinical use of the Nk1-r antagonist, Aprepitant, as an anti-emetic [1].

1.5.2.2 Glial cells

Microglia are the resident immune cells of the central nervous system, including the spinal cord, playing a crucial role in surveillance, inflammation regulation, and immune response. These small, highly dynamic cells constantly survey their environment, responding rapidly to injuries or infections by becoming activated, changing shape, and migrating to the site of injury to mediate immune and inflammatory processes.

Microglia express Toll-like receptors (TLRs) that recognize molecular patterns associated with pathogens or tissue damage. Activation of TLRs triggers the release of pro-inflammatory cytokines like interleukin-1β (IL-1β) and tumor necrosis factor-alpha (TNF-α), which can sensitize pain pathways and contribute to hyperalgesia [84; 129]. Microglia also express purinergic receptors, including P2X and P2Y receptors, which respond to ATP released during tissue damage. Activation of these receptors leads to the release of inflammatory mediators such as IL-1β, IL-6, and IL-18, which can contribute to the sensitization of pain pathways [128].

Astrocytes, on the other hand, are star-shaped glial cells that perform diverse functions within the spinal cord. They provide structural support, maintain the blood-brain barrier, regulate ion and neurotransmitter levels, and participate in the formation and elimination of synapses and neural circuits. Astrocytes are integral to maintaining the homeostasis of the spinal cord's microenvironment and contribute to neuroprotection and synaptic plasticity [120].

1.5.3 Pain in the brain

The spinothalamic tract is one of the main pathways responsible for transmitting pain signals from the spinal cord to higher brain centers. As the signals ascend through the spinal cord, they pass through multiple levels of processing and integration. Key structures and pathways are briefly described here:

1.5.3.1 The thalamus

The thalamus, a key first relay station in the brain, plays a pivotal role in directing pain signals to different regions of the cerebral cortex. The thalamus directly receives inputs from the projection neurons of the dorsal horn [2]. From the thalamus, pain signals are transmitted to the somatosensory cortex, where they are further analyzed and interpreted. The somatosensory cortex processes the sensory aspects of pain, such as its location, intensity, and quality.

1.5.3.2 The anterior cingulate cortex

Pain perception involves more than just sensory processing. Emotional and cognitive aspects of pain, including its unpleasantness and the emotional response it evokes, are encoded in areas of the brain associated with emotions, memory, and attention [213]. The anterior cingulate cortex and the insular cortex are among the brain regions involved in these processes, contributing to the multidimensional experience of pain.

1.5.3.3 The periaqueductal gray matter (PAG)

The PAG, located in the midbrain, is a key center for pain modulation. Activation of this center has resulted in analgesic effects in both rat and humans [24; 137]. It plays a crucial role in the descending pain modulation pathway, where its activation can trigger the release of endogenous pain-relieving substances, such as endorphins, to alleviate pain [89; 119].

1.5.3.4 Cuneiform Nucleus

Also situated in the midbrain, the cuneiform nucleus is involved in the descending pain modulation pathway. It is particularly associated with the inhibition of pain transmission and can influence pain perception by interacting with other brain regions [88; 237].

1.5.3.5 Caudal Medullary Ventrolateral Reticular Formation (VLM)

The caudal medullary ventrolateral reticular formation (VLM) is located in the medulla of the brainstem. It has been identified as an important inhibitory descending pain modulation pathway [218].

1.5.3.6 Dorsal Reticular Nucleus (DRt)

Also situated in the medulla, the DRt participates in shaping the brain's response to pain signals. Damaging the DRt results in a reduction of nociceptive reactions to both acute and inflammatory pain, while stimulation of this region produces the opposite outcome [112].

1.5.3.7 Nucleus Tractus Solitarius (NTS)

This nucleus, located in the medulla, is a key player in processing visceral pain information and integrating it with autonomic functions. It receives signals from the spinal cord and higher brain centers, contributing to the overall pain experience and autonomic responses related to pain [26].

1.5.3.8 Parabrachial Nucleus (PBN)

Found in the pons region of the brainstem, the PBN is involved in the emotional and affective aspects of pain perception. The PBN forms a cluster of neurons encircling the superior cerebellar peduncles in the dorsolateral pons. In rodents, the PBN can be classified into numerous subnuclei based on their cytoarchitecture [66].The medial PBN (mPBN) comprises a diverse array of neurons in terms of size and morphology, while the lateral PBN (lPBN) encompasses distinct homogeneous groups. The delineations established by cytoarchitecture within both the mPBN and lPBN are also distinguished by their distinct connectivity patterns and neurochemical characteristics. Nociceptive, pruritic, and thermal signals are channeled to the lateral parabrachial nucleus (lPBN) through the spinoparabrachial tract originating from the

trigeminal and spinal dorsal horns. The lPBN also engages in bidirectional connections with various brain structures, aligning with its function of integrating sensory input with behavioral and autonomic responses [31; 38; 90; 141].

1.6 Autonomous nervous system

The autonomic nervous system is a peripheral nervous system component that controls involuntary physiologic processes such as heart rate, blood pressure, respiration, digestion, and sexual arousal. It is divided into three anatomical divisions: sympathetic nervous system (SNS), parasympathetic nervous system, and enteric system.

1.6.1 Sympathetic neurotransmitters

Sympathetic neurotransmitters are chemical messengers that play a crucial role in transmitting signals within the sympathetic nervous system. The sympathetic nervous system is typically thought as the system responsible for the "fight or flight" response, which involves response to stressors by increasing heart rate, dilating airways, and redirecting blood flow to the muscles.

One of the primary sympathetic neurotransmitters is norepinephrine, also known as noradrenaline (NA). It is released from sympathetic nerve endings through vesicles, which can also contain ATP and dopamine β-hydroxylase and binds to adrenergic receptors on target cells. Norepinephrine's effects are diverse and can include increasing heart rate, constricting blood vessels, and mobilizing energy stores for immediate use. Another important sympathetic neurotransmitter is epinephrine, also known as adrenaline. While it is mainly produced and released by the adrenal medulla (part of the adrenal glands), epinephrine acts as a potent

sympathomimetic agent. It rapidly increases heart rate, dilates airways, and triggers the release of glucose from the liver to provide energy.

The effects of sympathetic neurotransmitters are mediated by specific receptors known as adrenergic receptors, which are categorized into two main types: alpha-adrenergic receptors and beta-adrenergic receptors. Each type has further subtypes (e.g., alpha-1, alpha-2, beta-1, beta-2, etc.), and their activation leads to distinct physiological responses [175]. For instance, activation of alpha-adrenergic receptors can lead to vasoconstriction (narrowing of blood vessels), increased blood pressure, and pupil dilation. Activation of beta-adrenergic receptors, on the other hand, can cause increased heart rate, bronchodilation, and mobilization of energy stores. Primary afferents have been identified as expressing alpha-adrenergic receptors, with highest expression of alpha-1A in naïve animals [242].

VMAT (Vesicular Monoamine Transporter) is a crucial protein responsible for packaging and transporting neurotransmitters, particularly monoamines, into vesicles within nerve terminals. These vesicles are then released into the synaptic cleft to transmit signals between neurons. VMAT exists in two isoforms, VMAT1 and VMAT2, and is particularly important in sympathetic neurons for the packaging and release of neurotransmitters like norepinephrine [55]. In sympathetic neurons, VMAT2 is the primary isoform responsible for packaging norepinephrine into vesicles.

A widely used medication for to lower high blood pressure is guanethidine, which uses this protein transporter system as mechanism of action. It belongs to a class of drugs known as sympathetic nervous system inhibitors or sympatholytics. Guanethidine is structurally similar to norepinephrine, allowing it to be taken up by VMAT2 into the vesicles. Once inside the vesicles, guanethidine displaces norepinephrine from the vesicles and takes its place, and in turn

effectively depletes the vesicles of norepinephrine. This can help lower blood pressure by decreasing the effects of norepinephrine on blood vessels and the heart [17].

1.6.2 Sensory-sympathetic coupling

Sensory sympathetic coupling refers to a phenomenon in which sensory nerve fibers interact with sympathetic nerve fibers within a tissue or organ. This interaction allows sensory signals, which are typically associated with transmitting sensory information such as touch, temperature, and pain, to also influence the activity of the sympathetic nervous system, and vice versa.

Sympathetic neurotransmitter release from sympathetic neurons onto sensory neurons has been shown to modulate pain-related withdrawal responses [194]. For example, intra-dermal administration of NA in neuropathic human subjects worsened pain and hyperalgesia [34; 52]. Further investigation showed that Aδ fibers and mostly C fibers are sensitized in this process [173]. Interestingly, in chronic inflammation and neuropathic pain conditions, sympathetic fibers have been found to closely associate with sensory fibers in areas of the skin where they are usually absent [11; 76; 169; 176; 246]. These sprouting anomalies drive interest in understanding changes in sensory and sympathetic innervations in arthritis, which has recently been demonstrated by our lab in inflammatory arthritis, but are yet to be investigated in osteoarthritis [117].

These changes described above highlight the complex and interconnected nature of the nervous system, where different types of nerve fibers can communicate and influence each other's activities to achieve specific physiological outcomes.

1.7 Anatomy of the synovial joint

The synovial joint is comprised of hyaline cartilage (more specifically articular cartilage) subchondral bone, the synovial fluids that fill the joint cavity, the synovium (or synovial membrane), and the articular capsule that surrounds all these structures. The capsule connects to the two bones that comprise the joint via ligaments. Figure 1.5 shows a representation of those structures in the healthy joint.

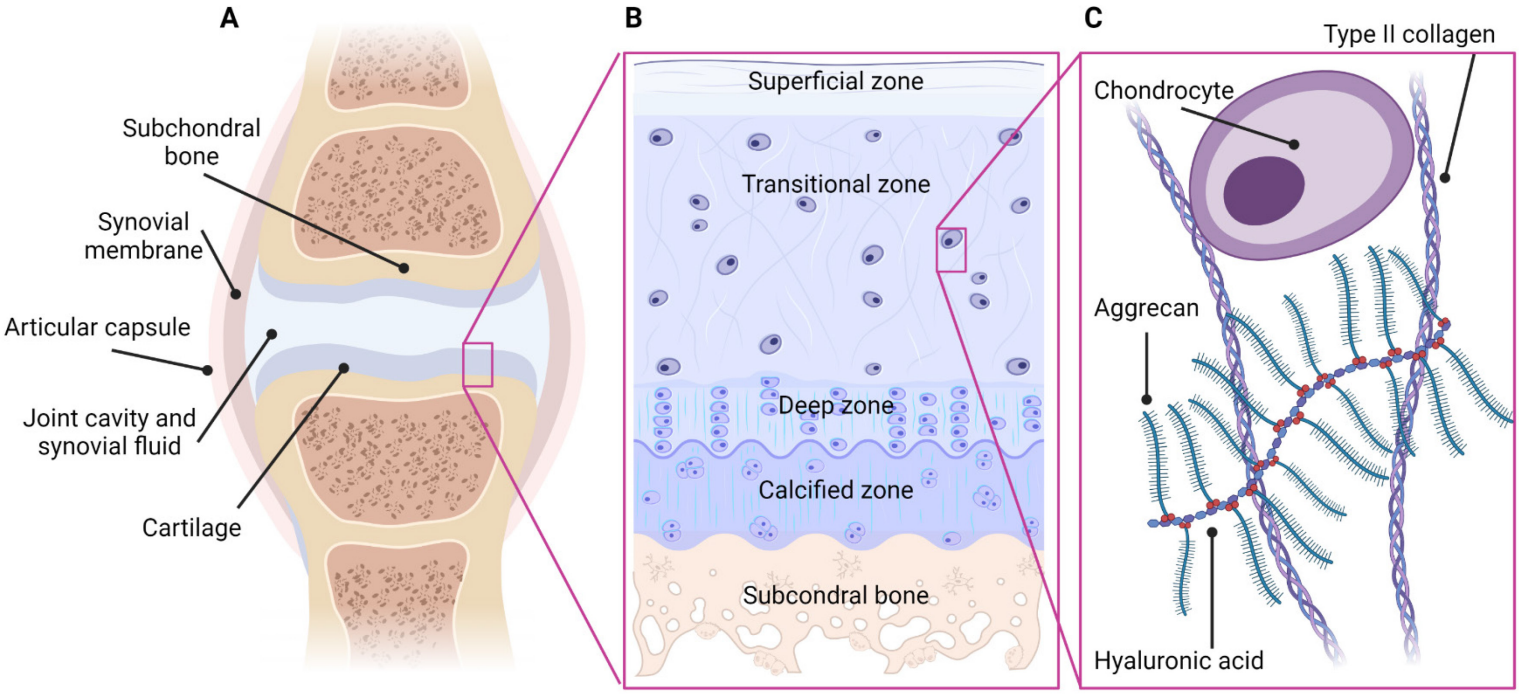

Chapter 1 Figure 5: Schematic representation of the anatomy of the healthy synovial joint.

A) Anatomical representation of joint components B) A magnified schematic of the articular cartilage organization. C) A magnified schematic of the extracellular matrix of the articular cartilage transitional zone. Original image created with BioRender.

1.7.1 Articular cartilage

The articular cartilage protects the subchondral bone by facilitating the impact of loads to the joint with a low friction coefficient (between 0.002 and 0.01 in healthy cartilage) [30; 64; 130]. It is composed of chondrocytes, which are the single cell type of the cartilage, and rich extracellular matrix (ECM) made up mostly of water, type II collagen, and proteoglycans such as aggrecan (Figure 1.5C) [75]. Chondrocytes are sparsely distributed in the cartilage and are responsible for the synthesis and breakdown of the molecules that make up the ECM, where collagen turnover is relatively slow compared to proteoglycans [144]. Unfortunately, cartilage has a limited capacity for repair: if chondrocytes are unable to maintain homeostasis, the integrity of the structure can be compromised and lead to irreversible degeneration [83]. In fact, articular cartilage is avascular and aneural, therefore, it relies on diffusion of nutrients from the synovial fluid for its maintenance. This is facilitated by the increase and decrease in interstitial fluid pressure that occur when forces are applied to the joint, allowing nutrients to reach chondrocytes in all zones of the articular cartilage [62; 65; 126]. Figure 1.5B shows the structure of the cartilage zones. The superficial zone represents 10-20% or cartilage thickness and contains flattened chondrocytes and collagen parallel to the surface of the joint. The transitional zone represents 40-60% of cartilage thickness and contains round chondrocytes and oblique collagen fibrils. The deep zone represents 30% of articular cartilage thickness and is characterized by columnar bundles of chondrocytes as well as perpendicular large caliber collagen fibrils that defend the bone from compressive forces. Finally, the calcified zone contains infrequent chondrocytes and allows the articular cartilage to securely attach to the subchondral bone [206].

It is unclear what cellular event might lead to the initiation of this degenerative cascade. Infiltration of synovial macrophages leads to the release of proinflammatory cytokines, like TNFα,

IL-1 and IL-6 [209]. These cytokines can bind to their receptors on chondrocyte to activate the release of metalloproteinases which directly leads to inhibition of type II collagen production and therefore perpetrating the dissolution of the articular cartilage [29].

1.7.2 Subchondral bone

The subchondral bone is composed of cortical bone bordering the cartilage on one side, and the growth plate on the other. The subchondral bone contains numerous canals containing their supply of vasculature and innervation (Figure 1.6). Although calcified cartilage seals the surface between the subchondral bone and the cartilage, "microcracks" start to appear and propagate in OA [182], which is believed to allow for the invasion of vascularization and innervation into the cartilage in the disease state [214]. Normal bone mass is achieved by the equilibrium between bone resorption by osteoclasts and bone formation by osteoblasts [61]. Bone degeneration in OA is associated with abnormal increased density, or sclerosis, of the subchondral bone and thickening of the cortical plate. This is normally accompanied by significant bone remodelling and formation of osteophytes at the joint margin [28; 220]. Compared to subchondral osteoblasts in healthy joints, osteoblasts located in osteophytes produce higher levels of IL-6, IL-8, and MMP-13 in OA-affected joints [181]. Interestingly, the nociceptive peptide SP has been associated with bone metabolism: macrophages and stromal cells originating from the bone marrow, which are precursors to osteoclasts and osteoblasts respectively, both express the NK1-r [230]. It is possible that neurogenic SP could potentiate the imbalance in bone resorption and formation, therefore contributing to abnormal bone and cartilage degeneration [110; 149].

1.7.3 Synovial membrane and synovial fluid

The inner surface of the articular capsule is lined with the synovial membrane which is rich is vascularization. The synovium is responsible for producing the synovial fluids, as well as the

nutrients required by the chondrocytes [144]. Contrary to historical beliefs, in the OA disease state, the synovium becomes inflamed, and likely contributes to the pathogenesis [57; 63; 160; 204]. Characteristic of this inflammation, or synovitis, is the infiltration of neutrophils, T lymphocytes, monocytes and increased vascularisation and hyperplasia of the synovium [41; 187]. Patients with advanced OA also show increased levels of SP in the synovial fluid [166] and SP-immunoreactive (ir) nerve endings in the synovial membrane [180]. Evidence suggests that synovitis may be a initiating factor of OA, as synovial tissue from early-stage OA patients show an over expression of inflammatory mediators [20].

1.7.4 Innervation of the joint

The synovial joint receives the majority of its nerve supply from unmyelinated afferents, with some myelinated afferents [104]. Peptidergic C fibers are located in all structures of the joint, with the exception of the cartilage which is aneural [125; 205]. Sympathetic efferent fibers closely adjoined to vasculature are also present in those structures [7]. In the subchondral bone, circular concentric clusters of osteocytes form a canal, called the Harversian canal, where thin myelinated fibers run alongside blood vessels and sympathetic efferents (Figure 1.6). Non-peptidergic nociceptors are absent from those structures, as they are almost exclusively located in skin tissue [219].

In the synovial joint, there exist several classes of proprioceptors that innervate various structures : 1) free nerve endings, which are the most numerous type of joint receptor, in the connective tissue; 2) Golgi endings which are found in the joint ligaments; and Ruffini endings that are found in the joint capsule [174].

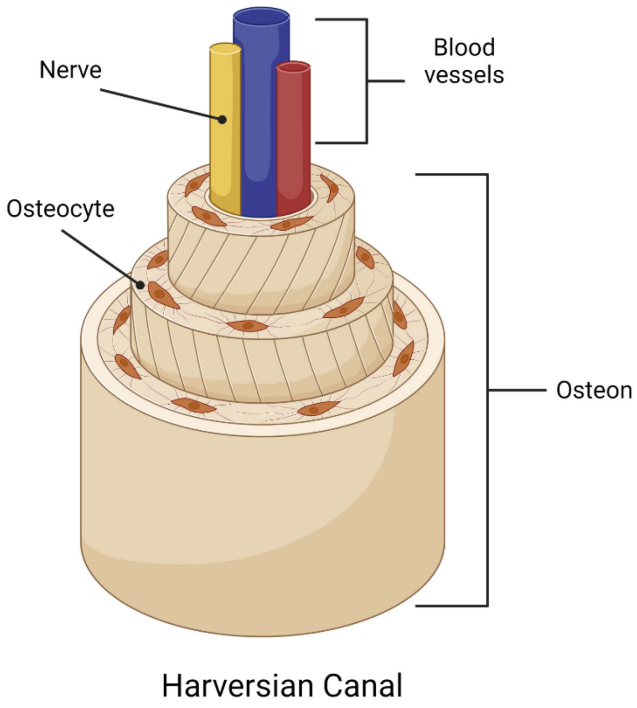

Chapter 1 Figure 6: Schematic representation of the Harversian canal.

Original image created with BioRender.

1.8 Animal models of OA

Comparative medicine is the process by which we use other species to study physiological processes in humans. Rats and mice are ideal species to research disease as 95% of their 30 000 genes are shared with humans [72; 103; 227; 233]. We owe a lot to animals for their contributions to advances in research and medicine, including advances in our understanding of OA. Since the creation of the first knock out mouse in 1987 and subsequent rapid evolution of genetic techniques, mouse models have taken over the biological research literature and offer great opportunities to perform functional studies [68; 221]. While the generation of genetically engineered rat models has evolved in the past two decades [249], with their larger size, rats offer the possibility to perform

complex procedures. There exist multiple approaches to induce OA in experimental animals, but none have received the consensus of scholars as being the gold standard. In this section, we will discuss the benefits and limitations of using various types of animal models of OA, including surgical, spontaneous, genetic, and chemical models.

1.8.1 Surgical models

Surgical procedures are used to destabilize joints in both mouse and rat by creating a structure lesion, such as a medial meniscal tear (MMT), partial medial meniscectomy (PMM), destabilization of the medial meniscus (DMM), and anterior cruciate ligament transection (ACLT). These procedures are invasive but generate relatively rapid signs of OA. In mice, starting at 4 weeks post-surgery, initial signs of cartilage fraying can be observed, and 8 weeks post-surgery, advanced cartilage destruction and subchondral bone sclerosis develop, while osteophyte develop at 12-weeks post-surgery [73; 74; 122; 235].

1.8.2 Spontaneous models

A spontaneous model refers to a disease that occurs naturally in the animal being studied. Aging genetic models such as transgenic guinea pigs (Dunkin-Hartley strain) and C57/BL6 black mice have been shown to develop signs of OA spontaneously at about 3 and 17 months of age respectively [93; 236; 253]. A spontaneous obesity mouse model also exists, which develops spontaneous OA with by administering high-fat diet over a period of 12 weeks [77]. Although very simple, spontaneous models tend to have very long end-points due to a slow progression of the disease, as be limited due to the variability between animals of a same cohort.

1.8.3 Genetic models

As of 2013, up to 135 strains of genetically modified mice had been developed to study OA [114]. Del1+/- mice, which carry a mutation in the type II collagen gene, also develop

spontaneous OA, and have been used in combination with surgical procedures to accelerate the development of the disease in the animal [177; 232]. Col2a1-Cre^{ERT2}, Agc1-Cre^{ERT2} and Prg4-Cre^{ERT2} are all transgenic mouse models of OA that are chondrocyte-specific. Col2a1-Cre^{ERT2} and Agc1-Cre^{ERT2} target chondrocytes in the growth plate cartilage, articular cartilage and temporomandibular joint [33; 85], while Prg4-Cre^{ERT2} targets chondrocytes residing in the superficial zone of the cartilage [101]. Studies utilizing OA genetic models are very valuable in studying disease initiation and progression and are less often used to study pain as it usually appears late in the disease process.

1.8.4 Chemical models

Chemical models of OA can be performed in mice or rats and have the advantage to be minimally invasive. Collagenase injected intra-articularly in the knee generates OA by digesting the type II collagen present in the extra-cellular matrix therefore disrupting cartilage integrity [98]. This is followed by bone lesions similar to what is described in the clinic [225; 226]. This model was also used to study OA-associated pain, where pain-related behavior was observed 6 weeks after injection [5]. Interestingly, there have been concerns regarding the external validity of the collagenase injection as a model for OA due to its strong inflammatory component resembling RA [115], but others are adamant that it does not qualify as RA due to a lack of autoimmune degeneration in non-injected joints [159].

Mono-iodoacetate (MIA) is a glycolytic inhibitor which chemically induces OA by disrupting glycolysis of chondrocyte, resulting in cell death. MIA induced-pain and histopathological features make this model superior to other chemically induced models [10]. The MIA model is typically induced in the knee joint of rat or mice. The knee-joint model has been extensively studied in terms of disease progression and inflammatory infiltration. It has previously

been shown that chondrocyte degeneration and necrosis appear at days 1–7 post-MIA, increased osteoclasts and osteoblasts in subchondral bone occur by day 7, focal fragmentation and collapse of bony trabeculae with fibrosis by day 28, and large areas of bone remodeling by day 56 [79; 100]. Additionally, there is increase tumor necrosis factor-α (TNF-α) and interleukin-6 (IL-6) in the knee synovium and capsule between days 1 and 28 post-MIA injection, with highest levels measured on day 4 post-MIA injection [156].

1.8.5 Studying pain with animal models of OA

It is important to realize that most, if not all, of the animal models described in this section were developed and characterized with the objective of studying disease-modifying agents or preventative measures for the degeneration of the joint. While these efforts are commendable and have provided valuable insight on the disease, they have not yet yielded satisfying therapeutic options. Chronic pain is the main symptom associated with OA, yet our knowledge of the underlying mechanism contributing to chronic pain in OA is still limited. To study the mechanisms that are involved in the maintenance of pain in OA, an experimenter must produce a cohort of animals with consistent pain behavior, which is best achieved by an advanced stage of OA. Surgical procedures should be minimally invasive in order to avoid pain originating from confounding tissue and nerve damage. From this perspective, chemical models of OA, particularly the one generated with MIA, are promising for the study of pain in OA.

Although a neuropathic pain-like component is suspected in OA, changes associated with peripheral nerve injury are infrequently investigated in the animal models of OA listed above. Many animal models of peripheral nerve injury of the sciatic nerve of rodents have been developed to replicate neuropathic pain conditions observed in humans. These include the complete transection of the sciatic nerve [228], the chronic constriction injury (CCI) [22], the partial sciatic

nerve ligation (PSNL) [189], the spared nerve injury model (SNI) [42], the spinal nerve ligation model (SNL) [87], and the polyethylene cuff model [19; 143; 164]. Schematic representations of these peripheral nerve injury models can be found in Figure 1.7. In the Sprague Dawley rat, the sciatic nerve projects mostly to the L4 and L5 segments of the spinal cord, with some contributions to L6 [15; 42; 172; 215]. While most, if not all, of the surgical and chemical animal models of OA are induced in the knee joint, the knee joint is supplied by branches from the femoral, tibial, common peroneal, and obturator nerves, which distribute to the L2-L4 segments of the spinal cord [69]. The ankle joint, however is mostly supplied by branches from the sciatic nerve (tibial, sural, deep peroneal) and saphenous nerves, with innervation from the spinal cord at the level of lower lumbar regions (L3-L6) [70]. In theory, an animal model targeting the ankle joint could allow for a more relevant comparison of changes occurring in OA to those occurring in sciatic nerve injury models used to study neuropathic pain.

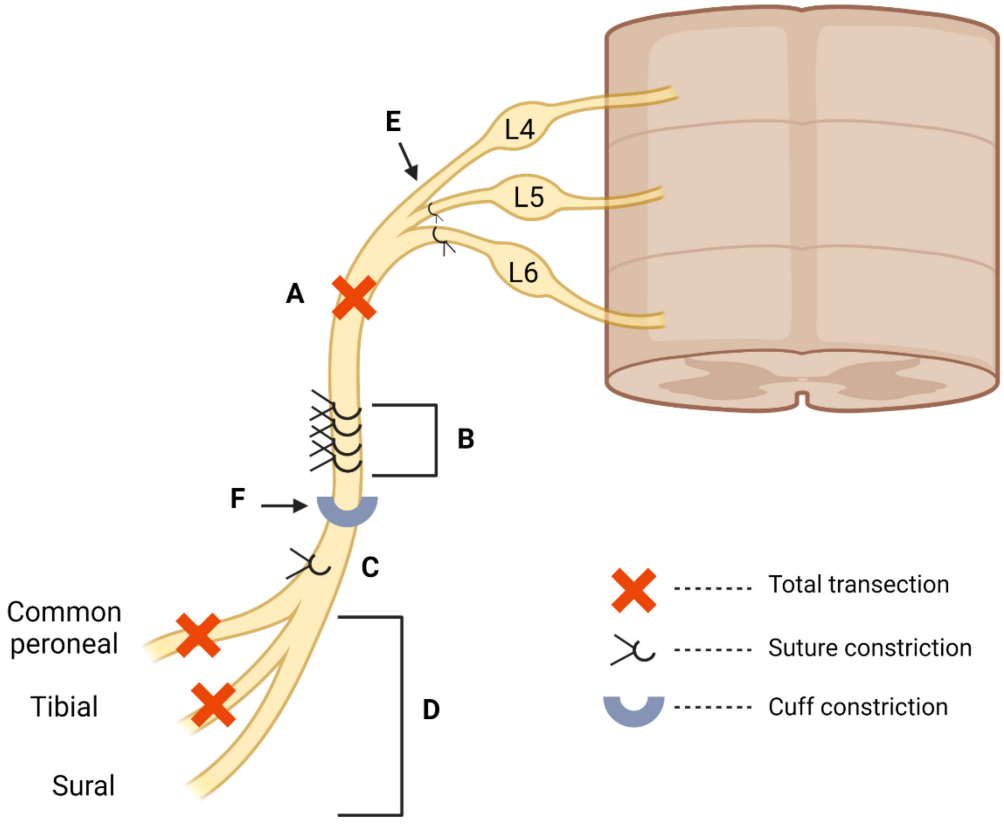

Chapter 1 Figure 7: Illustration of surgical models of peripheral nerve injury used to study neuropathic pain.

This includes sciatic nerve transection (A), chronic constriction injury (B), partial sciatic nerve ligation (C), spared nerve injury (D), spinal nerve ligation (E), and the polyethylene cuff around the main branch of the sciatic nerve (F). Original image created with BioRender.

1.8.6 Conservation between species

There are a few differences relevant to pain between rats and mice that have been reported in the literature and that should be taken into contemplation when choosing an animal model. TRPV1 expression in nociceptors is observed on peptidergic fibers only in mice, but in rats and

humans they are also observed on non-peptidergic IB4+ fibers [153]. Conversely, the member of the EF-hand calcium-binding protein (CaBP) superfamily secretagogin (Scgn) has been found to colocalize with CGRP in the DRG of mice and humans and to distribute similarly in LIIi of the dorsal horn (and LI, LIII-V in lower number) and in ventral horn neurons [199]. This pattern was similar to human Scgn expression, but not to rat. The general lack of translational studies in the literature that directly compare the biology of rats and mice makes it difficult to evaluate and compare cross-species (and even cross-strain) reported findings. It is unclear whether such investigations would reveal the ideal organisms represent human biology, as this remains a contested area of pain science [139].

1.9 Therapeutic approaches for the treatment of OA

As the molecular mechanisms involved in OA initiation and progression are still poorly understood, there are currently no interventions to restore degraded cartilage or to even decelerate the progression of the disease. Instead, current standards of care focus on the management and alleviation of OA in those affected. Despite the administration of conventional analgesic drugs, the quality of life of patients deteriorates as osteoarthritic pain persists. The first line of pharmacological treatment consists of oral/topical nonsteroidal anti-inflammatory drugs (NSAIDs) or acetaminophen. Additionally, patients are encouraged to seek non-pharmacological approaches to their treatment plan, such as aerobic exercise, swimming, and a weight loss diet, as well as psychological support. This approach to pain treatment is called the bio-psycho-social model.

Patients with knee or hip osteoarthritis may also receive intra-articular corticosteroid injections. However, if no improvement is observed after 12 weeks of treatment, a patient may be

eligible for total arthroplasty, a rather drastic but unavoidable alternative in many cases [203]. Additionally, a subset of osteoarthritis patients who have undergone successful total arthroplasty report sustained levels of pain after healing from surgery [121]. Indeed, the persistence of pain in some osteoarthritis patients, after removal of the diseased joint, suggests that this disease can lead to neuropathy and central sensitization.

1.10 Thesis rationale and general objectives

As described in this chapter, pain associated with OA remains a major clinical burden to our society. Despite the extensive pre-clinical and clinical innovations in OA research, we are still unable to provide patients with a curative treatment. Instead, we rely on multidisciplinary biopsychosocial pain management to provide relief, as analgesic options by themselves are unsatisfactory.

Investigations of in various animal models of chronic pain, including models of neuropathic pain and inflammatory arthritis, have uncovered growing evidence of neuroplastic changes occurring in the peripheral and central nervous systems that contribute to the maintenance of pain. Whether these structural and morphological changes are also occurring in OA is speculative, but clinical evidence certainly points to OA being more than a mechanical disease. To be able to describe these changes in a preclinical model of OA would build a foundation for future studies using mechanism-based interventions.

The goal of this body of work is two-fold. The first is to provide the field of pain science with strong and valid methodologies for studying pain associated with the disease of osteoarthritis.

The second is to shine a light on the complexity of OA pain by investigating peripheral and central contributors to pain transmission.

This thesis includes the following 3 manuscripts and 1 supplementary data chapter, which aim to:

1 Describe a robust methodology for detecting changes occurring in bone, including the detection of nerve fibers in models of OA, osteoporosis and fracture models.

2 Use a combination of behavioral, histopathological and pharmacological approaches to investigate peripheral and central mechanisms contributing to the maintenance of pain in OA, including the presence of a neuropathic-like component in OA using a novel MIA model in the rat ankle-joint.

3 Investigate the contribution of proprioceptors to pain-related behavior in OA by using histopathological and imaging techniques to study changes occurring in the PNS.

Supplementary Data: Describe changes in Nk1-r immuno-reactivity of projection neurons in OA and investigate activation of that circuitry using a treadmill model of exercise in male and female rats.

CHAPTER 2

An optimization of DAB-based immunohistochemical detection of nerve fibers in rat and mouse decalcified bone

Valerie Bourassa, Miyako Suzuki-Narita, Laura S. Stone, Alfredo Ribeiro-da-Silva

To be submitted to *Bone*

2.1 ABSTRACT

This report provides a detailed description of the optimisation of a diaminobenzidine (DAB)-based immunohistochemistry (IHC) protocol for detection of nerve fibers in rat and mouse decalcified bone. Research exploring innervation in healthy and remodelling bone has been impaired by technical challenges associated with obtaining convincing images of innervation in compact bone. Here we focussed on optimization of the detection of pain-sensing primary nociceptors and sympathetic fibers using antibodies against calcitonin gene-related peptide (CGRP) and vesicular mono-amine transporter 2 (VMAT-2), respectively. The approach was tested in animal models of bone pathologies where changes in bone innervation have been implicated: an osteoarthritis model in the rat ankle joint, a mouse open osteotomy fracture model, and an ovariectomy mouse model of osteoporosis. The optimized protocol is a considerable improvement over available approaches for the IHC detection of nerve fibers in bone in normal conditions and in animal models of bone pathology.

2.2 INTRODUCTION

Clinical evidence shows that bone pathologies are highly prevalent [22; 31; 34] and are often associated with pain, including osteoarthritis, osteoporosis and bone fractures. While pharmacological efforts to manage pain associated with these diseases, such as administration of NSAIDS, opioids, and antibodies against nerve growth factor (NGF) have shown promise, life-threatening and considerable side effects have been reported, such as gastro-intestinal track toxicity, respiratory depression and altered bone remodelling [5; 10; 11; 16; 17; 23-25]. These observations stress the importance of identifying alternative therapeutic targets such as neural mechanisms that contribute to the pain. Indeed, there is a growing appreciation for changes in

innervation in bone and interactions between the nervous system and bone tissue. However, our understanding of the intricacies of the nervous system's role in bone pain have been impaired by a difficulty in the detection of the innervation of bone itself by immunohistochemistry (IHC).

Although some studies have successfully characterized the organization of sensory innervation in the periosteum and bone marrow through IHC [3; 21], adequate penetration of antibodies in calcified structures such as compact bone, subchondral bone and remodelling bone remains challenging for many laboratories. In fact, very few research groups have demonstrated convincing images of innervation of compact bone [4].

Bone presents a unique challenge for IHC: it normally needs to be decalcified first and then embedded in plastic or paraffin prior to sectioning to maintain structural integrity. The loss of antigenicity associated with embedding leads to difficulties detecting nerve fibers. However, unsuitable decalcification and processing of bone tissue can also lead to problems, including loss of antigenicity and distorted morphology. All these challenges, if not properly addressed, can impact the quality of IHC.

Another factor that affects the visualization of the innervation of hard tissues (bone and cartilage) and bone marrow, when using fluorescence microscopy, is the presence of autofluorescence. Bone marrow displays intense autofluorescence; sources in bone marrow include collagen [26; 27; 35; 36], flavoprotein-associated granules in macrophages [14; 18], and lipofuscin, which fluoresces in most channels [6; 13; 15]. The latter also contribute to the autofluorescence associated with vasculature in Haversian canals in bone where sensory and sympathetic fibers travel and innervate blood vessels. Thus, autofluorescence may be mistakenly interpreted as innervation in the absence of appropriate controls. Due to these limitations, a bright

field, diaminobenzidine (DAB)-based IHC approach can be advantageous in detecting targets in those structures, namely nerve fibers, for the study of pain mechanisms.

Based on the above, we underwent an extensive series of experiments to improve protocols to study innervation in hard tissues in animal models of pathologies where changes in innervation have been reported or are likely to occur. These conditions include a mono-iodoacetate (MIA) model of osteoarthritis in the rat ankle joint, a mouse open osteotomy fracture model, and an ovariectomy mouse model of osteoporosis. We optimized the protocols for the detection in these models of markers for sensory nociceptive fibers and sympathetic fibers using antibodies detecting calcitonin gene-related peptide (CGRP) and vesicular mono-amine transporter 2 (VMAT-2), respectively. We expect that the improved methodology described here will facilitate research investigating changes in innervation associated with joint and bone pathologies.

2.3 METHODS

All experiments followed the guidelines contained in the Care and Use of Experimental Animals of the Canadian Council on Animal Care, and studies were approved by the Faculty of Medicine Animal Care Committee of McGill University. Moreover, the studies were conducted in accordance with the Guidelines for Animal Research by the International Association for the Study of Pain.

2.3.1 Animal models:

2.3.1.1 Osteoarthritis:

Osteoarthritis (OA) was induced chemically using the glycolytic inhibitor MIA. Sprague Dawley male rats (Charles Rivers Laboratories) 7 weeks of age and weighing 175-200 g at the

beginning of the study were anesthetized with 5 % isoflurane in O_2 and given a single administration of 2.4 mg of MIA (Sigma) in 40 µl saline through an intra-articular injection in the tibio-talar junction of the ankle joint as previously described by our group [2]. At 5 weeks post-injection, a timepoint at which OA pain and degenerative bone changes are established, animals were sacrificed for tissue collection.

2.3.1.2 Osteoporosis:

A model of post-menopausal osteoporosis was generated by bilateral ovariectomy (OVX) in female C57Bl/6j mice, 6 weeks of age and weighing 18.2 ± 0.42g, under anesthesia with 5% isoflurane in O_2 as we have previously described [29; 30]. Bone loss following OVX has been extensively described [19; 32; 33]. Experimental time point was 8-weeks post-surgery, when mice were sacrificed for tissue collection.

2.3.1.3 Tibia fracture:

We followed the open osteotomy model of tibia fracture [7; 9]. Female C57BL/6j mice, 18 months of age were anesthetized using 5% isoflurane in O_2. Intramedullary stabilization was performed through the insertion of the internal wire guide of a 25 gauge BDTM spinal needle into the medullary canal. Subsequently, a mid shaft transverse osteotomy was performed on the tibial bone [1]. At 5 weeks post-surgery, animals were sacrificed for tissue collection.

2.3.2 Perfusion fixation:

Animals were first deeply anesthetized with an intra-peritoneal injection of Equithesin (a mixture of 12.75 mg chloral hydrate, 3 mg sodium pentobarbital, and 6.4 mg magnesium sulfate in a volume of 0.3 mL per 100 g of body weight). Following a vascular rinse with 0.1% $NaNO_2$ and 0.05% $NaHCO_3$ in 0.01M phosphate buffered saline (PBS), animals were perfused with 3% paraformaldehyde in 0.1 M phosphate buffer (PFA), pH 7.4, with 15% (v/v) saturated picric acid,

for 30 minutes. Rat ankle joints, mouse tibias, and mouse spines were extracted and post-fixed in the same fixative for 4 hours at 4˚C, and subsequently placed in 10 % sucrose in 0.1 M cacodylate buffer overnight, at 4˚C.

2.3.3 Decalcification and sectioning:

Extracted joints and bone tissue were decalcified in 10 % ethylenediaminetetraacetic acid (EDTA) pH 7.4 in PBS at 4˚C on a shaker for 4 weeks for rat ankle joints, while mouse tibias and spines were decalcified for 2 weeks. The EDTA solution was changed twice a week. Subsequently, tissue samples were cryo-protected in 30% sucrose solution in cacodylate buffer at 4˚C overnight. Tissues were embedded and frozen in O.C.T. compound (Tissue-Tek, Torrance, CA, USA) and sectioning was performed using a cryostat (Leica). Serial sections, 25 µm in thickness for ankle, 20 µm tick for tibia and 16 µm thick for spine, were collected and thaw mounted onto gelatin-coated slides.

2.3.4 Preparation of gelatin-coated slides

The preparation of gelatin-coated slides was performed using 15 grams of gelatin (Sigma G2625 type A) and 1.5 g of chromium potassium sulfate dodecahydrate (MW 499.40; Sigma: 60152) in 3 L of ddH_2O were heated to 60˚C until dissolved. Fisher brand pre-cleaned SuperFrost slides (12-550-143, 25x75 mm) were slowly dipped in the gelatin solution for 30 seconds, then placed in a 37˚C incubator for at least 48 hours or until dry.

2.3.5 DAB – based immunohistochemistry:

A breakdown of the IHC parameters for each animal model is summarized in Table 1. Note that due to the tendency of bone tissue to detach from slides, shaking during incubations is not recommended. Instead, we used flexible plastic coverslips (EMD Millipore Corp. CAT #S7117) to protect the tissue during incubations (**Figure 1**). When applied carefully over tissues that have

a tendency to detach, the liquid on the slide is evenly distributed under the coverslip; we found that this prevents patchy staining patterns and tissue detachment. Note that it is also important to avoid air bubbles between the slide and the plastic coverslip. Another beneficial effect of the coverslip incubations was a reduction in the volume of primary and secondary antibodies. Normally for fixed tissue on slides that is too delicate to be incubated on a shaker, we recommend using 1 ml of liquid for proper incubation and washes. With the plastic coverslip, the volume of antibodies – and avidin-biotin complex – can be reduced to 150 µl per slide.

Decalcified ankle joints, spines, and tibias were pre-incubated on-slide with excess PBS with 0.2% Triton X-100 (PBS+T) for 24 hours at 4°C. Slides were then incubated for 30 minutes with 50% ethanol in water and for 30 or 60 minutes of 0.3% H_2O_2, with three 10 min washes with PBS between each incubation. Slides were left for 1 h at room temperature in 3-5% normal goat or donkey serum (Invitrogen) in PBS+T or PBS with 0.3% Triton X-100 to block unspecific labeling. To detect immunoreactivity of the peptidergic or sympathetic fiber populations, the sections were then incubated for 48 to 72 hours at room temperature or 4°C using a rabbit anti-calcitonin gene-related peptide (CGRP) antibody (Sigma-Aldrich #C8198), or goat anti-vesicular monoamine transporter-2 (VMAT-2) antibody (abm #Y213391) at dilutions of 1:2500 and 1:250, respectively. Following 3 rinses in PBS+T, sections were incubated at 4°C or room temperature for 24 to 72 hours in goat anti-rabbit IgG biotinylated antibody (Vector #BA-1000; 1:400) or donkey anti-goat IgG biotinylated antibody (Jackson #705-066-147; 1:250). The avidin-biotin complex (ABC) solution was prepared (1:400) in PBS+T (Vector Elite PK-6100) and added to the slides for incubation at room temperature for 1 hour. Diaminobenzidine (DAB) was added to the sections on-slide for 15 minutes, and then a 1% H_2O_2 DAB in PBS solution was added for 10 to 12 minutes. Slides were subsequently rinsed with PBS and PBS+T, dehydrated with ascending

concentrations of ethanol, cleared with xylene, and cover-slipped with Entellan mounting medium (Electron Microscopy Sciences). Bright field images were obtained using a Zeiss Axioplan 2 imaging microscope with a 40x oil-immersion objective, a high-resolution color camera and the Zeiss Zen software version 2.3.

2.4 RESULTS

In this study, we optimized the conditions for the bright field IHC staining for three types of joint and bone tissue (rat ankle joints, mouse tibia and spine) compared to the conventional approaches using either bright field or fluorescence.

Decalcification was monitored to ensure preservation of tissue morphology: rat ankle-joints were decalcified for 4 weeks, while mouse tibias and spines were decalcified for 2 weeks only. In all circumstances, the EDTA solution was changed twice a week, where bone softness was assessed. Bone should be soft enough so that it can be cut through manually with a blade with considerable force. If the bone is too soft, morphology and antigenicity will be lost.

We found that pre-incubating bone sections with PBS+T for 24 hours at room temperature prior to initiation of the IHC staining was crucial. This is likely because Triton X-100 results in permeabilization of the tissue that allows the penetration of the immunoreagents. Additionally, further improvement was obtained by extending incubation times from 24 hours to 48-72 hours for primary, and from 2 hours to 24 hours for secondary antibodies. It is interesting to note that the temperature at which the incubations were carried out had a different effect on each type of material. Some tissues, such as the subchondral bone of MIA-treated rats and the bone marrow of OVX mice, benefited from primary antibody incubations at room temperature. On the other hand,

the best quality staining of compact bone and bone marrow of the mouse fractured tibia was obtained when the secondary antibody incubation was at room temperature. These observations suggest that the temperature of the antibody incubations is a useful parameter to explore when optimizing staining of difficult tissues such as bone. Finally, we found that endogenous peroxidases were still active in the spine of OVX mice after a 30 minute incubation in H_2O_2 and required a second 30 minute incubation with fresh H_2O_2. We suspect hormonal changes in this model account for this observation. IHC parameters for each condition are summarised in Table 1.

We concluded that bright field, DAB-based IHC was clearly superior to immunofluorescence for bone tissue. Indeed, decalcified tissue is often associated with autofluorescence that can be mistaken for specific immunoreactivity as illustrated in **Figure 2**. **Figure 2A, B** shows representative images of rat tibial subchondral bone decalcified sections following traditional IHC protocols with anti-CGRP antibody processed for immunofluorescence (**Figure 2A**) and DAB-based IHC (**Figure 2B**). We detected autofluorescence on the edges of structures where there was an interface, such as periphery of harversian canals. As blood vessels in compact bone are located mostly in haversian canals, the non-specific staining appearing as lines may either mask or simulate immunoreactive nerve fibres. This is shown in **Figure 2A**, in which the structures indicated with arrows likely represent background, and not the CGRP-positive fibres that we wanted to see. The difficulty of distinguishing bona fide from autofluorescence will obscure specific immunoreactivity. That is not an issue with DAB-based IHC. While DAB addresses the issue of autofluorescence, the use of the usual short incubations will often result in the absence of staining, as shown in Figure 1B. In contrast, the use of long incubations as described in **Table 1** will provide easy detection of nerve fibers in bone, as shown in **Figure 2C**, in which a

clear bundle of CGRP-immunoreactive (-ir) fibers in the rat tibial subchondral bone can be observed.

The application of the optimized protocol for each condition (see Table 1) resulted in clear immunostaining in the 3 animal models of bone pathology examined, as illustrated in **Figure 3**. In addition to the subchondral bone, the synovial membrane that encapsulates the joint has been implicated in OA-related pain [2]. Here, we show CGRP-ir (**Figure 3A**) and VMAT-2-ir (**Figure 3B**) in the synovium of the MIA model of OA in the rat ankle joint. In the OVX post-menopausal model of osteoporosis, the periosteum (**Figure 3C**), and the bone marrow (**Figure 3D**) are areas of interest to study neural sensitization; in both cases, we detected increased density of CGRP-ir fibers compared to sham controls (data not shown). In the open osteotomy fracture model, we detected CGRP-ir fibers in marrow (**Figure 3E**) as well as innervation in remodelled bone post-fracture (**Figure 3F**). The ability to identify innervation in subchondral bone and remodelled bone will enable increased understanding of bone-nerve interactions as convincing detection has previously been rare in the literature.

2.5 FIGURES AND TABLES

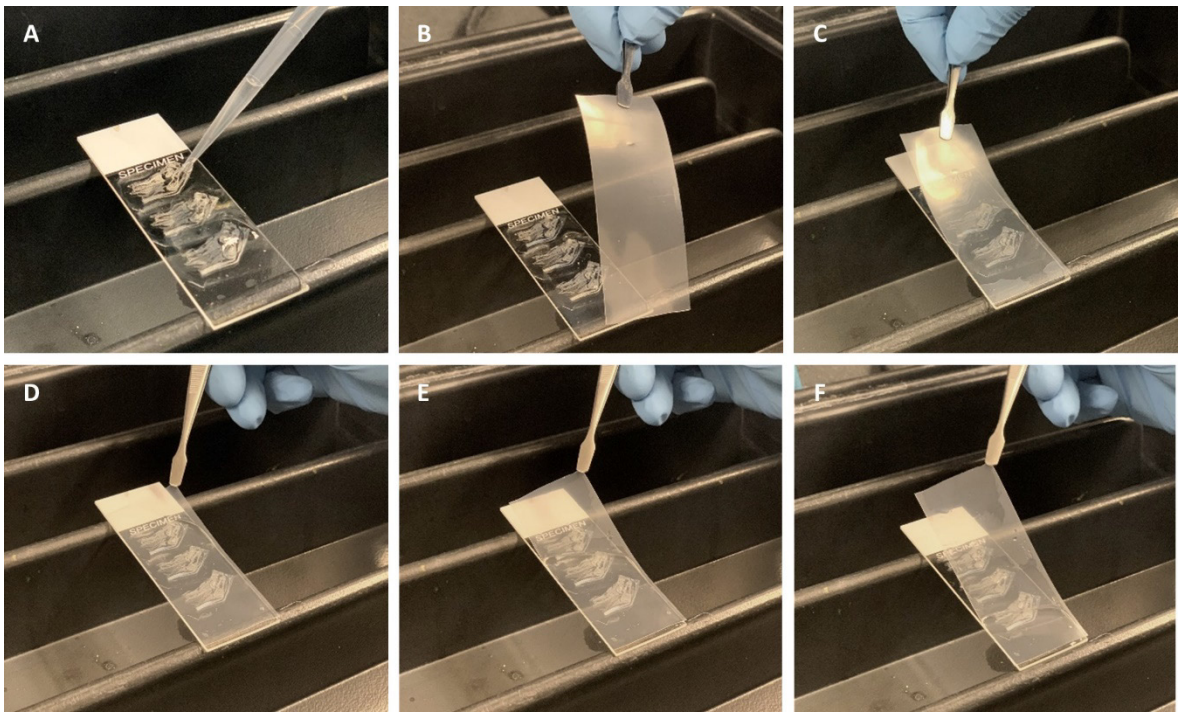

Chapter 2 Figure 1: Applying plastic coverslips for avidin-biotin complex, primary, and secondary antibody incubation.

A) A total of 150 µl of solution is applied to the slide. B, C) The plastic coverslip is applied from the bottom of the slide. Slowly press against the sections, making sure the liquid is spreading across the slide, and that no air bubbles are present on the sections. D – F) Once the incubation is complete, remove the plastic coverslip from the top of the slide. Slowly lift the plastic coverslip so that sections do not detach from the slide.

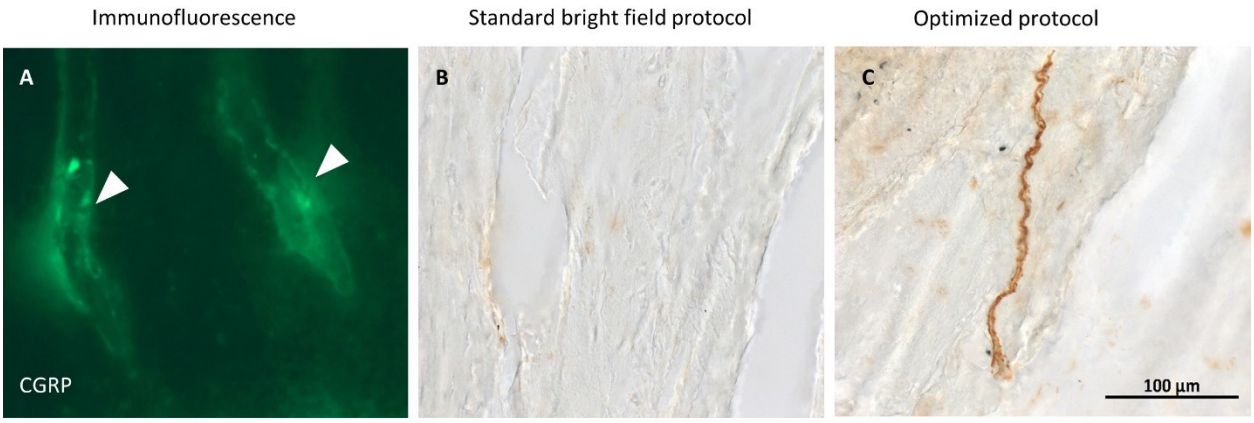

Chapter 2 Figure 2: Comparison on traditional immunofluorescence and immunohistochemistry to the optimized protocol.

Images were obtained using an anti-CGRP antibody in rat tibial subchondral bone in the MIA model of OA in the rat ankle joint 5 weeks post MIA injection. A) Illustration of challenges associated with autofluorescence and antibody penetration in an immunofluorescence representative image labelled with anti-CGRP antibody and a secondary antibody conjugated to Alexa 488; autofluorescence and trapping of fluorochrome to the blood vessel walls is observed (arrows), simulating nerve fibers. B, C) Images of DAB-IHC of a rat tibial subchondral bone labelled with anti-CGRP antibody. The image in B was acquired following the traditional IHC protocol, while C was acquired after optimization (see Table 1.).

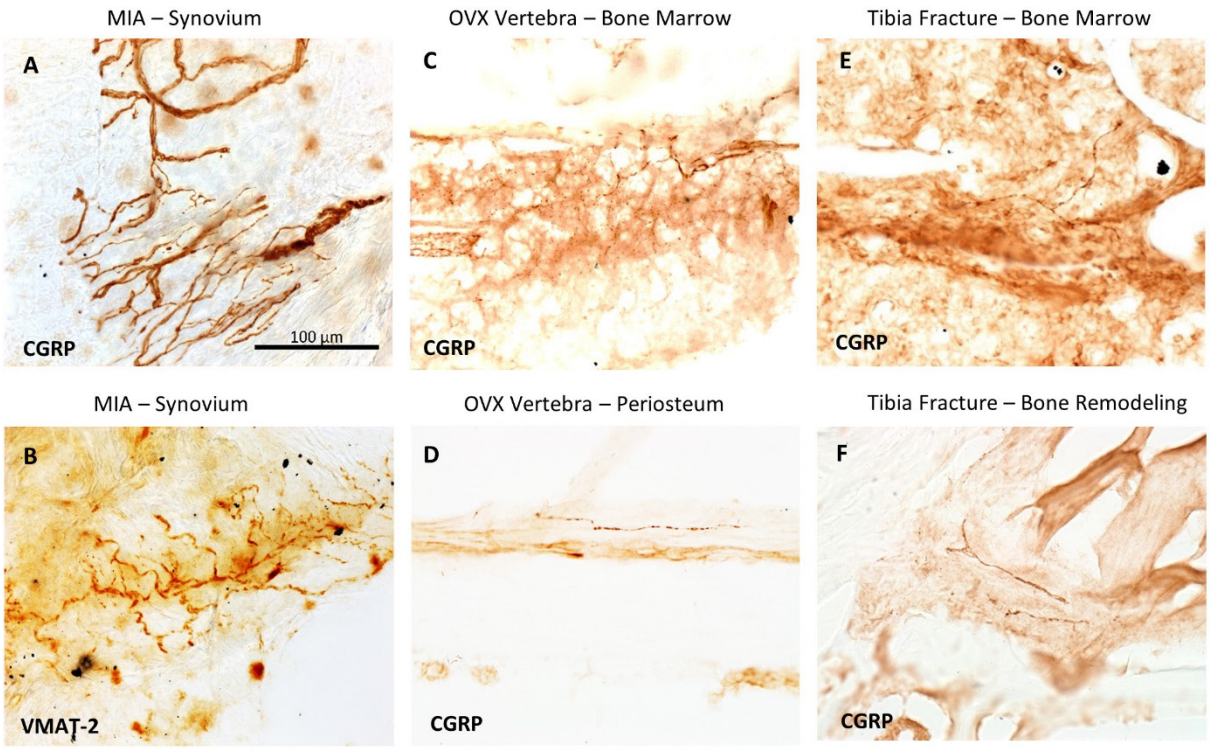

Chapter 2 Figure 3: Representative images of DAB-IHC staining optimization.

(A, B) show innervation of the synovium that encapsulates the tibio-talar compartment of the rat ankle joint at 5 weeks post MIA injection, labeled with anti-CGRP and anti-VMAT-2 antibodies, respectively. (C, D) show bone marrow (C) and periosteum (D) from OVX mice 8 weeks post-surgery, labelled with anti-CGRP antibody. (E, F) show bone marrow and remodelled bone at the fracture site of mice 5 weeks after an open osteotomy.

IHC Parameter	Traditional IHC	Subchondral Bone and Synovium	Cortical Bone	Bone Marrow	Bone Marrow and Periosteum
Animal model	All models	MIA	Fracture	Fracture	OVX
PBS+T preincubation	None	24 h	24 h	24 h	24 h
H_2O_2	30 min	30 min	30 min	30 min	2 X 30 min
Blocking serum	3 to 5% 0.2% to PBS+T	3% 0.3% PBS+T	3% 0.3% PBS+T	3% 0.3% PBS+T	3% 0.3% PBS+T
1˚ incubation	24h 4˚C 0.2% to PBS+T	48 h RT 0.2% PBS+T	72 h 4˚C 0.2% PBS+T	72 h 4˚C 0.2% PBS+T	48 h RT 0.2% PBS+T
2˚ incubation	2h RT	24 h 4˚C	24 h RT	24 h RT	24 h 4˚C
DAB/H_2O_2	5 – 12 min	12 min	10 min	10 min	10 min

Chapter 2 Table 1: Optimized protocols for diaminobenzidine (DAB)-based immunohistochemistry (IHC) staining in subchondral bone, synovium, bone marrow, periosteum and remodelled bone in 3 animal models of bone pathology.

PBS+T, PBS with 0.2% Triton X-100; PBS+0.3%T, PBS with 0.3% Triton X-100

2.6 DISCUSSION

The detection of nerve fibers in bone by IHC remains technically challenging and images of innervation of compact bone, in particular, are seldom published. The challenges of bone IHC directly impacts research efforts investigating innervation changes that accompany the onset and maintenance of pain in bone pathologies, as these rely on IHC for morphological assessments. Only a few groups have demonstrated consistent IHC detection of nerve fibers in their studies. In those cases, often images are shown from very young mice, where the bone is soft enough to be processed in the absence of decalcification, thus preserving antigenicity [4]. The exclusive use of young animals prevents incorporation of studies investigating pathologies that take time to develop, such as the OA and OVX models used here. In addition, joint and bone pathologies such as OA and osteoporosis are associated with aging and therefore should be studied in skeletally mature animals.

We addressed here some major challenges of bone tissue processing, which include autofluorescence and the issues related to fibre detection after decalcification. We also fully described optimized IHC protocols for various bone tissue types in animal models of osteoarthritis, osteoporosis, and tibial fracture, as these are often associated with innervation changes that need proper assessment.

Bone sectioning for IHC requires softening of the tissue which is achieved by sequestering the calcium content. The duration and degree of decalcification is affected by the chelating agent used, as well as by the size of the specimens to be decalcified. The most useful decalcifying method for IHC is treatment with ethylene diamine tetra-acetic acid (EDTA). This chelating agent has been shown to maintain tissue integrity better than alternatives, although it decalcifies hard tissues slowly [8; 12; 28]. However, it is important to monitor the decalcification degree, as failure to do

so can lead to over-decalcification, resulting to poor morphology and loss of IHC signal. Here, we optimized the decalcification time for each kind of specimen used.

Adhesion of sections from decalcified bone tissue to gelatin-subbed microscope slides is poor, making the use of a shaker during IHC incubations inadvisable. Instead, we recommend the use of plastic coverslips placed gently on top of each slide to ensure proper distribution and penetration of antibodies and other reagents such as avidin/biotin complexes in the tissue (see section 2.4).

Our study also revealed that immunofluorescence of bone marrow and bone structures that contain large blood vessels may be inadequate for morphological assessments of nerve sprouting due to high levels of unspecific labeling. Some of it represented autofluorescence, but there was clearly also a trapping of fluorochromes in the tissue. We found that with long pre-treatment of bone sections with PBS+T, and much longer than usual incubation times for both primary and secondary antibodies, DAB-based IHC was superior to immunofluorescence in detecting fibers in the bone marrow and in the harversian canals of the subchondral bone. As evidence of this superiority of this improved protocol, we detected strong CGRP-immunoreactivity in the remodelled bone at the tibial fracture site, which is has been difficult to detect in the past.

Studies from our group have used this improved methodology for nerve fiber detection in subchondral bone in animal models of inflammatory and osteoarthritis of the ankle joints to study quantitatively sensory and sympathetic nerve sprouting that contribute to pain-related behavior in these animal models [2; 20]. We hope the protocols and advice presented here will contribute to other advances in the understanding of neural mechanisms involved in bone pathologies.

2.7 CONCLUSION

The DAB-IHC protocols presented here represent a major improvement over currently used methodologies to process hard tissues to study the innervation in animal models of bone pathologies. This improved methodology could be applied in future research to investigate contributions of neural mechanisms to pain onset and maintenance in bone pathologies.

2.8 ACKNOWLEDGEMENTS

The authors wish to thank Manon St-Louis for laboratory expertise. Valerie Bourassa is a recipient of a studentship from the Louise and Alan Edwards Foundation. This work was funded by Canadian Institutes of Health Research Operating Grant MOP-136903 (to ARD), MOP-142291 to LSS, and an operating grant from the Louise and Alan Edwards Foundation to ARD. None of the authors have competing interests to disclose.

2.9 REFERENCES

[1] Al-Waeli H, Nicolau B, Stone L, Abu Nada L, Gao Q, Abdallah MN, Abdulkader E, Suzuki M, Mansour A, Al Subaie A, Tamimi F. Chronotherapy of Non-Steroidal Anti-Inflammatory Drugs May Enhance Postoperative Recovery. Scientific Reports 2020;10(1):468.

[2] Bourassa VD, Haley; Yousefpour, Noosha, Ftizcharles, Mary-Ann; Ribeiro-da-Silva, Alfredo. Pain-related behavior is associated with increased joint innervation, ipsilateral dorsal horn gliosis, and dorsal root ganglia activating transcription factor 3expression in a rat ankle joint model of osteoarthritis. Pain Reports 2020; In Press.

[3] Castañeda-Corral G, Jimenez-Andrade JM, Bloom AP, Taylor RN, Mantyh WG, Kaczmarska MJ, Ghilardi JR, Mantyh PW. The majority of myelinated and unmyelinated sensory nerve fibers that innervate bone express the tropomyosin receptor kinase A. Neuroscience 2011;178:196-207.

[4] Chartier SR, Mitchell SAT, Majuta LA, Mantyh PW. The Changing Sensory and Sympathetic Innervation of the Young, Adult and Aging Mouse Femur. Neuroscience 2018;387:178-190.

[5] Chrastil J, Sampson C, Jones KB, Higgins TF. Postoperative opioid administration inhibits bone healing in an animal model. Clin Orthop Relat Res 2013;471(12):4076-4081.

[6] Clark KGA, Davidson WM. Bone marrow lipofuscin. Journal of Clinical Pathology 1972;25(11):947.

[7] Collier CD, Hausman BS, Zulqadar SH, Din ES, Anderson JM, Akkus O, Greenfield EM. Characterization of a reproducible model of fracture healing in mice using an open femoral osteotomy. Bone Reports 2020;12:100250.

[8] Dey P. Decalcification of Bony and Hard Tissue for Histopathology Processing. In: P Dey, editor. Basic and Advanced Laboratory Techniques in Histopathology and Cytology. Singapore: Springer Singapore, 2018. pp. 35-39.

[9] Gerstenfeld LC, Cho TJ, Kon T, Aizawa T, Cruceta J, Graves BD, Einhorn TA. Impaired Intramembranous Bone Formation during Bone Repair in the Absence of Tumor Necrosis Factor-Alpha Signaling. Cells Tissues Organs 2001;169(3):285-294.

[10] Halter F. Mechanism of gastrointestinal toxicity of NSAIDs. Scand J Rheumatol Suppl 1988;73:16-21.

[11] Halvorson KG, Kubota K, Sevcik MA, Lindsay TH, Sotillo JE, Ghilardi JR, Rosol TJ, Boustany L, Shelton DL, Mantyh PW. A blocking antibody to nerve growth factor attenuates skeletal pain induced by prostate tumor cells growing in bone. Cancer Res 2005;65(20):9426-9435.

[12] Hillemann HH, Lee CH. Organic Chelating Agents for Decalcification of Bones and Teeth. Stain Technology 1953;28(6):285-287.

[13] Höhn A, Grune T. Lipofuscin: formation, effects and role of macroautophagy. Redox Biology 2013;1(1):140-144.

[14] Hulspas R, O'Gorman MRG, Wood BL, Gratama JW, Sutherland DR. Considerations for the control of background fluorescence in clinical flow cytometry. Cytometry Part B: Clinical Cytometry 2009;76B(6):355-364.

[15] Jain SK, Abreo K, Duett J, Sella M. Lipofuscin Products, Lipid Peroxides and Aluminum Accumulation in Red Blood Cells of Hemodialyzed Patients. American Journal of Nephrology 1995;15(4):306-311.

[16] Jimenez-Andrade JM, Martin CD, Koewler NJ, Freeman KT, Sullivan LJ, Halvorson KG, Barthold CM, Peters CM, Buus RJ, Ghilardi JR, Lewis JL, Kuskowski MA, Mantyh PW. Nerve growth factor sequestering therapy attenuates non-malignant skeletal pain following fracture. Pain 2007;133(1-3):183-196.

[17] Koewler NJ, Freeman KT, Buus RJ, Herrera MB, Jimenez-Andrade JM, Ghilardi JR, Peters CM, Sullivan LJ, Kuskowski MA, Lewis JL, Mantyh PW. Effects of a monoclonal antibody raised against nerve growth factor on skeletal pain and bone healing after fracture of the C57BL/6J mouse femur. J Bone Miner Res 2007;22(11):1732-1742.

[18] Li F, Yang M, Wang L, Williamson I, Tian F, Qin M, Shah PK, Sharifi BG. Autofluorescence contributes to false-positive intracellular Foxp3 staining in macrophages: A lesson learned from flow cytometry. Journal of Immunological Methods 2012;386(1):101-107.

[19] Li M, Shen Y, Wronski TJ. Time course of femoral neck osteopenia in ovariectomized rats. Bone 1997;20(1):55-61.

[20] Locke S, Yousefpour N, Mannarino M, Xing S, Yashmin F, Bourassa V, Ribeiro-da-Silva A. Peripheral and central nervous system alterations in a rat model of inflammatory arthritis. Pain 2020;161(7):1483-1496.

[21] Mach DB, Rogers SD, Sabino MC, Luger NM, Schwei MJ, Pomonis JD, Keyser CP, Clohisy DR, Adams DJ, O'Leary P, Mantyh PW. Origins of skeletal pain: sensory and sympathetic innervation of the mouse femur. Neuroscience 2002;113(1):155-166.

[22] Meling T, Harboe K, Søreide K. Incidence of traumatic long-bone fractures requiring in-hospital management: A prospective age- and gender-specific analysis of 4890 fractures. Injury 2009;40(11):1212-1219.

[23] Miller RE, Block JA, Malfait A-M. Nerve growth factor blockade for the management of osteoarthritis pain: what can we learn from clinical trials and preclinical models? Current opinion in rheumatology 2017;29(1):110-118.

[24] Pattinson KTS. Opioids and the control of respiration. BJA: British Journal of Anaesthesia 2008;100(6):747-758.

[25] Pountos I, Georgouli T, Calori GM, Giannoudis PV. Do nonsteroidal anti-inflammatory drugs affect bone healing? A critical analysis. ScientificWorldJournal 2012;2012:606404.

[26] Prentice AID. Autofluorescence of bone tissues. Journal of Clinical Pathology 1967;20(5):717.

[27] Ranjit S, Dvornikov A, Stakic M, Hong S-H, Levi M, Evans RM, Gratton E. Imaging Fibrosis and Separating Collagens using Second Harmonic Generation and Phasor Approach to Fluorescence Lifetime Imaging. Scientific Reports 2015;5(1):13378.

[28] Sanjai K, Kumarswamy J, Patil A, Papaiah L, Jayaram S, Krishnan L. Evaluation and comparison of decalcification agents on the human teeth. J Oral Maxillofac Pathol 2012;16(2):222-227.

[29] Suzuki M, Millecamps M, Naso L, Ohtori S, Mori C, Stone LS. Chronic Osteoporotic Pain in Mice: Cutaneous and Deep Musculoskeletal Pain Are Partially Independent of Bone Resorption and Differentially Sensitive to Pharmacological Interventions. J Osteoporos 2017;2017:7582716.

[30] Suzuki M, Millecamps M, Ohtori S, Mori C, Stone LS. Anti-nerve growth factor therapy attenuates cutaneous hypersensitivity and musculoskeletal discomfort in mice with osteoporosis. Pain reports 2018;3(3):e652-e652.

[31] Woolf AD, Pfleger B. Burden of major musculoskeletal conditions. Bull World Health Organ 2003;81(9):646-656.

[32] Wronski TJ, Cintrón M, Dann LM. Temporal relationship between bone loss and increased bone turnover in ovariectomized rats. Calcified Tissue International 1988;43(3):179-183.

[33] Wronski TJ, Dann LM, Horner SL. Time course of vertebral osteopenia in ovariectomized rats. Bone 1989;10(4):295-301.

[34] Zhang Y, Jordan JM. Epidemiology of Osteoarthritis. Clinics in geriatric medicine 2010;26(3):355-369.

[35] Zipfel WR, Williams RM, Christie R, Nikitin AY, Hyman BT, Webb WW. Live tissue intrinsic emission microscopy using multiphoton-excited native fluorescence and second harmonic generation. Proceedings of the National Academy of Sciences 2003;100(12):7075.

[36] Zoumi A, Yeh A, Tromberg BJ. Imaging cells and extracellular matrix in vivo by using second-harmonic generation and two-photon excited fluorescence. Proceedings of the National Academy of Sciences 2002;99(17):11014.

CONNECTING CHAPTER 2 TO CHAPTER 3

The investigation into the underlying mechanisms contributing to chronic pain in OA has revealed a complex interplay between pathological changes in the joint and nervous system dynamics. Chapter 2 presented a robust diaminobenzidine (DAB)-based immunohistochemistry (IHC) protocol optimized for the detection of nerve fibers in decalcified bone, thereby facilitating comprehensive exploration of bone innervation. Chapter 3 now seamlessly transitions to a study that builds on the insights gained from the optimized IHC protocol to unravel the intricate pain mechanisms underlying OA, shedding light on potential avenues for enhanced pain management and treatment. By merging the insights gained from advanced imaging techniques with the temporal characterization of pain-related behaviors and nerve sprouting, this collective body of research contributes to a more comprehensive grasp of OA pain etiology.

CHAPTER 3

Pain-related behavior is associated with increased joint innervation, ipsilateral dorsal horn gliosis and DRG ATF3 expression in a rat ankle joint model of osteoarthritis

Valerie Bourassa, Haley Deamond, Noosha Yousefpour, Mary-Ann Fitzcharles, Alfredo Ribeiro-da-Silva

Pain Reports 2020, Aug 25; 5 (5) : e846

3.1 ABSTRACT

3.1.1 Introduction:

Osteoarthritis (OA)-associated pain is often poorly managed, as our understanding of the underlying pain mechanisms remains limited. The known variability from patient to patient in pain control could be a consequence of a neuropathic component in OA.

3.1.2 Methods:

We used a rat Monoiodoacetate (MIA) model of the ankle joint to study the time-course of the development of pain-related behavior and pathological changes in the joint, dorsal root ganglia (DRG), and spinal cord, and to investigate drug treatments effects.

3.1.3 Results:

Mechanical hypersensitivity and loss of mobility (as assessed by treadmill) were detected from 4 weeks post-MIA. Cold allodynia was detected from 5 weeks. Using histology and x-ray microtomography, we confirmed significant cartilage and bone degeneration at 5 and 10 weeks. We detected increased nociceptive peptidergic and sympathetic fiber innervation in the subchondral bone and synovium at 5 and 10 weeks. Sympathetic blockade at 5 weeks reduced pain-related behavior. At 5 weeks, we observed, ipsilaterally only, DRG neurons expressing anti-activating transcription factor 3 (ATF3), a neuronal stress marker. In the spinal cord, there was microgliosis at 5 and 10 weeks, and astrocytosis at 10 weeks only. Inhibition of glia at 5 weeks with minocycline and fluorocitrate alleviated mechanical allodynia.

3.1.4 Conclusion:

Besides a detailed time-course of pathology in this OA model, we show evidence of contributions of the sympathetic nervous system and dorsal horn glia to pain mechanisms.

Additionally, late ATF3 expression in the DRG that coincides with these changes provides evidence in support of a neuropathic component in OA pain.

3.2 INTRODUCTION

Osteoarthritis (OA) is often classified as non-inflammatory or degenerative arthritis, in contrast to arthritis with a strong inflammatory component such as rheumatoid arthritis. However, the dichotomy between inflammatory and degenerative arthritis has become unclear as many inflammatory processes have been identified in OA [60]. Inflammation in OA affects a variety of tissues that are innervated by nociceptors; moreover cytokines and chemokines have been implicated in the signalling of these nociceptors (for review see [48]). Additionally, overexpression of NGF causes nociceptive fibers to sprout abnormally into inflamed joints [47], while anti-NGF neutralizing antibodies attenuate pain-related behavior [46]. Studies in inflammatory arthritis show that nerve fibres invade articular cartilage and sprout in the synovial membrane and adjacent bone [23; 39; 41] contributing to sensitization. In addition, different OA models have shown similar findings with innervation by Nav1.8-expressing and anti-calcitonin gene-related peptide (CGRP) positive fibers in the synovium [51; 53], as well as increased TRPV1 expression in the DRG [1]. Although it is likely that innervation changes contribute to the pain in OA, studies in OA models remain limited. Here, in our OA model, we investigated sympathetic and sensory fibre sprouting in subchondral bone and synovium.

In OA patients, there is poor correlation between radiographic changes and reported levels of pain [14]. Moreover, a subset of OA patients with successful total joint replacement surgeries report sustained levels of pain post-recovery [42]. Neuropathic pain (NP) is defined as pain following lesion or disease to the somatosensory nervous system (IASP). Indeed, the persistence

of pain in some OA patients, after removal of the diseased joint, suggests that this disease can result in neuropathy and central sensitization. In clinical cases of NP, gabapentin is commonly used as a treatment [68]. Interestingly, gabapentin is analgesic in some OA patients as well, supporting a possible NP-like component [17].

In animal models, NP is studied by inducing peripheral nerve damage, often of the sciatic nerve [31]. This consistently results in hypersensitivity that is accompanied by central changes, such as microgliosis, and activating transcription factor 3 (ATF3) expression in the DRG. Microgliosis, for instance, has also been observed in OA models [37; 57].

In this study, we provide an integrated time-course of peripheral and central pathological changes and correlate them with pain-related behavior in an OA model. Those changes include degradation of cartilage, degeneration of bone, sensory and sympathetic fiber innervation changes in the joint, glial activation in the dorsal horn and, at late time point, ATF3 expression in the DRG. To do this, we used the MIA model in the rat ankle joint, which we characterize for the first time here. The ankle receives most of its nerve supply from the sciatic nerve, which is lesioned in the most commonly used NP models. This facilitates the evaluation of possible mechanisms of OA pain that are also associated with NP. Subsequently, we used pharmacology to suppress components we believe contribute to pain in OA, including sympathetic sprouting, and glial changes.

3.3 METHODS

3.3.1 Induction of OA:

The entire experimental design followed the Care and Use of Experimental Animals of the Canadian Council on Animal Care guidelines. All animals were housed in pairs with soft bedding, food and water ad libitum, on a 12- hour light/dark cycle.

A total of 126 Sprague Dawley male rats (Charles Rivers Laboratories) weighing 175-200 g at the beginning of the study, with 6 animals per group, were anesthetized with 5 % isoflurane in O2, and given by intraarticular injection in the tibio-talar joint a single dose of 0.8, 1.6, 2.4 mg of MIA (Sigma) or saline, in a volume of 40 µL. Doses were selected based on a literature search of MIA concentrations administered in the more commonly used knee-joint model of OA [52].

3.3.2 Behavioral Assessments:

Pain-related behavior was assessed weekly by a blinded experimenter, while treadmill was assessed once each two weeks. Prior to each behavioral experiment, animals were accustomed to the testing environment by being placed in the corresponding cages for at least 30 minutes prior to testing. The baseline reaction values were measured in the morning of the MIA injections.

3.3.2.1 Mechanical Hypersensitivity:

Using a series of calibrated filaments (Stoelting, USA), the von Frey test was used to assess mechanical hypersensitivity. Animals were placed in individual cages on a mesh wire surface. Filaments were applied using the up/down method [5; 15] on the hind paw both ipsilaterally and contralaterally. The 50% withdrawal thresholds were calculated as previously described [55].

3.3.2.2 Cold Allodynia:

The acetone drop method was used to assess cold pain behavior on the plantar region of the hind paw [7]. Pain responses were graded as previously described [18].

3.3.2.3 Heat Hyperalgesia:

The Hargreaves's apparatus (UGO Basile) was used to measure latency of paw withdrawal to a heat stimulus, with a cut-off of 20 seconds of heat application, as previously described [41].

3.3.2.4 Changes associated with movement:

Six animals injected with a dose of 2.4 mg MIA and six saline-injected rats underwent a treadmill-test (Columbus Instrument Exer 3/6) each two weeks only (to avoid a training effect [35]). This was performed on a separate cohort of animals to avoid confounds with the other behavior assays. Each rat warmed-up at a speed of 15 m/min with no incline for 10 minutes. The speed was reduced to 10 m/min and increased by 5 m/min every 5 minutes until the rat was unable or unwilling to maintain pace with the treadmill belt. Prior to week 0, animals received a 5-day daily habituation run with the electric grid as a learning incentive. During experimental days manual encouragements were used instead (manually touching/flicking the tail).

3.3.3 Histopathology:

Rats were perfused intracardially with histological fixatives at 1, 2, 5, and 10 weeks post-MIA for subsequent immunohistochemical processing. Before sectioning, ankle joints were decalcified (see supplementary data for details).

3.3.3.1 Cartilage Degeneration Quantification:

Cartilage degeneration was visualized in the tibial articular surface of the tibio-talar compartment using the Safranin O (Sigma) and Fast Green (Fisher Scientific) staining method. A

Hematoxylin and Eosin (Sigma) staining was also used to better visualize chondrocytes. The timeline of cartilage degeneration was quantified by measuring the thickness of cartilage matrix stained by Safranin O with lacunae containing chondrocytes. Using the ImageJ tracing tool, we traced a line over the thickest region of safranin-stained chondrocytes, perpendicular to the surface of the tibia (4 images per animal, n = 6).

3.3.3.2 Bone Degeneration:

Ankle joints from the 5- and 10-weeks post MIA injection time-points were sent to the McGill University Bone Center for microtomography (µCT; using a SkyScan 1072) and x-ray imaging (using a Kubtec Xpert 80 apparatus), as well as for bone mineral density (BMD; using GE Lunar PIXImus) measurements (n=4). Ankle joints were then qualitatively evaluated for signs of degeneration.

3.3.3.3 Immunohistochemistry and Quantification:

After decalcification, joints were stained with rabbit anti-CGRP antibody (Sigma #C8198) or goat anti-vesicular monoamine transporter-2 (VMAT-2) antibody (abm #Y213391). Joint sections were incubated in goat anti-rabbit IgG biotinylated antibody (Vector #BA-1000; 1:400) and donkey anti-goat IgG biotinylated antibody (Jackson #705-066-147; 1:250) for DAB immunohistochemistry then imaged. CGRP and VMAT-2 fiber innervation densities were measured by a blinded experimenter using the ImageJ software tracing tool. Fibers measuring less than 5 µm-long were excluded from analysis to ensure the inclusion of genuine fibers only. See supplementary data for more detailed protocol.

L4 and L5 DRGs and lumbar spinal cord were sectioned and stained with rabbit monoclonal anti-ATF3 antibody (Abcam #ab207434; 1:500), or rabbit anti-ionized calcium binding adaptor molecule 1 (Iba1; Wako # 019-19741; 1:1000) and mouse anti-glial fibrillary

acidic protein (GFAP; Cell Signaling # 3670S; 1:1000). DRG and spinal cord sections were subsequently incubated with fluorochrome-labeled secondary antibodies (1:800, Invitrogen). DRG slides were incubated with red Nissl (Neurotrace 530/615 N-21482; 1:100). For the DRGs, total number of red Nissl-positive and ATF3-positive cells were counted and averaged for each animal (n = 4). For the spinal cords, extended depth of focus images were analyzed by a blinded experimenter and Iba1+ and GFAP+ cell counts were performed and dimensional ratios (Iba1+ only) were obtained using an ImageJ macro as previously described [27]. See supplementary data for a detailed protocol.

3.3.4 Pharmacology:

3.3.4.1 Sympathetic block:

Vehicle (saline) or 30 mg/kg guanethidine sulfate (Santa Cruz Biotechnology) were administered intraperitoneally (i.p.) twice with a 24 h interval [71] at 5 weeks post MIA injection. The von Frey and acetone tests described above were administered weekly up to 5-weeks post MIA injection (pre-drug) and 4 hours after the second dose of guanethidine. Animals were divided into the following groups: sham + vehicle, sham + guanethidine, MIA + vehicle, and MIA + guanethidine.

3.3.4.2 Glial inhibitors:

Vehicle (10µl saline), minocycline (100µg in 10µl saline; Sigma-Aldrich #13614-98-7) or fluorocitrate (1.0 nmol in 10 µl 2M HCl in saline; Sigma-Aldrich #100929-81-5) were administered intrathecally (i.t.) in the lumbar region of the spinal cord twice with a 24 hour interval at 5 weeks post-MIA injection. Von Frey and acetone tests (describe above) were administered weekly up to 5 weeks post MIA injection (pre-drug) and 4 hours after the second dose. Animals

were divided in the following groups: MIA + fluoro, MIA + mino, MIA + veh. A second blinded experimenter performed the behavior assessments.

3.3.5 Statistical analysis:

All behavioral measurements were analyzed using repeated measures two-way ANOVA. Time-courses of changes in innervation, microgliosis, astrocytosis and microglia morphology were assessed using two-way ANOVA. Singular comparisons were analyzed with a one-tailed Student t-test. For multiple comparisons tests, we employed the Bonferroni correction.

3.4 RESULTS

3.4.1 Pain-related behavior changes and establishment of the effective MIA dose:

Twenty four Sprague-Dawley rats that were saline-injected, or received either 0.8, 1.6 or 2.4 mg of MIA were tested weekly for 10 weeks to establish dose of MIA for subsequent experiments. Compared to saline-injected controls, mechanical hypersensitivity became significant at 7-weeks, 5-weeks, or 4-weeks, when a dose of 0.8 mg, 1.6mg, and 2.4mg of MIA was used, respectively (Figure 1A). It should be noted that with doses of 1.6 and 2.4 mg MIA, from 6 weeks onwards, mechanical hypersensitivity was at the maximum (Figure 1A). Cold allodynia, assessed with acetone was consistently detected only with 1.6 and 2.4 mg MIA doses, appearing at 4 and 5 weeks, respectively (Figure 1C). No heat hyperalgesia was detected by the Hargreaves' test in the ipsilateral paw at any time point with any dose (Figure 1E). Additionally, none of the behavior tests revealed contralateral effects (Figure 1B, D, F). The 2.4 mg dose of MIA resulted in consistent cartilage degeneration across animals (data not shown). Based on this observation and the behavioral outcomes, the 2.4 mg MIA was selected for all subsequent analyses.

3.4.2 Joint function deterioration:

We observed that 2.4mg MIA-injected animals spent significantly less time on the treadmill starting at 4 weeks post-injection compared to controls (Figure 2).

3.4.3 Histopathological changes:

The time-course of histopathological changes was assessed using a Safranin (cartilage) and Fast Green (contrast) staining (Figure 3A-E). Joints from the control group maintained an intact articular surface, with perfect cartilage integrity, as shown by the intense red Safranin staining (Figure 3A). MIA-injected animals displayed progressive loss of cartilage matrix staining, as well as considerable cartilage thinning (Figure 3B, C, D). Complete loss of the articular cartilage was observed by week 10, leaving the subchondral bone exposed (Figure 3E). These observations were confirmed by quantifying healthy cartilage thickness over time. A decrease in intact cartilage thickness is observed between SHAM and the 1 week post-MIA timepoint. There was no statistical difference in cartilage thickness between weeks 1 and 2. However, at week 5, we observed a significant decrease in intact cartilage thickness, followed by total delamination at week 10 (Figure 3K). Similar findings were observed using hematoxylin and eosin staining (Figure 3F-J), which confirmed the timeline of cartilage cell death. Damage to the bone in the subarticular cartilage location (subchondral bone), such as disrupted surface integrity, was prominent at week 10, when possible signs of remodelling were seen (Figures 3E, J).

3.4.4 Radiological and bone mineral density changes:

We performed microtomography (μCT) x-ray scans with 3D visualization throughout the entire ankle joint at 5 and 10-weeks post injection. Significant signs of bone erosion and fibrillation (arrows) were observed on the talus (yellow) of MIA animals at 5- and 10-weeks post injection (Figure 4C, D, G, H). Signs of bony outgrowths, indicating osteophyte formation, on the calcaneus

bone adjacent to the ankle joint (red circle on Figure 4H) were visible in the MIA group at 10-weeks post injection. Conventional x-ray images (Figure 4I, J) revealed joint space narrowing in MIA-injected animals as compared to sham animals at 5 (Figure 4I) and 10 weeks (Figure 4J).

Bone mineral density (BMD) scans were obtained (Figure 4K, L). A small but significant reduction in BMD of the whole ankle joint was detected at 10-weeks post injection in MIA compared to control animals (Figure 4L).

3.4.5 Changes in sensory and sympathetic innervation of joints:

Peptidergic nociceptive fibre as well in sympathetic fibre innervation was assessed in the tibial subchondral bone of the tibio-talar junction (Figure 5A, B, E, F) and in synovial membrane connecting the tibia and talus (Figure 5C, D, G, H). We used DAB-based immunohistochemistry with antibodies against the peptidergic nociceptive fiber marker CGRP (Figure 5A, B, C, D) and sympathetic fiber marker VMAT-2 (Figure 5E, F, G, H). Figure 5A-F shows representative images of innervation patterns at 10 weeks post-MIA or sham injection. We observed that in the OA-associated subchondral bone, VMAT-2 and CGRP nerve fibers sprouted outside the harversian canals (arrows; Figure 5B, F). Our quantification revealed major innervation increases in the subchondral bone and synovial membrane by both sensory and sympathetic fibers at 5 weeks and 10 weeks (Figure 5G, H, I, J). The increase of innervation was particularly marked for the CGRP-immunopositive fibres in the subchondral bone at 5- and 10-weeks post MIA (Figure 5I). No innervation changes were found at 1- and 2-weeks post-MIA injection.

To further investigate the contribution of the sympathetic nervous system to pain-related behavior, we administered guanethidine (known to produce a long term sympathetic blockade [34; 45]), at 5 weeks post MIA, a time point where we observed consistent and irreversible pain

behavior. We observed a significant alleviation of both mechanical hypersensitivity and cold allodynia following guanethidine administration (Figure 6A, C).

3.4.6 ATF3 expression in the ipsilateral DRG:

To assess neuronal stress associated with the nociception in this model of OA, ATF3 expression in the DRG was investigated. At 5-weeks post MIA injection, the contralateral DRG had no expression of ATF3 (Figure 7A, C), as in sham animals (data not shown). Interestingly, in the ipsilateral DRG we observed ATF3 expression in a small, but consistent, number of DRG neurons (Figure 7B, C).

3.4.7 Changes in microgliosis and astrogliosis in the spinal cord:

Microgliosis has previously been detected in the MIA model of OA [37; 57; 61], and in a model of destabilization of the medial meniscus (DMM) [65]. The time-course of microgliosis and astrocytosis, in this ankle MIA model, was investigated using Iba1 and GFAP immunoreactivities (Figure 8). We observed increased microglia cell counts at 5 and 10-weeks post-MIA injection (Figure 8J), and an astroglia density increase at week 10 (Figure 8K). These increases were observed in laminae II-III of the two medial thirds of the spinal dorsal horn (see Figure 8A-I), where most primary afferents innervating the ankle-joint terminate. As we expected for this OA model, the localization of the gliosis in the dorsal horn matches observations in NP models of the sciatic nerve [32].

In addition, we also observed changes in microglia morphology similar to that previously observed by our group in an inflammatory model [40], indicative of a reactive microglial phenotype. Indeed, microglia in the ipsilateral dorsal horn had a larger cell body, with retracted processes, compared to mostly ramified cells in the contralateral dorsal horn (Figure 9A, B, C, D).

These changes, as assessed by an increased dimensional ratio, were significant at 5 and 10-weeks post-MIA (Figure 9E).

To understand the contribution of microgliosis and astrocytosis to pain-related behavior, we administered the glial inhibitors minocycline and fluorocitrate at 5-weeks post MIA. Minocycline is widely accepted as a glial inhibitor, proposed to act by preventing the transition of microglia into the pro-inflammatory state [36]. However, the effect of minocycline on astrocyte function is unclear. Fluorocitrate is a metabolic toxin that is selectively taken up by astrocytes [16]. We observed a partial but significant alleviation of mechanical allodynia following both minocycline and fluorocitrate administration, with a larger effect observed with the minocycline treatment (Figure 10A). No drug effect was observed on the cold allodynia behavioral assessment (Figure 10C).

3.5 FIGURES

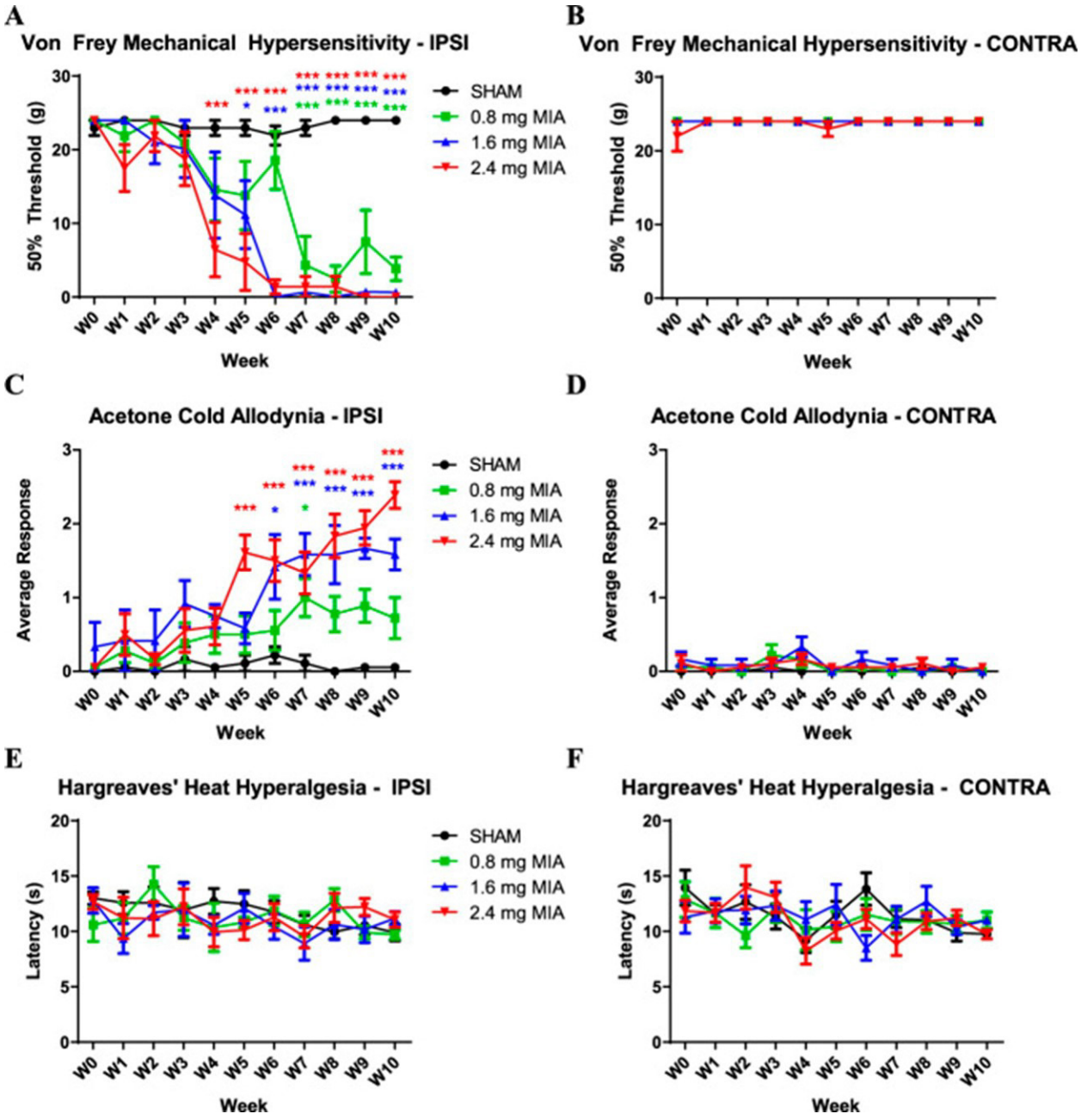

Chapter 3 Figure 1: Pain-related behavior in sham rats and animals injected with three different doses of MIA analyzed by two-way ANOVA with Bonferroni corrections.

Mechanical hypersensitivity as tested by the Von Frey fibers was first detected at 4 weeks post injection using the 2.4 mg MIA dose ($P < 0.001$), while appearing later at 5 and 7 weeks in the 1.6 ($P < 0.05$) and 0.8 mg MIA ($P < 0.001$) groups respectively (A). The acetone test yielded similar findings, with cold allodynia appearing at the earliest at 5 weeks post 2.4 mg MIA ($P < 0.001$), and at 6 weeks post-1.6 mg MIA ($P < 0.05$) (C). Pain thresholds of the 2.4 mg MIA dose were significantly lower than for the 1.6 mg dose at the 5-week time point ($P < 0.05$). No heat hyperalgesia, as tested by Hargreaves' test, was detected in the ipsilateral paw (E). For all tests, no contralateral effects were observed (B, D, F). Data from A-F were analyzed with two-way repeated measures ANOVA with Bonferroni correction ($N = 6$).

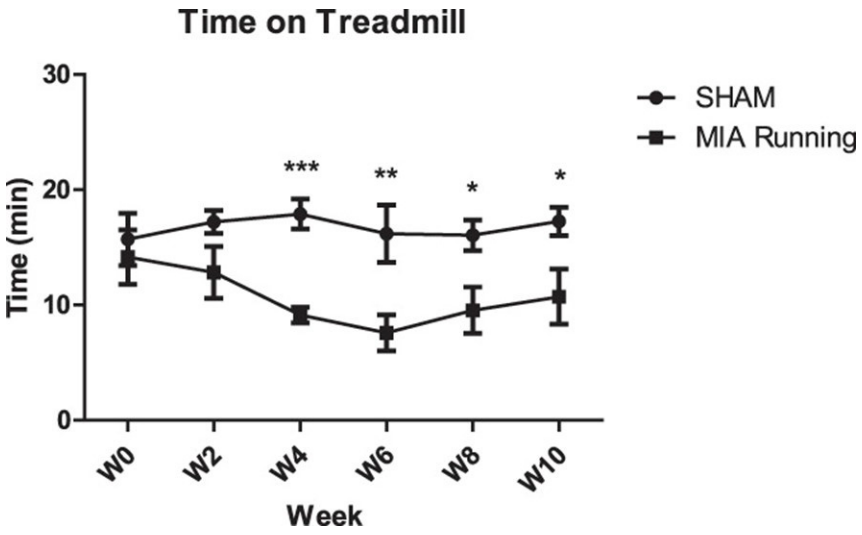

Chapter 3 Figure 2: Biweekly running in a treadmill.

Animals treated with 2.4 mg MIA had significantly reduced ability to stay on the treadmill as compared to controls starting at 4 weeks post injection ($P<0.0001$) and lasting until at least 10 weeks ($P = 0.0175$). Two-way ANOVA with Bonferroni correction for multiple comparisons. N =6

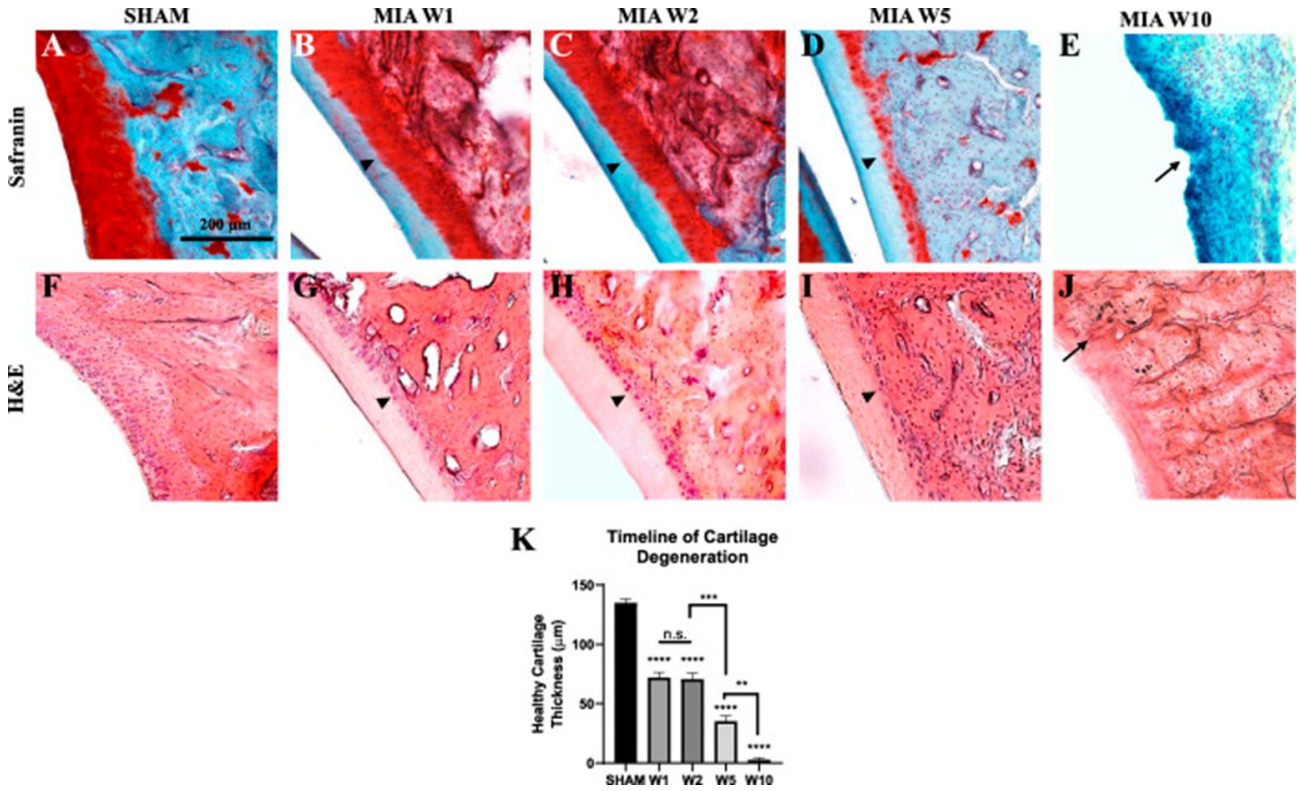

Chapter 3 Figure 3: Histopathological changes at 1, 2, 5 and 10 weeks post 2.4 mg MIA injection, using Safranin O and H&E stains.

A, F show an intact surface of healthy cartilage of SHAM animals. B – D and G – I show progressive loss of matrix staining of the outer 2/3 of the cartilage at 1, 2, and 5 weeks post injection (arrowheads). E, J show a complete loss of cartilage at 10 weeks post injection as only subchondral bone is visible (arrow). Note the disappearance of cartilage and disrupted integrity of subchondral bone (arrows) at 10 weeks post injection not detectable at earlier time points. K shows measurements of intact cartilage thickness over time using the Safranin O stain. As significant difference was observed between SHAM groups of each timepoint, they were grouped for this figure. There was a strong decrease in cartilage thickness at 1 week post MIA compared to SHAM controls. No significant difference was observed between week 1 and week 2. Another significant decrease in cartilage thickness was detected at 5 weeks post-MIA, followed by a

*complete delamination of cartilage at 10 weeks post MIA. Bars represent means ± SEM; * P < 0.05, ** P < 0.01, *** P < 0.001, **** P < 0.0001. Two-way ANOVA with Bonferroni correction for multiple comparisons N = 6.*

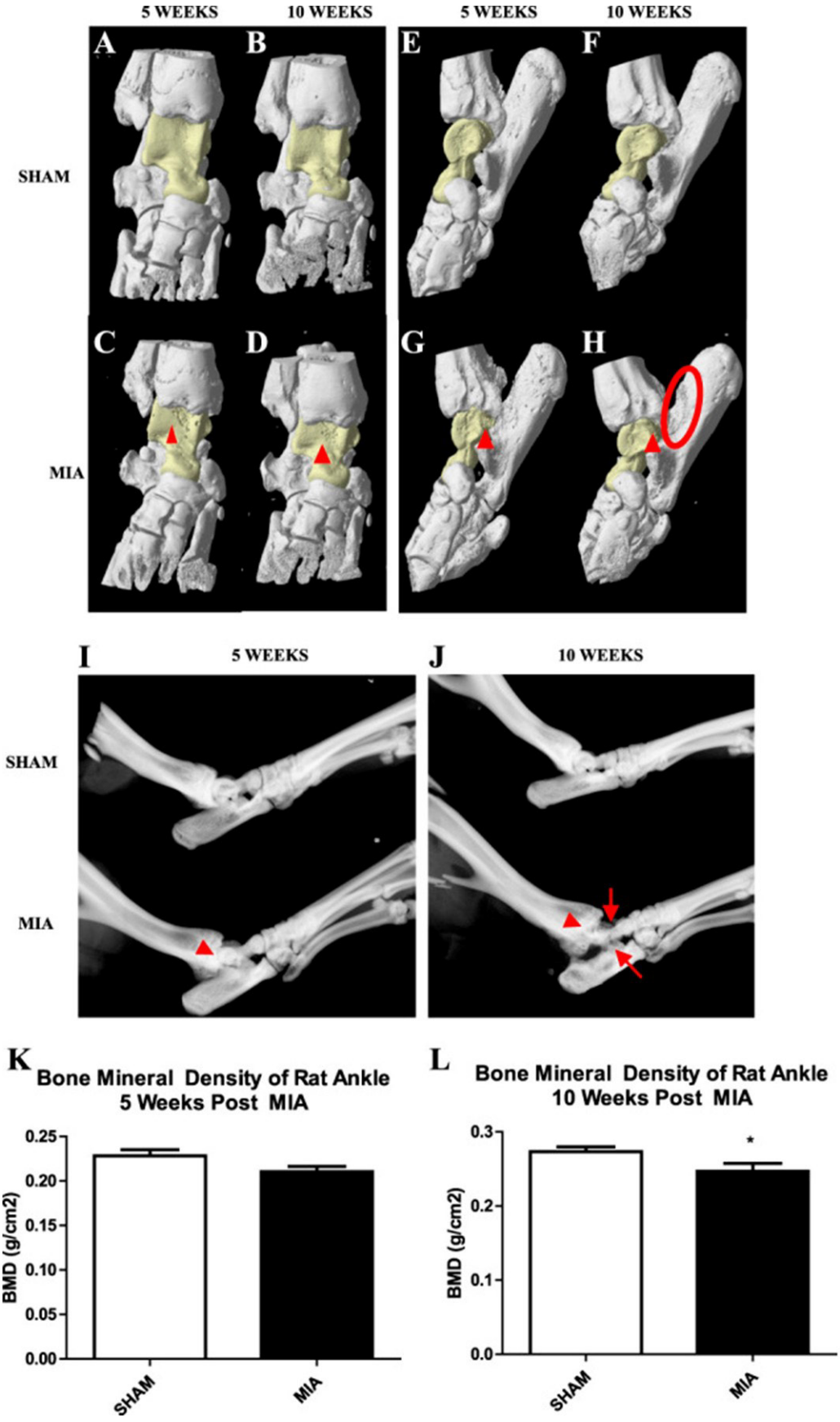
5 WEEKS
10 WEEKS
5 WEEKS
10 WEEKS
A
B
E
F
SHAM
C
D
G
H
MIA
I
5 WEEKS
J
10 WEEKS
SHAM
MIA
K
Bone Mineral Density of Rat Ankle
5 Weeks Post MIA
BMD (g/cm2)
0.25
0.20
0.15
0.10
0.05
0.00
SHAM
MIA
L
Bone Mineral Density of Rat Ankle
10 Weeks Post MIA
BMD (g/cm2)
0.3
0.2
0.1
0.0
*
SHAM
MIA

Chapter 3 Figure 4: Radiographic changes of the MIA rat ankle joint model of OA.

A-H: X-Ray imaging of the rat ankle joints at 5- and 10-weeks post MIA injection. A-H show microtomography (μCT) of SHAM (A, B, E, F) and MIA-treated joints (C, D, G, H) with the talus bone highlighted in yellow. A-D show the dorsal view, and E-H show the medial view of the ankle joints. G, H illustrate irregular new bony growths on the calcaneus bone (red circle), and fibrillations on the surface of the talus (arrowhead). C, D, Ventral view of the ankle also shows surface fibrillations in the talus (arrowhead). I, J, Conventional X-ray images of a SHAM and MIA-treated joint at 5- and 10-weeks post injection. The MIA joint at 10 weeks post injection shows significant irregularities surrounding the talus and calcaneus bones (arrows). Important loss of joint space is also visible at both time points (arrowheads). K, L, One-tailed Students t-test revealed a reduction in bone mineral density of the ankle joint at 10 weeks post injection in MIA as compared to control animals (P = 0.0374). No differences were detected at the 5-week time point. N=4

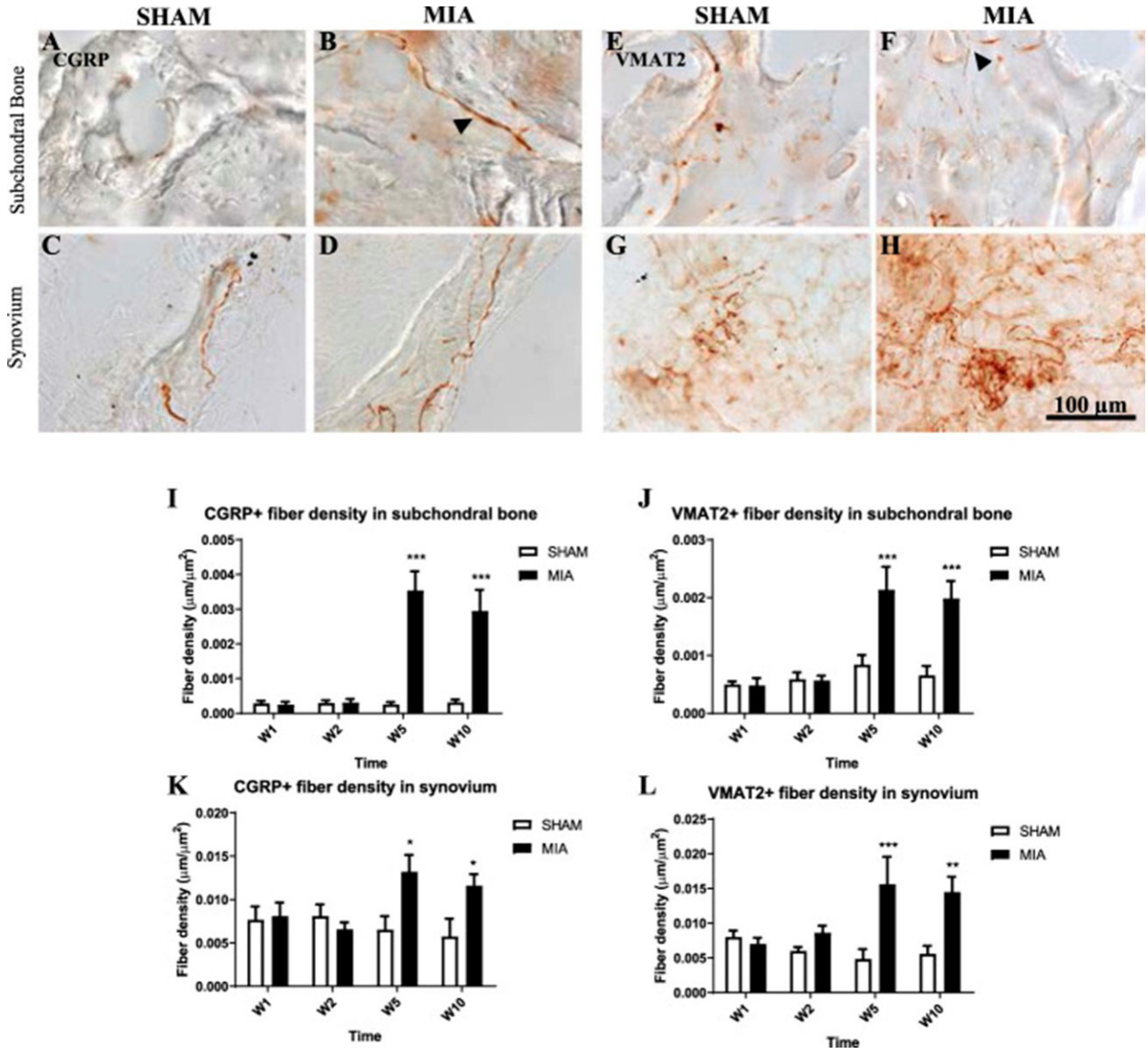

Chapter 3 Figure 5: Sensory and innervation as detected by CGRP antibody using bright field immunohistochemistry in the tibial subchondral bone (A, B) and tibio-talar synovial membrane (C, D) decalcified tissue at 1,2,5 and 10 weeks post injection of 2.4 mg MIA.

E-H, Sympathetic innervation as detected by vesicular monoamine transporter 2 (VMAT2) using DAB immunohistochemistry of the tibial subchondral bone (E, F) and tibio-talar synovial membrane (G-H) decalcified at 10 weeks post injection of 2.4 mg MIA. Anomalous fibers sprouting outside of harversian canals are shows in B and F (arrows). Quantification of fiber densities

revealed significant increase in innervation of CGRP+ fibers of the subchondral bone ($P<0.001$) (I), synovial membrane ($P<0.05$) (K) at 5- and 10-weeks post MIA. Increased innervation of VMAT-2+ fibers in the subchondral bone ($P<0.001$) (J) and synovium ($P<0.001$ at 5 weeks, $P<0.005$ at 10 weeks) (L) at 5- and 10-weeks post MIA injection. No significant changes were observed at 1- and 2-weeks post MIA. Data were analyzed with two-way ANOVA with Bonferroni correction. $N = 6$.

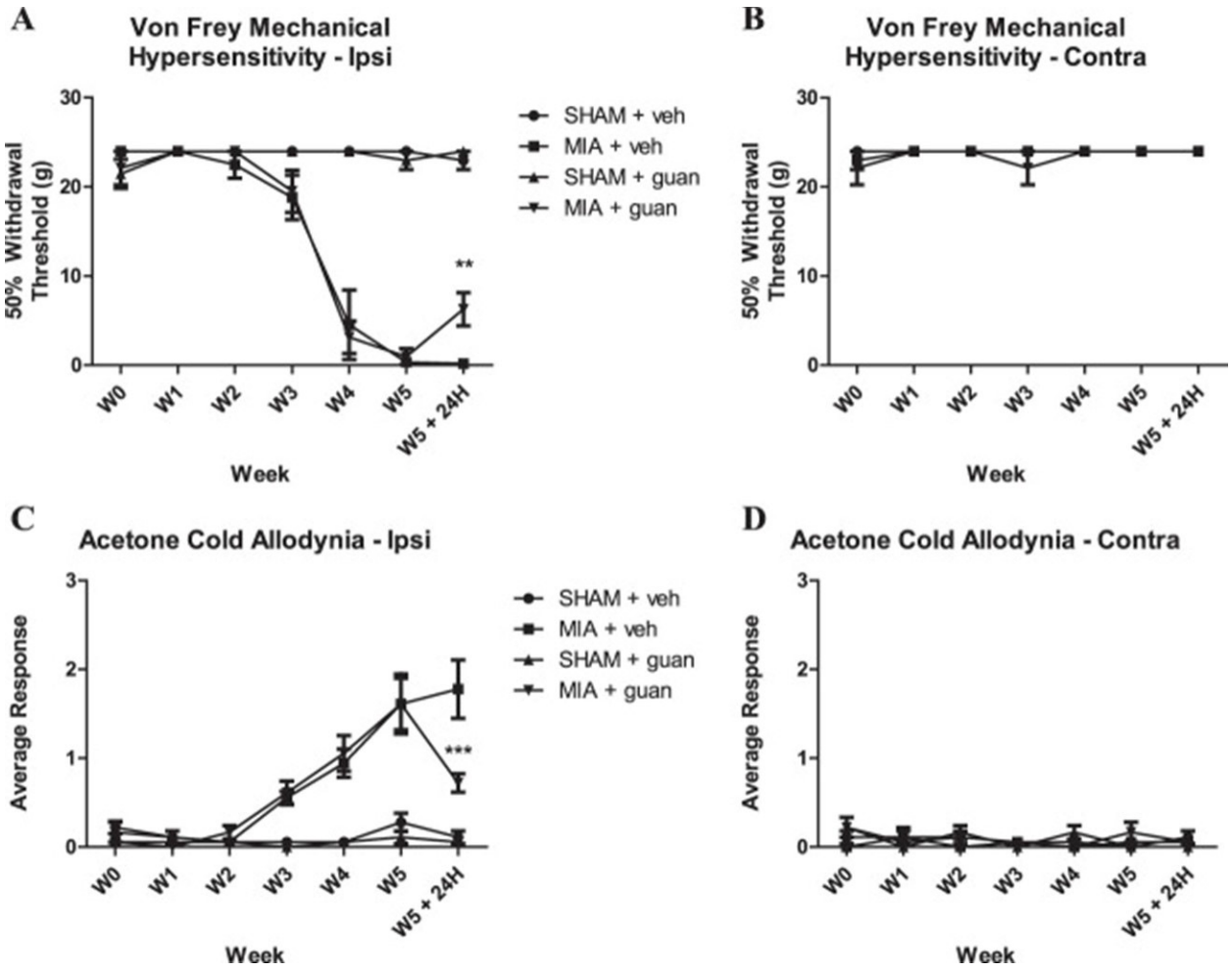

Chapter 3 Figure 6: Behavioral assessments following sympathectomy using guanethidine.

Note partial alleviation of mechanical hypersensitivity (P<0.005) (von Frey hairs) (A) and cold allodynia (P<0.001) (C) in MIA animals at the 5-week time point, 24 hours following the second injection of guanethidine i.p. Contralateral behavior data are shown in B and C. Data were analyzed with two-way repeated measures ANOVA with Bonferroni correction. Bars represent means ± SEM. N = 6.

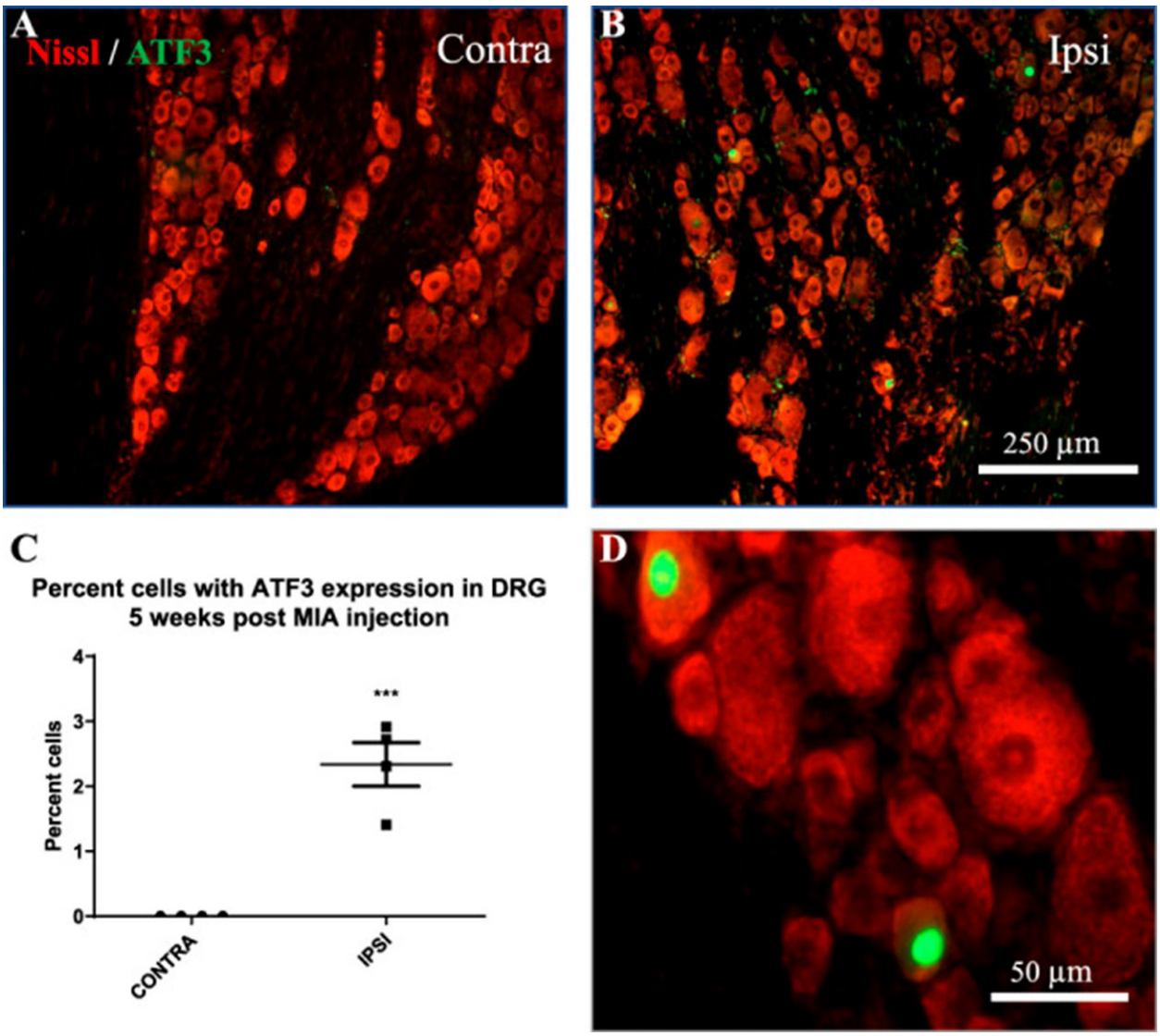

Chapter 3 Figure 7: Activating transcription factor 3 (ATF3) expression in lumbar DRG 5 weeks post MIA injection.

*Low magnification images show no expression of ATF3 in the contralateral DRG (A), and increased expression in the ipsilateral DRG (B), quantified in C. D represents a higher magnification image clearly showing localization of the ATF3 signal in the nucleus. Data were analyzed a one-tailed unpaired t-test. Bars represent means ± SEM; *** $P < 0.001$. $N = 4$.*

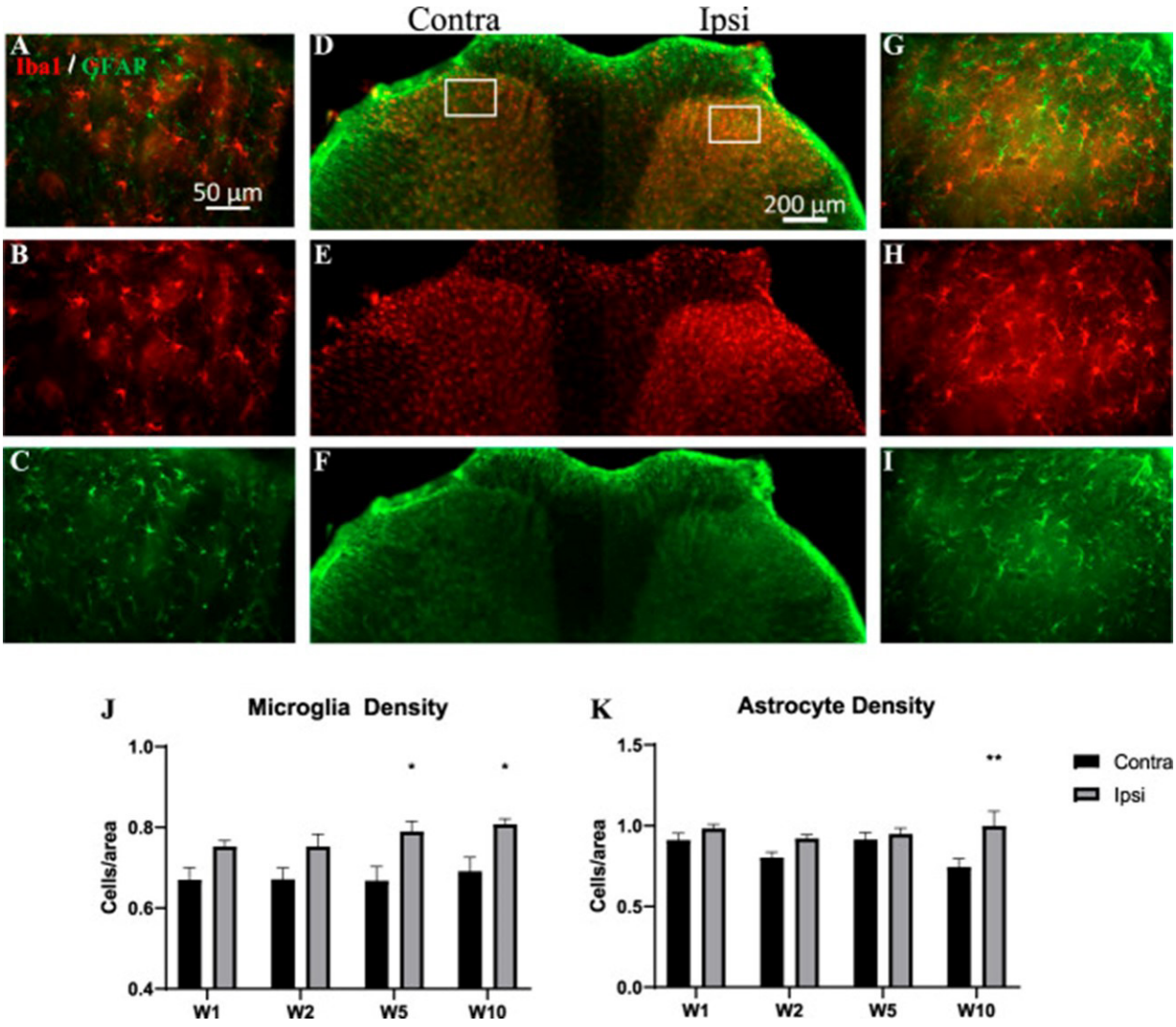

Chapter 3 Figure 8: Microgliosis (Iba1) and astrocytosis (GFAP) in the laminae II-III of the spinal dorsal horn.

*A-I, Representative fluorescence micrographs showing increased immunoreactivity of Iba1 and GFAP in ipsilateral dorsal horn of MIA-treated animals 10 weeks post injection compared to contralateral. G, E, F, are low magnification micrographs of the dorsal horn showing where images in A-C and G-I were obtained (framed areas). J, K, show a time-course of microglia and astrocyte cell densities at 1, 2, 5 and 10 weeks post injection. Data were analyzed with two-way ANOVA with Bonferroni correction. Bars represent means ± SEM; * $P < 0.05$, ** $P < 0.01$, ****

$P < 0.001$. $N = 6$. Note also the difference in morphology in the Iba1 immunoreactivity in the ipsilateral dorsal horn compared to the contralateral.

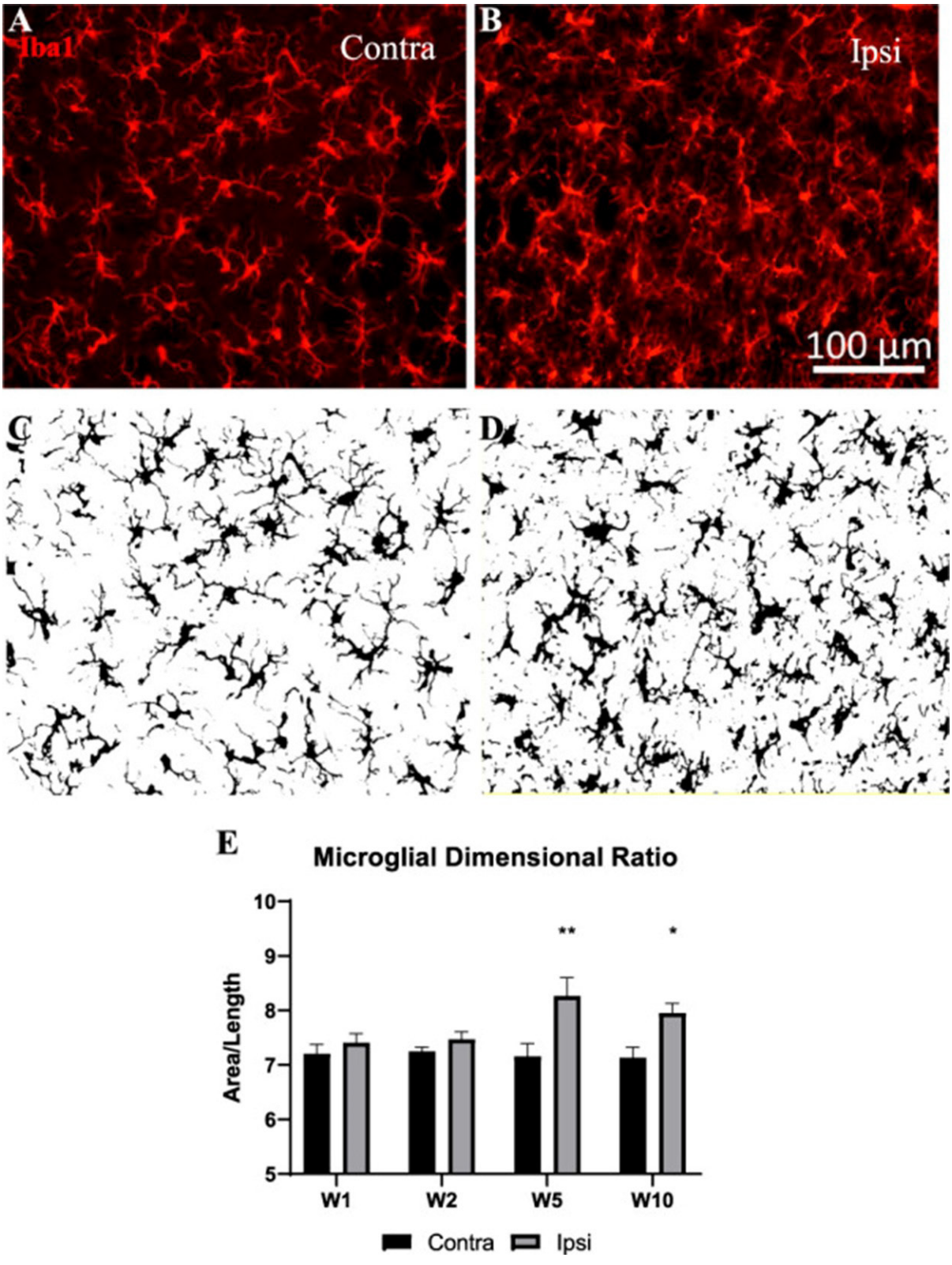

Chapter 3 Figure 9: Microglia shape changes.

*Microglia morphology was assessed by Iba1 immunoreactivity in contralateral (A) and ipsilateral (B) laminae II-III (shown images from lamina II at the 10-week timepoint). Binary images (C, D) were skeletonized and the dimensional ratio (length of cells/area of cells) calculated by the software. E, shows increased dimensional ratio in the ipsilateral dorsal horn of MIA-treated animals at 5- and 10-weeks post injection. Data were analyzed with two-way ANOVA with Bonferroni correction. Bars represent means ± SEM; * $P < 0.05$, ** $P < 0.01$, *** $P < 0.001$. $N = 6$.*

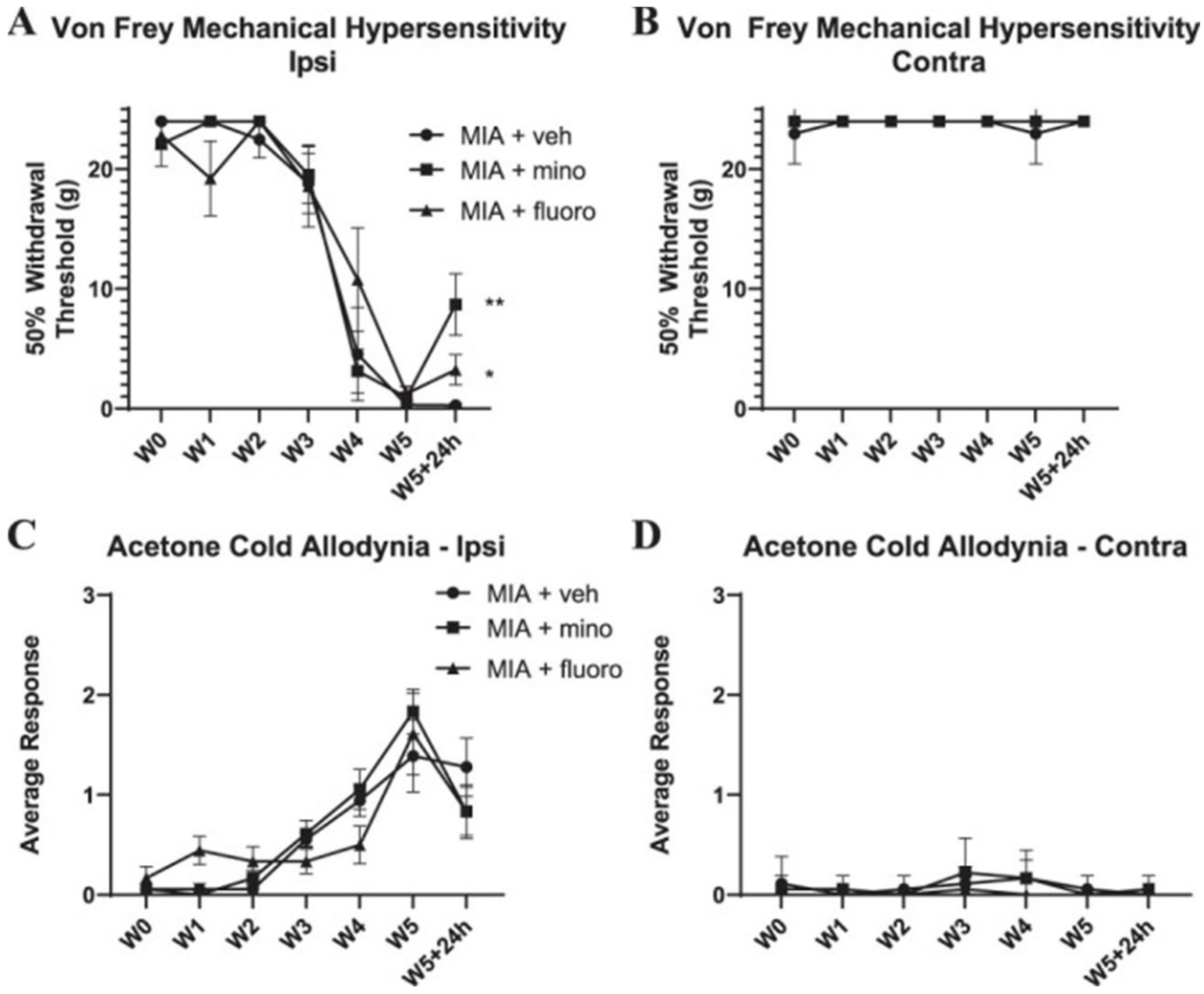

Chapter 3 Figure 10: Behavioral assessments following glial inhibitors minocycline and fluorocitrate.

Note partial alleviation of mechanical hypersensitivity (A) by minocycline ($P < 0.01$) and fluorocitrate ($P < 0.05$) at the 5-week time point, 24 hours following the second injection of the glial inhibitor. No significant alleviation of cold allodynia was observed (C). B, D show no contralateral effect. Data were analyzed with two-way repeated measures ANOVA with Bonferroni correction. Bars represent means ± SEM. N = 6

3.6 DISCUSSION

We provide an integrated time-course of the development of pain-related behavior and pathological changes in the joint and spinal cord of this OA model of the rat ankle joint. We described the time-course of nociceptive sensory and sympathetic innervation changes and found significant innervation increases at time points in which there was marked mechanical and cold allodynia. Pain-related behavior was also associated with ATF3 expression in the DRG as well as microglia and astrocyte changes in the dorsal horn. Using pharmacology, we supressed the function of putative contributors to pain in OA, including sympathetic fibers, microglia, and astrocytes. The changes described above include the presence of primary afferent stress and central changes - known descriptors in NP.

3.6.1 Characterization of the ankle joint MIA model

In the literature, most rodent models of OA involve the knee-joint, given the high prevalence of knee OA in the clinic. With our ankle-joint model, direct comparisons to changes in the spinal cord in established NP models can be made, as similar nerves are affected. The ankle joint is mostly supplied by branches from the sciatic nerve (tibial, sural, deep peroneal) and saphenous nerves [21], with innervation from the spinal cord at the level of lower lumbar regions (L3-L6). The knee joint is supplied by branches from the femoral, tibial, common peroneal, and obturator nerves [20], which have different distributions at the spinal cord (L2-L4). Our laboratory has been using this OA model as well as an inflammatory arthritis model of the ankle joint to investigate NP-like features of arthritis in the spinal cord. In fact, the localization of the gliosis observed in this model matched observations in several NP models involving injury to the sciatic nerve [32]. Additionally, we were able to detect cold allodynia, which is seldom reported in knee-joint models although it is clinically relevant [49; 70]. Moreover, loss of mobility was detected

which aligns with clinical investigations that show a strong correlation between pain and functional limitations of the joint in patients with OA [25; 50; 69].

3.6.2 Morphological changes in the joint and presence of fiber sprouting

We observed signs of bone remodelling, presence of osteophytes, and joint-space narrowing in this model, which are important changes associated with OA in humans [2]. Although progressive cartilage loss, bone deformation and remodelling often result in joint pain and increased functional disability, 50% of patients with these structural changes are asymptomatic [26]. Conversely, a minority of patients with minimal, and even radiographically undetectable damage suffer from OA-related incapacitating pain [14; 33]. One possible explanation for this discrepancy is the existence of a variable neuropathic component to osteoarthritic pain.

We observed increased densities of sensory and sympathetic fibers in the synovium and subchondral bone correlating with pain-related behavior. Persistence of pain in patients with OA has been associated with increased peptidergic free nerve endings in synovial tissue, and high concentrations of the nociceptive peptide, substance P [58]. We suspect that neurogenic inflammation as well as increased NGF released by inflammatory cells [44] and chondrocytes [43], are major drivers of pain in this model.

The sympathetic sprouting that we observed reproduce abnormal innervation patterns that are observed in neuropathic-pain models. In these, we have seen close appositions of sensory and sympathetic fibers in skin of the territory affected by the lesion [24; 73]. Functional studies of sensory-sympathetic coupling show that the sympathetic effect on sensory neurons is excitatory [4; 6; 13], and the abnormal coupling suggest modulation of C-fiber excitability through norepinephrine release [72]. In fact, sympathetic blockade remains a recommended treatment for some peripheral neuropathies [28]. In agreement with our previous data using a CFA model of the

ankle joint [41], we observed that sympathectomy partially attenuated pain-related behavior. This change, however, was relatively minor suggesting that modulation of sensory fibers excitability through the sympathetic system is not sufficient for pain maintenance in this model.

3.6.3 ATF3 expression in the DRG

ATF3 expression in DRG has been described as a marker for neurons axotomized by peripheral nerve injury. ATF3 is not detectable in intact primary sensory neurons [63; 66], but is consistently upregulated in the nucleus of injured peripheral neurons [38; 66]. In addition to models of peripheral nerve injury, ATF3 has been detected in an in vitro model of diabetic neuropathy [56], in a mice rheumatoid arthritis model [8], and in a MIA model of OA in the rat knee-joint [30; 64]. However, these OA studies only detected ATF3 at early time-points, and it is unclear whether this should be interpreted as toxicity from the MIA compound, or axon degeneration caused by the underlying disease. For this reason, we studied ATF3 expression in our MIA model only at 5 weeks post-injection, a time point where we observed consistent and irreversible mechanical and cold hypersensitivity, as well as sensory fiber sprouting in the periphery. We detected a small but consistent number of ATF3-expressing neurons in the ipsilateral DRG, but not contralaterally. We believe this is a consequence of ongoing OA, which results in hyperinnervation of bone with likely repeated nerve terminal injury in exposed bone. At 5 weeks, it is unlikely that this is a consequence of MIA toxicity, although this could be a factor at earlier time points. Rather, we believe these results indicate the presence of primary afferent injury.

3.6.4 Microgliosis and astrocytosis

Recently, a surge of novel findings attribute an important role to microglia in the development and maintenance of chronic pain [59]. A common feature of the neuropathic

phenotype is disruption of excitatory and inhibitory transmission in the dorsal horn [11; 67]. Activated microglia drive this disinhibition by releasing BDNF, which through its trkB receptor causes the downregulation of the potassium-chloride co-transporter KCC2 in spinal neurons [10]. In this study, we observed an increased density and activation of microglia starting at 5 weeks. Microglia activity suppression by minocycline partially relieved mechanical allodynia. Together these findings suggest that pro-inflammatory changes caused by microglia activation contribute to pain in OA at late stages.

Like microglia, astrocytes enter a reactive state after peripheral nerve injury [9; 22]. However, the participation of astrocytes in MIA models of OA is unclear; some groups report increased GFAP immunoreactivity [57], while others report lack of response [54]. In this study, we observed a minor but significant increase in astrocyte number at 10 weeks only, in contrast to 5 weeks for microgliosis. This data aligns with the finding that activated microglia precede the activation of astrocytes, and may in fact play a role in astrocyte reactivity [62]. Dimensional ratio of astrocyte morphology was not calculated, as GFAP immunoreactivity is not a reliable marker of cell shape. Fluorocitrate, a suppressor of astrocyte activity, partially alleviated mechanical allodynia. A larger effect may have been observed if the drug had been administered at the 10 week time-point. Therefore, our data suggests that astrocytes play a minor role in pain in OA.

3.6.5 Limitations

Ankle osteoarthritis is relatively uncommon compared to knee and hip osteoarthritis in patients [12], which is a limitation of this study. However, we believe the ankle model was the correct model to identify peripheral and central changes associated with the neuropathic-pain phenotype and correlate these changes with pain-related behavior. These findings remain relevant for the clinic: although not very frequent, some patients develop ankle arthritis, predominantly as

post-traumatic arthritis [12; 29]. Moreover, the ankle joint model of MIA presented here displays a much slower progression of changes which allows for a time-dependent analysis of the emergence of features associated with OA. This contrasts with the rat knee joint in which mechanical hypersensitivity has been detected as early as 5 days post-injection with significant cartilage damage at 20 days [17]. It is important to note that a high number of individuals suffering from OA report pain sensations comparable to those described in neuropathies [3; 19].

3.6.6 Conclusions

In this study, we investigated the time-course of changes in joint innervation, ATF3 expression in DRG, and spinal dorsal horn glia and found that their onset correlated with pain-related behaviour and extensive structural damage in the joint. We also observed that the pharmacological suppression of sympathetic fiber function, of microglia reactivity and astrocyte function led to mild ameliorations of pain-related behavior. Taken together, our data reinforced the concept that multiple factors are contributing to pain in OA, including features that are commonly described in models of NP. Our objective was to provide a multi-facetted time-course of relevant changes in OA using a robust animal model that can be directly compared to animal models of NP. We believe that further investigation of a neuropathic phenotype in OA pain has important implications for the development of therapeutic approaches.

3.7 ACKNOWLEDGMENTS

The authors wish to thank Manon St. Louis for laboratory expertise, and the McGill Bone Center for their services. Valerie Bourassa, and Noosha Yousefpour acknowledge doctoral studentships from the Louise and Alan Edwards Foundation. Haley Deamond is a recipient of studentship from the McGill University Faculty of Medicine. This work was funded by Canadian

Institutes of Health Research Operating Grant MOP-136903 and a grant from the Louise and Alan Edwards Foundation. None of the authors have competing interests to disclose.

3.8 SUPPLEMENTARY METHODS

3.8.1 Histopathology

Animals were perfused through the left cardiac ventricle with histological fixatives at 1, 2, 5, and 10 weeks post-MIA injections. For this, animals were first deeply anesthetized with an intra-peritoneal injection of Equithesin (a mixture of 12.75 mg chloral hydrate, 3 mg sodium pentobarbital, and 6.4 mg magnesium sulfate in a volume of 0.3 mL per 100 g of body weight). Following a vascular rinse (0.1% $NaNO_2$ and 0.05% $NaHCO_3$ in PBS), rats were perfused with 4 % paraformaldehyde in 0.1 M phosphate buffer (PFA), pH 7.4, with 15% (v/v) saturated picric acid, for 30 minutes. Spinal cords and L4-L6 DRGs were extracted and post-fixed for 2 hours at 4˚C in 4% PFA, then placed in 30 % sucrose in 0.1 M phosphate buffer. Spinal cords were sectioned in 50 µm-thick transverse sections in a sledge freezing microtome (Leica) and placed in PBS with 0.2% Triton X-100 (PBS+T) in wells of a 24-well tissue culture plate. DRGs were sectioned in 50 µm-thick transverse sections in a sledge freezing microtome (Leica) and collected directly on gelatin-subbed slides. Ankle joints were extracted and post-fixed in the same fixative for 4 hours at 4ºC, and subsequently placed in 10 % sucrose and 0.1 M cacodylate buffer solution overnight, at 4ºC. Ankle joints were then decalcified in 10 % ethylenediaminetetraacetic acid (EDTA) in phosphate buffered saline for 4 weeks at 4ºC on a shaker; the solution was changed twice a week. Subsequently, ankle joints were cryo-protected in 30% sucrose solution in cacodylate buffer at 4ºC overnight. To standardize sectioning of one ankle to the next, ankles were placed flat with the medial side facing down on the cryostat

(Leica) specimen holder and covered with O.C.T. compound (Tissue-Tek, Torrance, CA, USA). After freezing, the ankles were trimmed by cutting 100 µm sections until a point was reached in which the talus appeared bean-shaped. Then, serial sections, 25 µm in thickness, were collected on gelatin-subbed slides, 3 sections per slide. Slides were numbered in order of collection. For each ankle-joint staining described below, 4 sections per animal were utilized, respecting the same slide numbering for each animal. This was done in order to normalize the region of interest of the tibial articular joint across all animals.

3.8.2 Immunohistochemistry

3.8.2.1 Ankle Joints

Decalcified ankle joints were pre-incubated on-slide with excess PBS+T for 24 hours at 4°C. Slides were then incubated with 30 minutes of 50% ethanol and 30 minutes of 0.3% H_2O_2, with three 10 min washes with PBS between each incubation. Slides were left for 1 h at room temperature in 10% normal goat or donkey serum (Invitrogen) in PBS to block unspecific labeling. To detect immunoreactivity of the peptidergic and sympathetic fiber populations, the sections were then incubated for 48 hours at room temperature using a rabbit anti-calcitonin gene-related peptide (CGRP) (Sigma #C8198) antibody or goat anti-vesicular monoamine transporter-2 (VMAT-2) antibody (abm #Y213391) at dilutions of 1:2500 and 1:250, respectively. Following 3 rinses in PBS+T, sections were incubated at 4°C for 24 hours in goat anti-rabbit IgG biotinylated antibody (Vector #BA-1000; 1:400) and donkey anti-goat IgG biotinylated antibody (Jackson #705-066-147; 1:250). The A+B solution was prepared (1:400) in PBS+T (Vector Elite PK-6100) and added to the slides for incubation at room temperature for 1 hour. Diaminobenzidine (DAB) was added to the sections on-slide for 15 minutes, and then H_2O_2 was added for 8 to 10 minutes. Slides were subsequently rinsed with PBS and PBS+T,

dehydrated with ascending concentrations of ethanol, cleared with xylene, and cover-slipped with Entellan mounting medium (Electron Microscopy Sciences). Bright field micrographs of the tibial articular surface of the tibio-talar joint were obtained using a Zeiss Axioimager M2 microscope with a 40x oil-immersion objective, a high-resolution color camera and the Zeiss Zen software version 2.3.

Quantification involved six animals per time point, four sections per animal, and five images per section (of subchondral bone of tiba in the tibio-talar junction and synovium connecting the tibia and talus bones) for each time point (1, 2, 5, and 10 weeks post MIA injection).

3.8.2.2 DRGs and spinal cord

On-slide DRG sections and free-floating spinal cord sections were washed with three 10-minute incubations in PBS+T, and then blocked in 10% normal donkey serum (Invitrogen) for 1 hour at room temperature on a shaker. DRG sections were incubated in 5% NDS in PBS+T and rabbit monoclonal anti-activating transcription factor 3 (ATF3; Abcam #ab207434; 1:500) primary antibody overnight at 4 ˚C. Spinal cord sections were incubated in 5% NDS in PBS+T and rabbit anti-ionized calcium binding adaptor molecule 1 (Iba1; Wako # 019-19741; 1:1000) and mouse anti-glial fibrillary acidic protein (GFAP; Cell Signaling # 3670S; 1:1000) primary antibodies overnight at 4 ˚C. The following day, sections and slides were washed with three 10-minutes incubations in PBS+T and then incubated with fluorochrome-conjugated secondary antibodies in PBS+T for 2 hours at room temperature (donkey anti-rabbit Alexa 568 (Invitrogen Thermo Fisher Cat # A10042, 1:800) and donkey anti-mouse Alexa 488 (Invitrogen Thermo Fisher Cat # A21202, 1:800) for spinal cord sections, or donkey anti-rabbit Alexa 488 (Invitrogen Thermo Fisher Cat # A21206, 1:800) for DRG slides). Finally, sections were washed

with three10-minute incubations of PBS+T. DRG slides were incubated with red Nissl (Neurotrace 530/615 N-21482; 1:100) in PBS-T for 30 minutes on a shaker at room temperature, washed for 10 minutes in PBS-T, followed by two 10-minute washes in PBS, and cover-slipped with mounting medium (Aqua Polymount). Spinal cord sections were mounted on gelatin subbed-slides and cover-slipped with mounting medium (Aqua Polymount). Immunofluorescence micrographs were obtained using a Zeiss Axioplan 2 imaging microscope (with 10x or 20x objectives), a high-resolution camera monochrome camera and the Zeiss Zen software version 2.3.

3.8.2.3 Quantification of DRG neurons and ATF3 expression

Low magnification images (10X) used for quantification were taken to cover the whole DRG, and higher magnification images (20X) were obtained in order to show localization of the ATF3 signal in the nuclei of DGR neurons. At the lower magnification, one image per DRG section and 3 sections per animal were taken. The total number of cells stained with red Nissl and the number of ATF3-positive cells were counted and averaged for each animal (n = 4).

3.8.2.4 Quantification of glial cell density and dimensional ratio

Each image was taken so that the upper limit of the photographic field was at the junction of laminae I and II and comprised part of laminae II-III. For each time point (1, 2, 5, and 10 weeks post MIA injection), quantification involved 5-6 animals, 6 sections per animal, and 1 image for each ipsilateral and contralateral dorsal horn. Extended depth of focus images were analyzed and Iba1+ and GFAP+ cell counts were performed and dimensional ratios (Iba1+ only) were obtained using an ImageJ macro as previously describe [74].

3.8.2.5 Antibody Specificity

We assessed the quality of all staining by omitting either primary or secondary antibodies in some sections. In absence of these antibodies, we observed no labelling. Specificity of the primary antibodies used in the experiments has been well validated in the literature. Anti-ATF3 was generated in rabbit and recognizes ATF3 in rat tissue; its specificity was tested via western blot of ATF3 knock outs in HeLa and HAP1 cell lysates (data supplied by abcam). The anti-Iba1 antibody was generated in rabbit and recognizes rat tissue. Its specificity has been validated using Iba1 expression in COS-7 cells ligated with an Iba1 cDNA fragment, where untreated COS-7 and anti-sense COS-7 showed no Iba1 signal on a western blot [75]. Anti-GFAP was generated in mouse and its specificity has been tested in SNB19 cells that show strong anti-GFAP labelling, while the HeLa cells used for negative control did not (data supplied by Cell Signalling). Anti-CGRP was generated in rabbit and its specificity was previously assessed via dot-blot against rat CGRP conjugated to BSA (data supplied by Sigma), and staining has been shown to be abolished when preincubated with rat CGRP [73]. Anti-VMAT2 was generated in goat against the SYPIGEDEESESD peptide sequence and the antibody was purified by affinity chromatography and shown to recognize VMAT2 in several species (Human, Mouse, Rat, Bovine) (data supplied by abm); we tested its specificity in lab by performing a co-localization study with another sympathetic fiber marker, a dopamineβ-hydroxylase monoclonal antibody (Medimabs Canada) and co-localization was 100%.

3.9 REFERENCES

[1] Adães S, Mendonça M, Santos TN, Castro-Lopes JM, Ferreira-Gomes J, Neto FL. Intra-articular injection of collagenase in the knee of rats as an alternative model to study nociception associated with osteoarthritis. Arthritis Res Ther 2014;16(1):R10-R10.

[2] Altman RD, Gold GE. Atlas of individual radiographic features in osteoarthritis, revised. Osteoarthritis and cartilage 2007;15 Suppl A:A1-56.

[3] Blikman T, Rienstra W, van Raay J, Dijkstra B, Bulstra SK, Stevens M, van den Akker-Scheek I. Neuropathic-like symptoms and the association with joint-specific function and quality of life in patients with hip and knee osteoarthritis. PLoS One 2018;13(6):e0199165.

[4] Burchiel KJ. Spontaneous impulse generation in normal and denervated dorsal root ganglia: sensitivity to alpha-adrenergic stimulation and hypoxia. Experimental neurology 1984;85(2):257-272.

[5] Chaplan SR, Bach FW, Pogrel JW, Chung JM, Yaksh TL. Quantitative assessment of tactile allodynia in the rat paw. Journal of neuroscience methods 1994;53(1):55-63.

[6] Chen Y, Michaelis M, Janig W, Devor M. Adrenoreceptor subtype mediating sympathetic-sensory coupling in injured sensory neurons. Journal of neurophysiology 1996;76(6):3721-3730.

[7] Choi Y, Yoon YW, Na HS, Kim SH, Chung JM. Behavioral signs of ongoing pain and cold allodynia in a rat model of neuropathic pain. Pain 1994;59(3):369-376.

[8] Christianson CA, Corr M, Firestein GS, Mobargha A, Yaksh TL, Svensson CI. Characterization of the acute and persistent pain state present in K/BxN serum transfer arthritis. Pain 2010;151(2):394-403.

[9] Colburn RW, Rickman AJ, DeLeo JA. The effect of site and type of nerve injury on spinal glial activation and neuropathic pain behavior. Experimental neurology 1999;157(2):289-304.

[10] Coull JA, Beggs S, Boudreau D, Boivin D, Tsuda M, Inoue K, Gravel C, Salter MW, De Koninck Y. BDNF from microglia causes the shift in neuronal anion gradient underlying neuropathic pain. Nature 2005;438(7070):1017-1021.

[11] Coull JA, Boudreau D, Bachand K, Prescott SA, Nault F, Sík A, De Koninck P, De Koninck Y. Trans-synaptic shift in anion gradient in spinal lamina I neurons as a mechanism of neuropathic pain. Nature 2003;424(6951):938-942.

[12] Cushnaghan J, Dieppe P. Study of 500 patients with limb joint osteoarthritis. I. Analysis by age, sex, and distribution of symptomatic joint sites. Ann Rheum Dis 1991;50(1):8-13.

[13] Devor M, Janig W, Michaelis M. Modulation of activity in dorsal root ganglion neurons by sympathetic activation in nerve-injured rats. Journal of neurophysiology 1994;71(1):38-47.

[14] Dimitroulas T, Duarte RV, Behura A, Kitas GD, Raphael JH. Neuropathic pain in osteoarthritis: a review of pathophysiological mechanisms and implications for treatment. Seminars in arthritis and rheumatism 2014;44(2):145-154.

[15] Dixon WJ. Efficient analysis of experimental observations. Annual review of pharmacology and toxicology 1980;20:441-462.

[16] Erlichman JS, Leiter JC, Gourine AV. ATP, glia and central respiratory control. Respir Physiol Neurobiol 2010;173(3):305-311.

[17] Fernihough J, Gentry C, Malcangio M, Fox A, Rediske J, Pellas T, Kidd B, Bevan S, Winter J. Pain related behaviour in two models of osteoarthritis in the rat knee. Pain 2004;112(1-2):83-93.

[18] Flatters SJ, Bennett GJ. Ethosuximide reverses paclitaxel- and vincristine-induced painful peripheral neuropathy. Pain 2004;109(1-2):150-161.

[19] French HP, Smart KM, Doyle F. Prevalence of neuropathic pain in knee or hip osteoarthritis: A systematic review and meta-analysis. Semin Arthritis Rheum 2017;47(1):1-8.

[20] Gardner E. The innervation of the knee joint. The Anatomical Record 1948;101(1):109-130.

[21] Gardner E, Gray DJ. The innervation of the joints of the foot. The Anatomical Record 1968;161(2):141-148.

[22] Garrison CJ, Dougherty PM, Kajander KC, Carlton SM. Staining of glial fibrillary acidic protein (GFAP) in lumbar spinal cord increases following a sciatic nerve constriction injury. Brain research 1991;565(1):1-7.

[23] Ghilardi JR, Freeman KT, Jimenez-Andrade JM, Coughlin KA, Kaczmarska MJ, Castaneda-Corral G, Bloom AP, Kuskowski MA, Mantyh PW. Neuroplasticity of sensory and sympathetic nerve fibers in a mouse model of a painful arthritic joint. Arthritis and rheumatism 2012;64(7):2223-2232.

[24] Grelik C, Bennett GJ, Ribeiro-da-Silva A. Autonomic fibre sprouting and changes in nociceptive sensory innervation in the rat lower lip skin following chronic constriction injury. The European journal of neuroscience 2005;21(9):2475-2487.

[25] Guccione AA, Felson DT, Anderson JJ, Anthony JM, Zhang Y, Wilson PW, Kelly-Hayes M, Wolf PA, Kreger BE, Kannel WB. The effects of specific medical conditions on the functional limitations of elders in the Framingham Study. Am J Public Health 1994;84(3):351-358.

[26] Hannan MT, Felson DT, Pincus T. Analysis of the discordance between radiographic changes and knee pain in osteoarthritis of the knee. The Journal of rheumatology 2000;27(6):1513-1517.

[27] Hanzel CE, Pichet-Binette A, Pimentel LS, Iulita MF, Allard S, Ducatenzeiler A, Do Carmo S, Cuello AC. Neuronal driven pre-plaque inflammation in a transgenic rat model of Alzheimer's disease. Neurobiol Aging 2014;35(10):2249-2262.

[28] Harden RN, Oaklander AL, Burton AW, Perez RS, Richardson K, Swan M, Barthel J, Costa B, Graciosa JR, Bruehl S. Complex regional pain syndrome: practical diagnostic and treatment guidelines, 4th edition. Pain medicine (Malden, Mass) 2013;14(2):180-229.

[29] Huch K, Kuettner KE, Dieppe P. Osteoarthritis in ankle and knee joints. Seminars in Arthritis and Rheumatism 1997;26(4):667-674.

[30] Ivanavicius SP, Ball AD, Heapy CG, Westwood FR, Murray F, Read SJ. Structural pathology in a rodent model of osteoarthritis is associated with neuropathic pain: increased expression of ATF-3 and pharmacological characterisation. Pain 2007;128(3):272-282.

[31] Jaggi AS, Jain V, Singh N. Animal models of neuropathic pain. Fundamental & Clinical Pharmacology 2011;25(1):1-28.

[32] Jergová S, Čížková D. Microglial activation in different models of peripheral nerve injury of the rat. Journal of Molecular Histology 2007;38(3):245-251.

[33] Kidd BL. Osteoarthritis and joint pain. Pain 2006;123(1):6-9.

[34] Kim SH, Na HS, Sheen K, Chung JM. Effects of sympathectomy on a rat model of peripheral neuropathy. Pain 1993;55(1):85-92.

[35] Knab AM, Bowen RS, Moore-Harrison T, Trynor Hamilton A, Turner MJ, Lightfoot JT. Repeatability of Exercise Behaviors in Mice. Physiology & behavior 2009;98(4):433-440.

[36] Kobayashi K, Imagama S, Ohgomori T, Hirano K, Uchimura K, Sakamoto K, Hirakawa A, Takeuchi H, Suzumura A, Ishiguro N, Kadomatsu K. Minocycline selectively inhibits M1 polarization of microglia. Cell Death & Disease 2013;4(3):e525-e525.

[37] Lee Y, Pai M, Brederson JD, Wilcox D, Hsieh G, Jarvis MF, Bitner RS. Monosodium iodoacetate-induced joint pain is associated with increased phosphorylation of mitogen activated protein kinases in the rat spinal cord. Mol Pain 2011;7:39.

[38] Lindå H, Sköld M, Ochsmann T. Activating Transcription Factor 3, a Useful Marker for Regenerative Response after Nerve Root Injury. Frontiers in Neurology 2011;2(30).

[39] Locke S, Yousefpour N, Mannarino M, Xing S, Yashmin F, Bourassa V, Ribeiro-da-Silva A. Peripheral and central nervous system alterations in a rat model of inflammatory arthritis. Pain 2020;Articles in Press.

[40] Locke S, Yousefpour, Noosha., Bourassa, Valerie. & Ribeiro-da-Silva, Alfredo. . Spinal Inhibitory Synapse Loss in Arthritis via a Microglial-Complement Pathway. Research Poster Abstracts, Canadian Journal of Pain 2019;3.

[41] Longo G, Osikowicz M, Ribeiro-da-Silva A. Sympathetic fiber sprouting in inflamed joints and adjacent skin contributes to pain-related behavior in arthritis. The Journal of neuroscience : the official journal of the Society for Neuroscience 2013;33(24):10066-10074.

[42] Lundblad H, Kreicbergs A, Jansson KA. Prediction of persistent pain after total knee replacement for osteoarthritis. J Bone Joint Surg Br 2008;90(2):166-171.

[43] Malfait AM, Miller RJ. Emerging Targets for the Management of Osteoarthritis Pain. Current osteoporosis reports 2016;14(6):260-268.

[44] Mantyh PW, Koltzenburg M, Mendell LM, Tive L, Shelton DL. Antagonism of nerve growth factor-TrkA signaling and the relief of pain. Anesthesiology 2011;115(1):189-204.

[45] Maxwell RA, Plummer AJ, Schneider F, Povalski H, Daniel AI. Pharmacology of [2-(octahydro-1-azocinyl)-ethyl]-guanidine sulfate (Su-5864). The Journal of pharmacology and experimental therapeutics 1960;128:22-29.

[46] McMahon SB, Bennett DL, Priestley JV, Shelton DL. The biological effects of endogenous nerve growth factor on adult sensory neurons revealed by a trkA-IgG fusion molecule. Nature medicine 1995;1(8):774-780.

[47] Mendell LM, Albers KM, Davis BM. Neurotrophins, nociceptors, and pain. Microscopy research and technique 1999;45(4-5):252-261.

[48] Miller RE, Miller RJ, Malfait A-M. Osteoarthritis joint pain: the cytokine connection. Cytokine 2014;70(2):185-193.

[49] Moss P, Knight E, Wright A. Subjects with Knee Osteoarthritis Exhibit Widespread Hyperalgesia to Pressure and Cold. PLoS ONE 2016;11(1):e0147526.

[50] Mottram S, Peat G, Thomas E, Wilkie R, Croft P. Patterns of pain and mobility limitation in older people: cross-sectional findings from a population survey of 18,497 adults aged 50 years and over. Qual Life Res 2008;17(4):529-539.

[51] Murakami K, Nakagawa H, Nishimura K, Matsuo S. Changes in peptidergic fiber density in the synovium of mice with collagenase-induced acute arthritis. Can J Physiol Pharmacol 2015;93(6):435-441.

[52] Nagase H, Kumakura S, Shimada K. Establishment of a novel objective and quantitative method to assess pain-related behavior in monosodium iodoacetate-induced osteoarthritis in rat knee. Journal of pharmacological and toxicological methods 2012;65(1):29-36.

[53] Obeidat AM, Miller RE, Miller RJ, Malfait AM. The nociceptive innervation of the normal and osteoarthritic mouse knee. Osteoarthritis and Cartilage 2019;27(11):1669-1679.

[54] Ogbonna AC, Clark AK, Gentry C, Hobbs C, Malcangio M. Pain-like behaviour and spinal changes in the monosodium iodoacetate model of osteoarthritis in C57Bl/6 mice. Eur J Pain 2013;17(4):514-526.

[55] Osikowicz M, Mika J, Makuch W, Przewlocka B. Glutamate receptor ligands attenuate allodynia and hyperalgesia and potentiate morphine effects in a mouse model of neuropathic pain. Pain 2008;139(1):117-126.

[56] Peeraer E, Van Lutsenborg A, Verheyen A, De Jongh R, Nuydens R, Meert TF. Pharmacological evaluation of rat dorsal root ganglion neurons as an in vitro model for diabetic neuropathy. J Pain Res 2011;4:55-65.

[57] Sagar DR, Burston JJ, Hathway GJ, Woodhams SG, Pearson RG, Bennett AJ, Kendall DA, Scammell BE, Chapman V. The contribution of spinal glial cells to chronic pain behaviour in the monosodium iodoacetate model of osteoarthritic pain. Mol Pain 2011;7:88.

[58] Saito T, Koshino T. Distribution of neuropeptides in synovium of the knee with osteoarthritis. Clinical orthopaedics and related research 2000(376):172-182.

[59] Salter MW, Stevens B. Microglia emerge as central players in brain disease. Nature medicine 2017;23(9):1018-1027.

[60] Sokolove J, Lepus CM. Role of inflammation in the pathogenesis of osteoarthritis: latest findings and interpretations. Therapeutic advances in musculoskeletal disease 2013;5(2):77-94.

[61] Sousa-Valente J, Calvo L, Vacca V, Simeoli R, Arevalo JC, Malcangio M. Role of TrkA signalling and mast cells in the initiation of osteoarthritis pain in the monoiodoacetate model. Osteoarthritis and cartilage 2018;26(1):84-94.

[62] Svensson M, Eriksson NP, Aldskogius H. Evidence for activation of astrocytes via reactive microglial cells following hypoglossal nerve transection. J Neurosci Res 1993;35(4):373-381.

[63] Takahashi N, Kikuchi S, Dai Y, Kobayashi K, Fukuoka T, Noguchi K. Expression of auxiliary beta subunits of sodium channels in primary afferent neurons and the effect of nerve injury. Neuroscience 2003;121(2):441-450.

[64] Thakur M, Rahman W, Hobbs C, Dickenson AH, Bennett DLH. Characterisation of a peripheral neuropathic component of the rat monoiodoacetate model of osteoarthritis. PLoS One 2012;7(3):e33730-e33730.

[65] Tran PB, Miller RE, Ishihara S, Miller RJ, Malfait AM. Spinal microglial activation in a murine surgical model of knee osteoarthritis. Osteoarthritis Cartilage 2017;25(5):718-726.

[66] Tsuzuki K, Kondo E, Fukuoka T, Yi D, Tsujino H, Sakagami M, Noguchi K. Differential regulation of P2X(3) mRNA expression by peripheral nerve injury in intact and injured neurons in the rat sensory ganglia. Pain 2001;91(3):351-360.

[67] van den Pol AN, Obrietan K, Chen G. Excitatory actions of GABA after neuronal trauma. The Journal of neuroscience : the official journal of the Society for Neuroscience 1996;16(13):4283-4292.

[68] Wiffen PJ, Derry S, Bell RF, Rice AS, Tolle TR, Phillips T, Moore RA. Gabapentin for chronic neuropathic pain in adults. Cochrane Database Syst Rev 2017;6:Cd007938.

[69] Wilkie R, Peat G, Thomas E, Croft P. Factors associated with restricted mobility outside the home in community-dwelling adults ages fifty years and older with knee pain: an example of use of the International Classification of Functioning to investigate participation restriction. Arthritis and rheumatism 2007;57(8):1381-1389.

[70] Wright A, Benson HAE, Will R, Moss P. Cold Pain Threshold Identifies a Subgroup of Individuals With Knee Osteoarthritis That Present With Multimodality Hyperalgesia and Elevated Pain Levels. The Clinical Journal of Pain 2017;33(9):793-803.

[71] Xanthos DN, Coderre TJ. Sympathetic vasoconstrictor antagonism and vasodilatation relieve mechanical allodynia in rats with chronic postischemia pain. The journal of pain : official journal of the American Pain Society 2008;9(5):423-433.

[72] Xie Y, Zhang J, Petersen M, LaMotte RH. Functional changes in dorsal root ganglion cells after chronic nerve constriction in the rat. Journal of neurophysiology 1995;73(5):1811-1820.

[73] Yen LD, Bennett GJ, Ribeiro-da-Silva A. Sympathetic sprouting and changes in nociceptive sensory innervation in the glabrous skin of the rat hind paw following partial peripheral nerve injury. The Journal of comparative neurology 2006;495(6):679-690.

[74] Hanzel CE, Pichet-Binette A, Pimentel LS, Iulita MF, Allard S, Ducatenzeiler A, Do Carmo S, Cuello AC. Neuronal driven pre-plaque inflammation in a transgenic rat model of Alzheimer's disease. Neurobiol Aging 2014;35(10):2249-2262.

[75] Imai Y, Ibata I, Ito D, Ohsawa K, Kohsaka S. A Novel Geneiba1in the Major Histocompatibility Complex Class III Region Encoding an EF Hand Protein Expressed in a Monocytic Lineage. Biochemical and Biophysical Research Communications 1996;224(3):855-862.

CONNECTING CHAPTER 3 TO CHAPTER 4

Chapter 3 provided an expansive characterization of the ankle joint OA model, untangling the dynamic interplay of pain-related behavior, sensory and sympathetic sprouting, gliosis, and ATF3 expression, highlighting the relevance of a neuropathic pain-like component in OA. Chapters 3 and 4 converge on ATF3 as a focal point in understanding the neuropathic dimensions of osteoarthritic pain. This focus broadens to encompass the discovery of ATF3 expression in proprioceptive neurons of the DRG, thus bringing the interest back to the joint to study changes in proprioceptive fiber density.

CHAPTER 4

ATF3 immuno-reactivity and decrease density of proprioceptive primary afferents are associated with pain-related behavior in a rat model of osteoarthritis

Valerie Bourassa, Noosha Yousefpour, Kito Doyle, Hannah Derue, Alfredo Ribeiro-da-Silva

Manuscript in preparation

4.1 ABSTRACT

Osteoarthritis (OA), the degenerative and most common form of arthritis, is a complex disease of the whole joint that affects 1 in 7 adults in Canada. To this day, there is no satisfactory method of relieving osteoarthritic pain. There are many clinical and pre-clinical lines of evidence suggesting a neuropathic component to OA pain. A putative mechanism for this neuropathic pain-like component of OA is the contribution of primary afferent damage following joint degeneration. To study this issue, we have used a rat model of osteoarthritis based on the intraarticular injection of monoiodoacetate (MIA) in the ankle joint. We have observed expression of Activating Transcription Factor 3 (ATF3), a marker of neuronal stress, principally in large-diameter dorsal root ganglia cell bodies in which it colocalizes with parvalbumin, a marker of proprioceptors. Our results also show a significant decrease in proprioceptive fiber density in the joint correlating with pain-related behaviour, which adds to the body of evidence that proprioceptors are affected in advanced and irreversible OA. This suggests that myelinated mechanoreceptors innervating the joint are preferentially affected following joint degeneration, which drives interest in understanding the contribution of lamina III-V that receives input from these fibers, in the persistence of OA pain.

4.2 INTRODUCTION

Osteoarthritis (OA) has traditionally been defined as a chronic disease caused by the breakdown of joint cartilage, exposing the underlying bone. However, in recent years, there has been strong support for a neuropathic component in OA pain, implying that OA is more complex than its mechanical manifestations. In the clinic, common symptoms include pain, stiffness, swelling, and inflexibility. OA is the most common type of arthritis, affecting one in every seven adults in Canada [1], and its prevalence is expected to rise in the future due to current ageing and obesity trends [17]. OA, on the other hand, is not limited to the elderly; according to the Arthritis Society of Canada, one in every three OA patients is diagnosed before the age of 45. This has major implications not only for the mental and physical wellbeing of these patients, but it also produces a significant burden on the Canadian economy as 42% of the working-age population (20-64 years old) with OA are unable to contribute to the labour force [1]. While OA has commonly been referred to as a non-inflammatory, degenerative joint disease that is distinct from inflammatory arthritis (IA), recent findings of inflammatory processes in OA blur this distinction [20]. OA is diagnosed with radiographical imaging analysis using X-Ray or MRI, however, there is relatively poor correlation between the severity of cartilage deterioration as indicated by the X-Ray and the level of patient-reported pain [8].

OA pain is poorly managed and therapeutic approaches are predominantly symptomatic, using pharmacological agents such as non-steroidal anti-inflammatory drugs (NSAIDs), which can have severe side effects such as cardiovascular, gastrointestinal, or renal toxicity [2]. In the absence of therapeutic strategies to halt the progression of the disease or provide effective long-term relief from OA pain, joint replacement surgery is currently the most effective treatment for OA-

associated pain [25]. However, a significant subset of patients who have undergone successful total joint replacement still experience pain in the joint region post-recovery [11].

The nature of osteoarthritis (OA)-associated pain is complex, and our understanding of its mechanisms is still limited. The classical description of OA pain as purely mechanical in origin has been challenged in recent years. Strong evidence of peripheral and central sensitization and contribution of immune cells to pain-related behaviour in animal models suggest a neuropathic component to OA pain. In addition, a recent publication from our lab revealed the expression of activating transcription factor 3 (ATF3) in the dorsal root ganglia (DRG) in an animal model of OA at 5 weeks post MIA injection [4]. ATF3 upregulation is indicative of neuronal stress and is a response to axonal damage. This upregulation has been associated with neuropathic pain (NP) models that involve crushed or ligated nerves. Previous studies from our lab have identified that peptidergic (nociceptive) and sympathetic sprouting occurs in the OA-affected joint, but density of innervation by proprioceptors has not been investigated yet [4].

In this study, we aimed to quantify changes in the proprioceptive innervation density in the ankle joint of an OA rat model through histological staining using an optimized diaminobenzidine (DAB) immunohistochemistry (IHC) protocol. Thick afferents represent almost exclusively proprioceptors in joints. The overall objective was to quantify the density of NF200-positive fibers in MIA-injected ankles in comparison to saline-injected ankle joints. Our results showed a statistically significant decrease in the innervation density of NF200-positive fibers in synovium of the MIA-injected OA rat model. These findings generate support for the presence of a neuropathic component in OA pain and provide a basis for further research into a neuropathic phenotype of OA pain.

4.3 METHODS

4.3.1 Animals:

Sprague Dawley male rats (175-200 g; Charles Rivers Laboratories) were used in this study. The rats were housed as pairs in cages with soft bedding on a 12-hour light/dark cycle where food and water were available ad libitum. All experimental protocols followed the guidelines on Care and Use of Experimental Animals of the Canadian Council on Animal Care and were approved by the McGill University Animal Care Committee.

4.3.2 Induction of Osteoarthritis and nerve lesion:

Under brief anesthesia using 5% isoflurane in O2, animals were injected intra-articularly in the right tibio-talar (ankle) joint with 2.4 mg of MIA (Sigma) in 40µl of saline, or vehicle. For comparison of the pattern of ATF3 expression in a neuropathic model and the MIA, we used C57BL/6 mice (8 weeks of age) with a spared nerve injury (SNI) from the cohort prepared for another publication [24]. Three mice were perfused at 3 days after lesion.

4.3.3 Histopathology:

At the 1, 2, 3, 4, 5, 6 and 10-week post-injection time-points, animals were sacrificed to collect tissue samples. Animals were first deeply anesthetized with Equithesin (0.3 mL per 100 g of body weight) via intra-peritoneal injection, then subject to vascular rinse using 0.1% NaNO2 and 0.05% NaHCO3 in 0.01M phosphate buffered saline (PBS). Animals were then perfused using 4% Paraformaldehyde (PFA) in 0.1M phosphate buffer solution (PBS) for 30 minutes. L4-L6 DRGs were extracted and post-fixed for 2 hours at 4˚C in 4% PFA, then placed in 30 % sucrose in 0.1 M phosphate buffer. Subsequently, they were sectioned in 50 µm-thick transverse sections in a sledge freezing microtome (Leica) and collected directly on gelatin-subbed slides. Mice were processed as described in [24] and DRG segment used was L4.

4.3.3.1 Processing and imaging of DRGs

DRGs were stained with a combination of the following primary anti-bodies: rabbit monoclonal anti-ATF3 antibody (Abcam #ab207434; 1:500), mouse monoclonal anti-CGRP (Sigma C7113, 1:500), goat anti-PV (Swant PVG-213, 1:8000), and mouse anti-NF200 (Sigma N0142, 1:1000). DRG and spinal cord sections were subsequently incubated with fluorochrome-labeled secondary antibodies (1:800, Invitrogen). DRG slides were also incubated with red Nissl (Neurotrace 530/615 N-21482; 1:100) or blue Nissl (Neurotrace 435/455 N-21479; 1:100) in PBS+T on shaker in foil for 30 min. Then, slides were washed for 10 minutes in PBS-T, followed by two 10-minute washes in PBS, and cover-slipped with mounting medium (Aqua Polymount). DRGs were imaged using a Zeiss Axioimager M2 microscope equipped with a high-resolution monochrome camera and the Zeiss Zen software version 2.3 (Zeiss Canada). In the DRGs, total number of Nissl-positive and ATF3-positive cells were counted and averaged for each animal (n = 4).

4.3.3.2 Processing of ankle joints

Following extraction, right ankle joints were placed in fixative for 4 hours, then 10% sucrose in 0.1 M cacodylate buffer overnight at 4°C. Ankles joints were decalcified in 10% ethylenediaminetetraacetic acid (EDTA) pH 7.4 in PBS at 4°C on a shaker for 3 weeks. The EDTA solution was changed biweekly for the first two weeks, then once in the final week. Joint samples were placed in 10% sucrose solution in sodium cacodylate buffer overnight at 4°C for cryo-protection, then set in OCT (Tissue-Tek, Torrance, CA, USA). Joints were then cut using the cryostat (Leica) into 25 µm sections and thaw-mounted onto gelatin-coated slides.

4.3.3.3 DAB Immunohistochemistry:

Decalcified ankle joints mounted on gelatin-subbed slides were pre-incubated with PBS with 0.2% Triton X-100 (PBS+T) at 4°C for 24 hours. Slides were then incubated in 50% ethanol in water then 0.3% H_2O_2 for 30 minutes each, with three 10-minute PBS washes between each incubation. To block unspecific labelling, slides were incubated in 3% normal goat serum (NGS) in 0.3% PBS+T for 1 hour. To detect proprioceptors, slides were incubated using mouse anti-NF200 (Sigma N0142, Lot #109M4754V) in 0.1% NGS in 0.1% PBS+T on a serial dilution ranging from 1:50 to 1:800. After 48 hours, slides were triple washed using PBS+T, then incubated in goat anti-mouse biotin (Life Technologies D20691, Lot #1712142; 1:400) overnight at 4°C. Slides were incubated for 1 hour at room temperature in a solution (1:400) of avidin-biotin complex (ABC) in PBS+T (Vector Elite PK-6100). Diaminobenzidine (DAB) was added to the sections on-slide for 10 minutes or 12 minutes, and then 1% H_2O_2 was added for 10 or 12 minutes. Following rinses with PBS+T and PBS, slides were dehydrated in ascending concentrations of ethanol and cleared with xylene for 20 minutes. Slides were finally cover-slipped using Entellan mounting medium and Gold Seal coverslips (Electron Microscopy Sciences) and stored at room temperature until microscopy analysis.

Bone tissue tends to easily detach from slides when subject to shaking during incubation; as such, we opted to use plastic coverslips (EMD Millipore Corp. CAT #S7117) for primary antibody, secondary antibody, and avidin-biotin complex (ABC) incubations as described in Chapter 2 of this thesis. Flexible coverslips, when carefully applied to prevent air bubbles, evenly distribute the volume of antibodies, allowing for a uniform staining pattern. Additionally, the plastic coverslips minimize the volume required to perform proper incubations in the absence of a shaker to evenly distribute antibody across the slide – see Chapter 2 for details.

4.3.3.4 Fiber Imaging and Quantification:

For joints, images were captured using a Zeiss Axioimager M2microscope equipped with a high-resolution color camera and the Zeiss Zen software version 2.3 (Zeiss Canada). For each animal, 2 slides with 3 sections each were collected for imaging analysis. Intact fiber-positive microscopic fields in the synovium were selected and imaged, for a total of 4 images per animal. Bright field Z-stack images were obtained using the 40x oil-immersion objective and exported as TIFF files which were then imported into ImageJ for quantification. A scale bar of 100µm on the first image was traced with the straight-line tool to establish the measurement scale. This scale was applied globally in the ImageJ software such that all subsequent images would have accurate measurements in µm. Typically, the afferent fibers did not span the entire image frame, so a live frame area (LFA) was designed and implemented in all images for consistency. Using the freehand line tracer tool, fibers within the live frame area were traced and measured in µm. All measurements were exported to Excel, then GraphPad for subsequent analysis.

4.4 RESULTS

4.4.1 ATF3 expression and colocalization in the DRG:

Figure 4.1 shows the pattern and time course of ATF3 in the DRG. We observed that in the mouse DRG of at 3 days after SNI there was extensive expression of ATF3 in neurons (Fig 4.1A). In MIA rats, in contrast, ATF3 expression in DRG followed biphasic pattern (Figure 4.1B) with an initial strong expression of ATF3 following MIA injection at week 1 (Figure 4.1C), which subsided completely by week 3 (Figure 4.1E). Interestingly, significant ATF3 expression returned at week 5 (Figure 4.1G). Higher magnification images were used in Figure 4.2 to analyze the distribution of ATF3 expression in DRG profiles at 5-weeks post MIA injection. Figure 2B shows the normal distribution of large caliber afferents (40-80 µm), which typically make up

approximatively 25% of the rat DRG [9; 16]. Figures 4.2C and D show that over 50% of ATF3-ir cells are large-caliber afferents, which is a notable abundance of expression in this smaller cell population. Interestingly, further analysis of ATF3 expression by immunohistochemistry at the 5-week time-point shows significant colocalization of ATF3 with parvalbumin (69.3%) and NF-200 (73.7%), markers for proprioceptors and myelinated fibers respectively (Figure 3E-H). Fewer ATF3+ colocalization was observed in CGRP-ir neurons (25.7%), while no colocalization with IB4 labeling was observed (Figure 4.3A-D).

4.4.2 Density of proprioceptive fibers in the ankle joint:

Proprioceptive fibre innervation was assessed in the synovial membrane connecting the tibia and talus (Figure 4.4). We used DAB-based immunohistochemistry with antibodies against the myelinated-fibre marker NF-200. Figure 4.4 shows representative images of innervation patterns at 6 weeks post-injection in sham (Figure 4.4A) and MIA (Figure 4.4B) animals. Our quantification revealed a significant innervation decrease in the synovial membrane in MIA-injected animals ($P < 0.05$) at a time-point that is associated with pain-related behavior (Figure 4.4C).

4.5 FIGURES

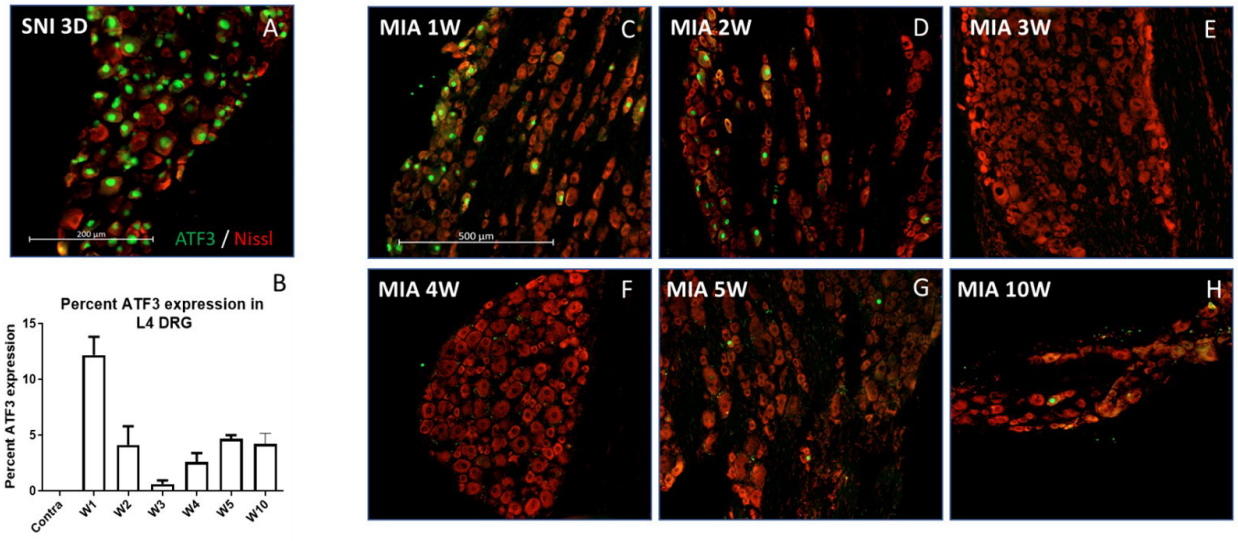

Chapter 4 Figure 1: Time-course of Activating transcription factor 3 (ATF3) expression in lumbar DRG at 1, 2, 3, 4, 5, and 10 weeks post MIA injection with red Nissl contrast stain.

A) Positive control of ATF3 expression in mouse spared-nerve injury (SNI) model of neuropathic pain at 3-days after injury. B) Quantification of ATF3 immunoreactivity in rat MIA OA shows a biphasic expression of ATF3, with high levels of expression at 1-week I, which subsides by week 3 (E), reappears at week 5 (G), and persists through week 10 (H). Bars represent mean ± SEM. N = 4.

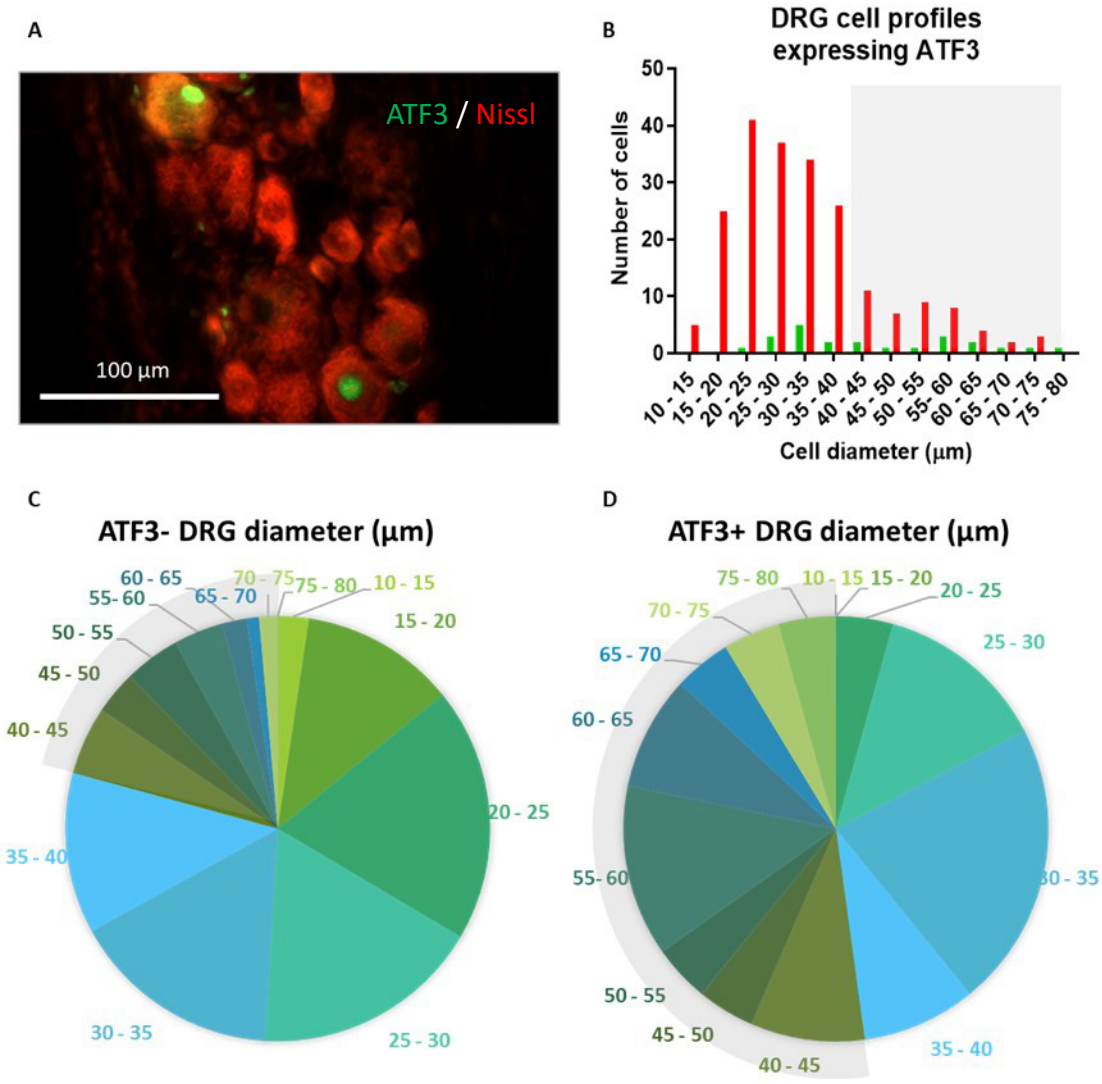

Chapter 4 Figure 2: DRG cell profiles expressing the Activating transcription factor 3 (ATF3) 5 weeks post MIA injection

A) shows a high magnification image of large caliber neurons expressing ATF3 with red Nissl contrast stain. B) Average diameter (in µm) of cell profiles of ATF3+ (green) and ATF3- (red) DRG neurons. Shaded area represents large-caliber neurons (40-80 µm). C,D) Pie charts depicts the proportion of ATF3- (C) and ATF3+ (D) that are large caliber neurons (shaded). N = 4.

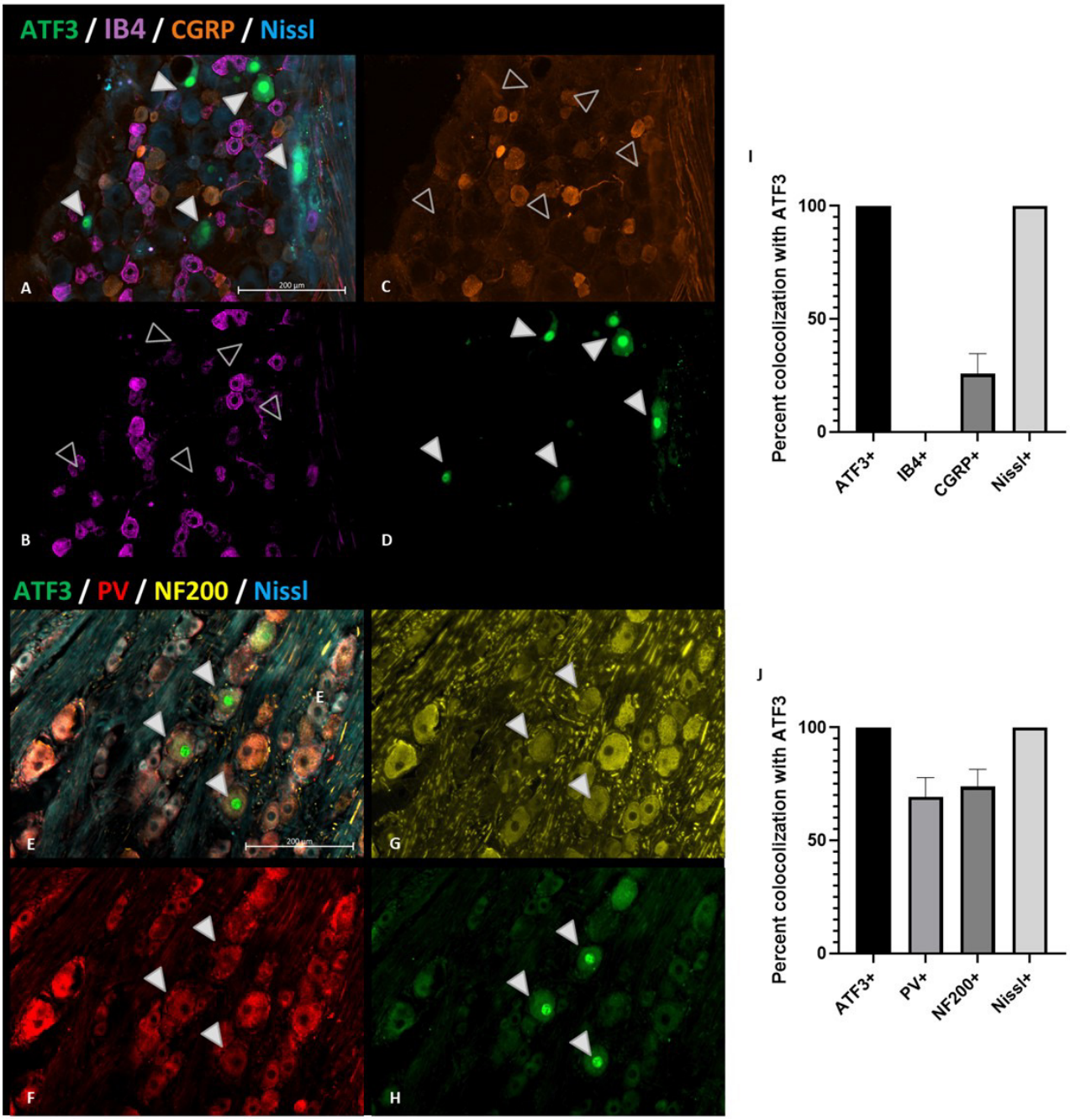

Chapter 4 Figure 3: Immunofluorescence images of ATF3 colocalization in ipsilateral DRG at 5 weeks post MIA injection.

A-D) Triple immunostaining with anti-ATF3, anti-IB4, anti-CGRP with blue Nissl shows absence of colocalization of CGRP-ir and IB4-ir (empty arrow heads) with ATF3-ir (full arrowheads). E-

H) Triple immunostaining with anti-ATF3, anti-PV, and anti-NF200 with blue Nissl stain shows colocalization of both PV-ir and NF-200-ir with ATF3-ir (full arrowheads) I-J) Quantification of percent colocalization with ATF3-ir. Bars represent mean ± SEM. N = 4.

Chapter 4 Figure 4: Bright field images of DAB immunohistochemistry showing innervation detected by NF200 (1:800) antibody, a marker of myelinated afferents, in the tibiotalar synovial membrane at 12-minute DAB incubation periods in SHAM (A) versus MIA (B) animals.

*C) NF200-positive fiber density in the synovial membrane of the ankle joint in SHAM versus MIA rats. Data were analyzed using an unpaired two-tailed t-test. Bars represent mean ± SEM; *P < 0.05, **P < 0.01, ***P < 0.001. N = 8 (Sham), 7 (MIA).*

4.6 DISCUSSION

Clinical and pre-clinical evidence suggests a neuropathic component to OA pain. We studied the possible contribution of primary afferent damage following joint degeneration to this neuropathic component by investigating a time-course of the expression of ATF3, a marker of neuronal stress, in various cell populations of the rat DRG.

Surprisingly, we observed bi-phasic expression of ATF3 in the DRG: first a high expression at 1 and 2 weeks post MIA injection, and a second moderate expression at 5 weeks post injection, which coincides with pain-related behavior that we established in previous work [4]. ATF3 expression in the rat DRG of a knee osteoarthritis model as evidence of neuropathic pain in OA has previously been described; however, the investigators studied this expression at 1 and 2 weeks post injection [21]. We suspect that these results, as well as our observation of high levels of ATF3 at 1 and 2 weeks were caused by the injection of the MIA toxin itself, rather than the presence of prolonged nerve damage that contribute to pain. MIA is a non-selective glycolytic inhibitor that causes rapid cells death. When injected in the joint cavity, it mostly affects chondrocytes, but we cannot exclude that more peripheral tissues can be affected, including peripheral nerves. We believe that the second phase of ATF3 expression that we observed represents more convincing evidence of the presence of neuropathy in this model of OA as it coincides with pain-related behavior and other pathological changes that we previously observed in our MIA model [4].

The majority of ATF3 positive DRG neurons were also immunoreactive for parvalbumin and NF-200. It is well known that in the periphery parvalbumin labels proprioceptors [6], which represent the main innervation of joint by thick afferents, and can be labeled with NF200. This

observation adds compelling evidence to the idea that damaged proprioceptors may play a role in OA pain. This suggest that thick afferents innervating the articular joint in OA pain are mostly affected following joint degeneration, which drives interest in understanding the changes in circuitry of lamina III-V of the spinal cord that receives input from these fibers, and which may contribute to the persistence of OA pain.

In IHC studies of innervation of the ankle joint, we discovered that the MIA rats had significantly less NF200+ fibre innervation in the synovial membrane of the ankle joint than SHAM animals. These findings contrast with previous observations in our lab for sensory and sympathetic fiber innervation in an inflammatory arthritis model, where we observed increases in sensory and sympathetic fiber densities in various structures of the joint [13]. Both peptidergic sensory and sympathetic primary afferents rely on nerve growth factor (NGF) for maintenance or survival [22]. Following peripheral nerve injury, NGF is upregulated by mast cells that accumulate at the site of injury and by Schwann cells in the distal nerve stump, resulting in increased innervation of sympathetic and peptidergic fibres [7; 12]. In contrast, proprioceptors, which comprise the majority of the thick myelinated afferent fibres in the ankle joint, use neurotrophin-3 (NT-3) and the corresponding TrkC receptor [5]. It should be noted that we previously observed in a neuropathic pain model a prolonged loss of skin innervation by thick afferents as detected by NF200 immunoreactivity [15], what gives support to findings of the current study.

We suspect that the reduction in proprioceptive innervation density observed in our MIA rats is directly linked to axonal injury. In response to axonal injury, macrophage recruitment, the production of cytokines and neurotrophins, and the proliferation of Schwann cells occurs [12]. Distal nerve injury cellular events create a microenvironment that promotes axonal regeneration

by stimulating regrowth of the proximal nerve stump towards the distal stump. Surprisingly, this sequence of events results in the accumulation of algesic factors and structural changes to the injured nerve, both of which contribute to the onset and maintenance of neuropathic pain (NP) [7; 23]. Importantly, the immature Schwann cells of the distal stump, which produce neurotrophic and neurotropic factors to attract regrowing axons of the proximal stump, do not upregulate NT-3 synthesis [7; 10]. In our OA model, the lack of guiding trophic factor NT-3 could explain the decreased proprioceptive density that occurs after peripheral nerve injury. Furthermore, sprouting proprioceptors that are unable to navigate to their target organ for functional re-innervation may play a role in long-term OA pain. Given this information, NT-3 manipulation could be a promising pharmacological avenue to pursue, as it has previously been shown to alleviate proprioceptive deficits and associated neuropathology in rats with large sensory-fiber peripheral neuropathy [12]. NT-3 has proprioceptor specificity and the ability to significantly reduce the effects of profound proprioceptive loss in clinical presentations of large fibre neuropathies [12]. Given the significant loss in proprioceptive density in our OA model, we believe that further research into NT-3 manipulation in this animal model of OA is the logical next step.

Large-fiber neuropathy refers to a type of peripheral neuropathy that primarily affects the larger nerve fibers responsible for transmitting sensory information related to touch, proprioception, and vibration. These nerve fibers, known as A-alpha and A-beta fibers, are essential for relaying signals related to position sense, coordination, and tactile sensations. Arthritis is typically not considered as a disease resulting from or maintained by large-fiber neuropathy, although OA patients do present with muscle weakness, protective movement avoidance and joint instability which can disrupt the normal proprioceptive signals that help the brain understand joint orientation. As a result, individuals with OA might experience difficulties in maintaining balance

and coordinated movements, underscoring the importance of rehabilitation strategies aimed at improving joint stability and proprioceptive function [14; 18; 19]. However, the relationship between pain and proprioception is generally understudied. In a study that examined the connection between knee joint proprioception, pain, and disability in a large group of knee OA patients, individuals with the worst and best proprioception didn't show significant differences in pain and disability [3]. Although this finding is puzzling, further investigation in the contribution of proprioceptors in in pain circuitry is warranted. Proprioceptors terminate predominantly in lamina III-V of the dorsal horn of the spinal cord.

Our current findings contribute to the growing body of evidence supporting the idea that pain experienced in osteoarthritis (OA) has an underlying neuropathic component. Moreover, our research underscores the potential significance of proprioceptors in the persistence of chronic pain within the context of OA. Proprioceptors appear to play a crucial role in mediating and perpetuating the sensation of chronic pain in individuals with OA. By highlighting the involvement of proprioceptors, our study deepens the understanding of the complex interplay between neural mechanisms and pain perception in OA, which has implications for the development of more targeted interventions and treatments aiming to alleviate the neuropathic aspects of OA pain.

4.7 ACKNOWLEDGEMENTS

The authors wish to thank Manon St. Louis for laboratory expertise. Valerie Bourassa, and Noosha Yousefpour acknowledge doctoral studentships from the Louise and Alan Edwards Foundation. This work was funded by Canadian Institutes of Health Research Operating Grant MOP-136903 and a grant from the Louise and Alan Edwards Foundation. None of the authors have competing interests to disclose.

4.8 REFERENCES

[1] Arthritis Society. What is Arthritis—Inflammatory Diseases Retrieved March 21, 2022, from https://arthritisca/about-arthritis/what-is-arthritis 2022.

[2] Balmaceda CM. Evolving guidelines in the use of topical nonsteroidal anti-inflammatory drugs in the treatment of osteoarthritis. BMC Musculoskelet Disord 2014;15:27.

[3] Bennell KL, Hinman RS, Metcalf BR, Crossley KM, Buchbinder R, Smith M, McColl G. Relationship of knee joint proprioception to pain and disability in individuals with knee osteoarthritis. Journal of Orthopaedic Research 2003;21(5):792-797.

[4] Bourassa V, Deamond H, Yousefpour N, Fitzcharles MA, Ribeiro-da-Silva A. Pain-related behavior is associated with increased joint innervation, ipsilateral dorsal horn gliosis, and dorsal root ganglia activating transcription factor 3 expression in a rat ankle joint model of osteoarthritis. Pain Rep 2020;5(5):e846.

[5] Chalazonitis A. Neurotrophin-3 as an essential signal for the developing nervous system. Molecular Neurobiology 1996;12(1):39-53.

[6] Dietrich S, Company C, Song K, Lowenstein ED, Riedel L, Birchmeier C, Gargiulo G, Zampieri N. Molecular identity of proprioceptor subtypes innervating different muscle groups in mice. Nat Commun 2022;13(1):6867.

[7] Dubovy P. Wallerian degeneration and peripheral nerve conditions for both axonal regeneration and neuropathic pain induction. Ann Anat 2011;193(4):267-275.

[8] Finan PH, Buenaver LF, Bounds SC, Hussain S, Park RJ, Haque UJ, Campbell CM, Haythornthwaite JA, Edwards RR, Smith MT. Discordance between pain and radiographic severity in knee osteoarthritis: findings from quantitative sensory testing of central sensitization. Arthritis Rheum 2013;65(2):363-372.

[9] Harper AA. Similarities between some properties of the soma and sensory receptors of primary afferent neurones. Exp Physiol 1991;76(3):369-377.

[10] Helgren ME, Cliffer KD, Torrento K, Cavnor C, Curtis R, DiStefano PS, Wiegand SJ, Lindsay RM. Neurotrophin-3 administration attenuates deficits of pyridoxine-induced large-fiber sensory neuropathy. J Neurosci 1997;17(1):372-382.

[11] Kurien T, Arendt-Nielsen L, Petersen KK, Graven-Nielsen T, Scammell BE. Preoperative Neuropathic Pain-like Symptoms and Central Pain Mechanisms in Knee Osteoarthritis Predicts Poor Outcome 6 Months After Total Knee Replacement Surgery. J Pain 2018;19(11):1329-1341.

[12] Locke S, Yousefpour N, Mannarino M, Xing S, Yashmin F, Bourassa V, Ribeiro-da-Silva A. Peripheral and central nervous system alterations in a rat model of inflammatory arthritis. Pain 2020;161(7):1483-1496.

[13] Longo G, Osikowicz M, Ribeiro-da-Silva A. Sympathetic fiber sprouting in inflamed joints and adjacent skin contributes to pain-related behavior in arthritis. J Neurosci 2013;33(24):10066-10074.

[14] Pai YC, Rymer WZ, Chang RW, Sharma L. Effect of age and osteoarthritis on knee proprioception. Arthritis & Rheumatism: Official Journal of the American College of Rheumatology 1997;40(12):2260-2265.

[15] Peleshok JC, Ribeiro-da-Silva A. Delayed reinnervation by nonpeptidergic nociceptive afferents of the glabrous skin of the rat hindpaw in a neuropathic pain model. J Comp Neurol 2011;519(1):49-63.

[16] Price J. An immunohistochemical and quantitative examination of dorsal root ganglion neuronal subpopulations. J Neurosci 1985;5(8):2051-2059.

[17] Rahman MM, Cibere J, Goldsmith CH, Anis AH, Kopec JA. Osteoarthritis incidence and trends in administrative health records from British Columbia, Canada. J Rheumatol 2014;41(6):1147-1154.

[18] Sharma L. Proprioceptive impairment in knee osteoarthritis. Rheumatic Disease Clinics 1999;25(2):299-314.

[19] Sharma L, Pai Y-C. Impaired proprioception and osteoarthritis. Current opinion in rheumatology 1997;9(3):253-258.

[20] Sokolove J, Lepus CM. Role of inflammation in the pathogenesis of osteoarthritis: latest findings and interpretations. Ther Adv Musculoskelet Dis 2013;5(2):77-94.

[21] Thakur M, Rahman W, Hobbs C, Dickenson AH, Bennett DL. Characterisation of a peripheral neuropathic component of the rat monoiodoacetate model of osteoarthritis. PLoS One 2012;7(3):e33730.

[22] Thoenen H. The changing scene of neurotrophic factors. Trends Neurosci 1991;14(5):165-170.

[23] Üçeyler N, Sommer C. Wallerian degeneration and neuropathic pain. Drug Discovery Today: Disease Mechanisms 2006;3(3):351-356.

[24] Yousefpour N, Tansley SN, Locke S, Sharif B, Parisien M, Deamond H, Rodrigues R, Mathur V, Yednock TA, Austin JS, Bourassa V, Wang C, Cabana V, Wong C, Lister K, St-Louis M, Andrews-Zwilling Y, De Koninck Y, Mogil JS, Seguela P, Diatchenko L, Khoutorsky A, Ribeiro-da-Silva A. Complement protein C1q is a therapeutic target for neuropathic pain. Nature Communications 2021;Revised version under consideration(Available online as a preprint):https://www.researchsquare.com/article/rs-1016420/v1016421.

[25] Yusuf E. Pharmacologic and Non-Pharmacologic Treatment of Osteoarthritis. Current Treatment Options in Rheumatology 2016;2(2):111-125.

CONNECTING CHAPTER 4 TO CHAPTER 5

Chapter 4 contributes to the strong body of evidence that a neuropathic pain-like component is present in OA with the time-course of ATF3 expression in the DRG. Chapter 4 also adds to the complexity of osteoarthritic pain mechanisms by identifying proprioceptive afferents as potential contributors to chronic pain in OA. What this work does not elucidate yet is the role of proprioceptive afferents in shaping spinal cord circuitry changes and their contribution to pain in OA. The following chapter describes preliminary data on spinal cord dorsal horn circuitry changes in OA with morphological analyses of projection neurons known to relay pain-related information to the brain, and internalization of the neurokinin-1 receptor (NK1-r) after exercise. Further studies will need to be undertaken to study the changes associated with proprioceptive afferents in the dorsal horn. Understanding changes in established spinal cord pain circuitry, including the dynamics of Nk1-r-ir projection neurons, in the MIA ankle joint model of OA serves as a foundational step toward building an integrated understanding of the disease.

CHAPTER 5

SUPPLEMENTARY DATA

Internalization of the substance P receptor following treadmill exercise in an ankle joint model of osteoarthritis

Valerie Bourassa, Haley Deamond, Alfredo Ribeiro-da-Silva

5.1 ABSTRACT

The internalization of the receptor for substance P, the neurokinin-1 receptor (NK1-r) on lamina I projection neurons of the spinal dorsal horn has been used as a marker of nociceptive responses. Lamina I is an important centre for the modulation and forwarding to the brain of pain-related information. Therefore, changes in the properties of lamina I projection neurons may be important for pain. Previous work from our lab has shown increased expression of NK1-r on lamina I pyramidal neurons in both neuropathic pain and inflammatory arthritis models. In addition to this, we have shown that forced movement of an inflamed joint or intradermal injection of capsaicin leads to NK1-r internalization. This project aims to investigate whether internalization of the receptor on NK1-r positive neurons will occur in a rat ankle joint model of osteoarthritis (OA) after a treadmill exercise. Using rats of both sexes, OA was induced using an injection of the glycolytic inhibitor mono-iodoacetate (MIA) into the right tibio-talar joint. At 8 weeks post MIA injection, a time where OA-related pain is consistent and irreversible, animals were forced to run for 10 minutes at a speed of 15 m/min on a treadmill and immediately perfused. NK1-r internalization was then analyzed using immunocytochemistry and confocal microscopy. Analysis of our results showed increased NK1-r immunoreactivity in MIA animals, and that running MIA animals underwent significant internalization of the NK1-r as compared to non-running MIA animals and vehicle-injected controls. This suggests that movement during a treadmill exercise results in pain, which is of significance as pain during movement is a major complaint of osteoarthritis patients.

5.2 INTRODUCTION

The neurokinin 1 receptor (NK1-r) plays an important role in the pain processing pathway within the spinal cord. It belongs to the family of the class I (rhodopsin-like) cell surface G protein-coupled receptors (GPCRs) and, in the spinal cord, is primarily associated with dorsal horn neurons involved in the transmission of pain-related information to higher centres.

The spinal cord serves as a vital relay station for sensory information, including nociceptive signals traveling from the periphery to the brain. Upon activation by its endogenous ligand, substance P, the NK1-r initiates a cascade of intracellular events that favor the amplification of nociceptive signaling within the spinal cord [8; 9; 14; 15; 17].

Several studies have shown a correlation between NK1-r function and heightened pain sensitivity [3; 6; 7; 18-20; 22]. Namely, studies from our laboratory have shown an upregulation of NK1-r in chronic pain models of neuropathic pain and inflammatory arthritis [3; 18]. Additionally, in arthritis, forced movement of the affected joint resulted in internalization of the receptor in projection neurons [19].

In should be clarified that, although the NK1-r has been considered as important in pain mechanisms in the spinal dorsal horn, and its antagonists considered at one time as potential novel analgesics, such promised was not confirmed in clinical trials. However, despite the lack of efficacy of NK1-r antagonists as analgesics in clinical trials, these receptors are still important as they are critical in the development of sensitization and, therefore, the etiology of chronic pain [5; 11; 12]. In agreement with this idea, in past studies we have found a novel expression of these receptors in a dorsal horn neuronal population which is thought to be normally non-nociceptive [10], in both neuropathic and inflammation with arthritis pain conditions [3; 18]. This *de novo* expression of NK1-r was accompanied by an abundant innervation by peptidergic nociceptive

fibres, indicative of strongly increased noxious input, and by receptor internalization following noxious stimulation in a neuropathic pain model [18]. Therefore, the expression level and internalization of the NK1-r is an important marker of pain mechanisms.

In a previous study from our laboratory, we have described peripheral and central mechanisms that likely contribute the development and maintenance of chronic pain in the mono-iodoacetate (MIA) ankle-joint model of osteoarthritis (OA) [4] – see chapter 3. The objective of the current study was to study the changes in expression and internalization of the NK1-r in our model of MIA-induced OA in the ankle joint as evidence of the similarity of certain pain mechanisms to those of inflammatory arthritis and neuropathic pain models

Given the common complaint of pain during movement in osteoarthritis patients [16], we chose to utilize a treadmill in our study to investigate NK1-r internalization following movement.

5.3 METHODS

5.3.1 Induction of OA:

The entire experimental design followed the Care and Use of Experimental Animals of the Canadian Council on Animal Care guidelines. All animals were housed in pairs with soft bedding, food and water ad libitum, on a 12- hour light/dark cycle.

A total of 36 Sprague Dawley female and male rats (Charles Rivers Laboratories) weighing 175-200 g at the beginning of the study, with 3 animals per group, were anesthetized with 5 % isoflurane in O2, and given by intraarticular injection in the tibio-talar joint a single dose of 2.4 mg of MIA (Sigma) or saline, in a volume of 40 µL [4]. A total of 9 groups were divided as follows for SHAM (Male Running, Male Non-Running, Female Running, Female Non-Running), MIA

(Male Running, Male Non-Running, Female Running, Female Non-Running) and naïve male non-running.

5.3.2 Treadmill habituation and forced movement before perfusion

Rats were habituated to treadmill exercise over an eight-week period with weekly 30 -minute sessions on a motorized treadmill, during which manual encouragement was provided to ensure consistent participation. At the eight-week time point, animals were subjected to a final treadmill session immediately before perfusion and tissue extraction. During this session, rats were exercised at a speed of 15 meters per minute (m/min) for 10 minutes, representing a moderate-intensity exercise bout.

5.3.4 Histopathology:

At the 8-week post-injection time-point, animals were sacrificed to collect tissue samples. Animals were first deeply anesthetized with Equithesin (0.3 mL per 100 g of body weight) via intra-peritoneal injection, then subject to vascular rinse using 0.1% $NaNO_2$ and 0.05% $NaHCO_3$ in 0.01M phosphate buffered saline (PBS). Animals were then perfused using 4% Paraformaldehyde (PFA) in 0.1M phosphate (PB) for 30 minutes.

Lumbar spinal cords were sectioned on the horizontal plane and stained with a rabbit anti-NK1-r antibody (Sigma S8305; 1:10 000). L4-L5 segments were used. Sections were subsequently incubated with fluorochrome-labeled secondary antibodies (1:800, Life Technology). Slides were incubated with red Nissl (Neurotrace 530/615 N-21482; 1:100). Z-stack images were captured with confocal microscopy (LSM 710 and Zeiss AxioObserver) and the classification of lamina I neurons into morphological types and presence/absence of NK1-r internalization were analyzed by an experimenter blinded to the experimental groups.

5.4 RESULTS

5.4.1 Upregulation of NK1-r at the cellular membrane

At the 8 week time point, consistently with previous studies from our laboratory, Figure 1 shows distinct lamina I NK1-r neuronal populations that were distinguished based on their dendritic arborization and cell body shape when observed in the horizontal plane. Fusiform neurons exhibited a spindle-shaped soma, with a single dendrite emerging from each end of the cell body (Figure 1A). Multipolar neurons were identified by the presence of four or more primary dendrites originating from the cell body, irrespective of the soma shape (Figure 1B). Pyramidal neurons displayed a triangular soma, with a primary dendrite arising from each corner (Figure 1C). Note that Figure 1C shows a pyramidal neuron in the MIA group, with prominent immunoreactivity for the NK1-r, to better illustrate the morphology of this cell type. Some neurons exhibited features that were transitional between two of the described cell types and did not meet the criteria for the main categories due to their atypical appearance. Additionally, certain neurons had a portion of the cell body and/or proximal dendritic tree truncated by sectioning. Both cells were deemed unclassifiable and were categorized as "unclassified" for the purposes of our quantitative analyses.

Overall, we detected an increase of NK1-r immunoreactivity in all cell types. In particular, we observed a significant increase in the number of cells with NK1-r immunoreactivity in MIA animals in the pyramidal projection neuron category. This suggests a recruitment of these cells to the pain circuitry in the OA-disease state, as pyramidal neurons do not normally express detectable levels of NK1-r immunoreactivity, but upregulate in to

detectable levels in a considerable number of cells [18]. There were no significant differences between male and female rats and thus data from both sexes was pooled

5.4.2 Internalization of the NK1-r following forced treadmill

A 10 minute treadmill running session at 30 meters per minute was used as a forced movement exercise immediately before perfusion to induce internalization. In the past, this had been achieved by the experimenter manually moving the affected joint in a CFA-arthritis model while the animal was sedated and awaiting perfusion [192]. The use of the treadmill aligns with this A 10 minute treadmill running session at 30 meters per minute was used as a forced movement exercise immediately before perfusion to induce internalization. In the past, this had been achieved by the experimenter manually moving the affected joint in a CFA-arthritis model while the animal was sedated and awaiting perfusion [19]. The use of the treadmill aligns with this laboratory's objective to study movement-induced pain an exercise in OA. Confocal microscopy was employed to visualize the internalization of the NK1-r by after immunofluorescence labelling and Nissl staining. Figure 2 A-D depict projection neurons in male subjects from the SHAM (A, B) and MIA (C, D) groups, with B and D representing the running groups. Meanwhile, Figures E-H display projection neurons in female subjects from the SHAM (E, F) and MIA (G, H) groups, where F and H correspond to the running groups. Notably, only images D and H, representing the male MIA running and female MIA running groups respectively, show internalized NK1-r. These images revealed the presence of distinct NK1-r immunoreactive intracellular clusters (indicated by arrows), a characteristic hallmark of receptor internalization.

There were no differences in the percentage of cells showing internalization between male and female MIA running groups.

5.5 FIGURES

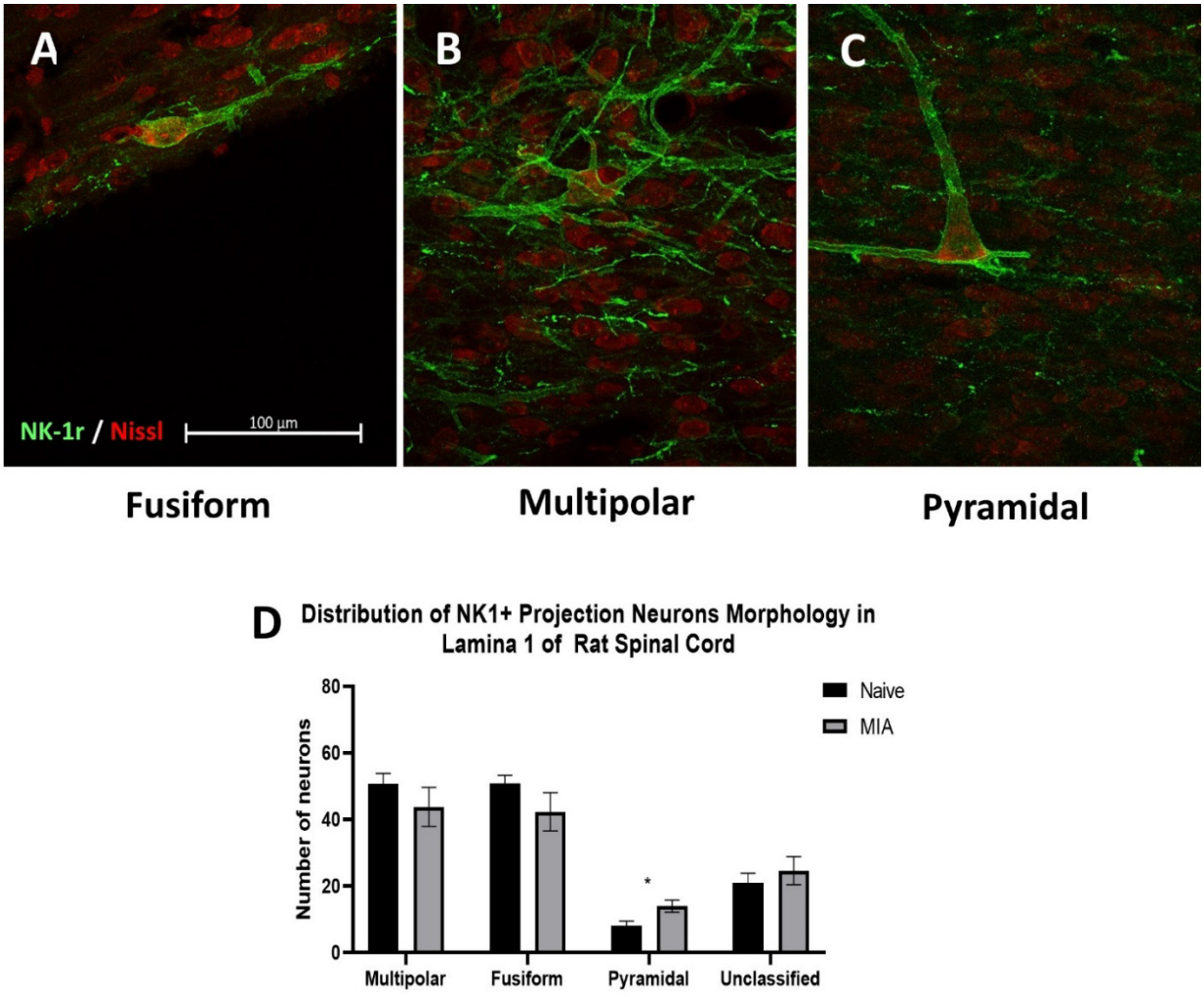

Chapter 5 Figure 1: Confocal microscopy images representing the 3 morphological cell types of projection neurons expressing NK1-r.

F*usiform (A), multipolar (B) and pyramidal (C). Note that A & B are from naïve animals while C is from the MIA group to best illustrate the morphology of this cell type, which normally express very low levels of NK1-r. The distribution of each morphological type in naïve and MIA animals is shown in D and reflects the upregulation of NK1-r in multipolar neurons, as in the absence of*

*another marker few cells of the pyramidal type are detected in naïve animals. Bars represent mean ± SEM. *P < 0.05, **P < 0.01, ***P < 0.001. N = 6*

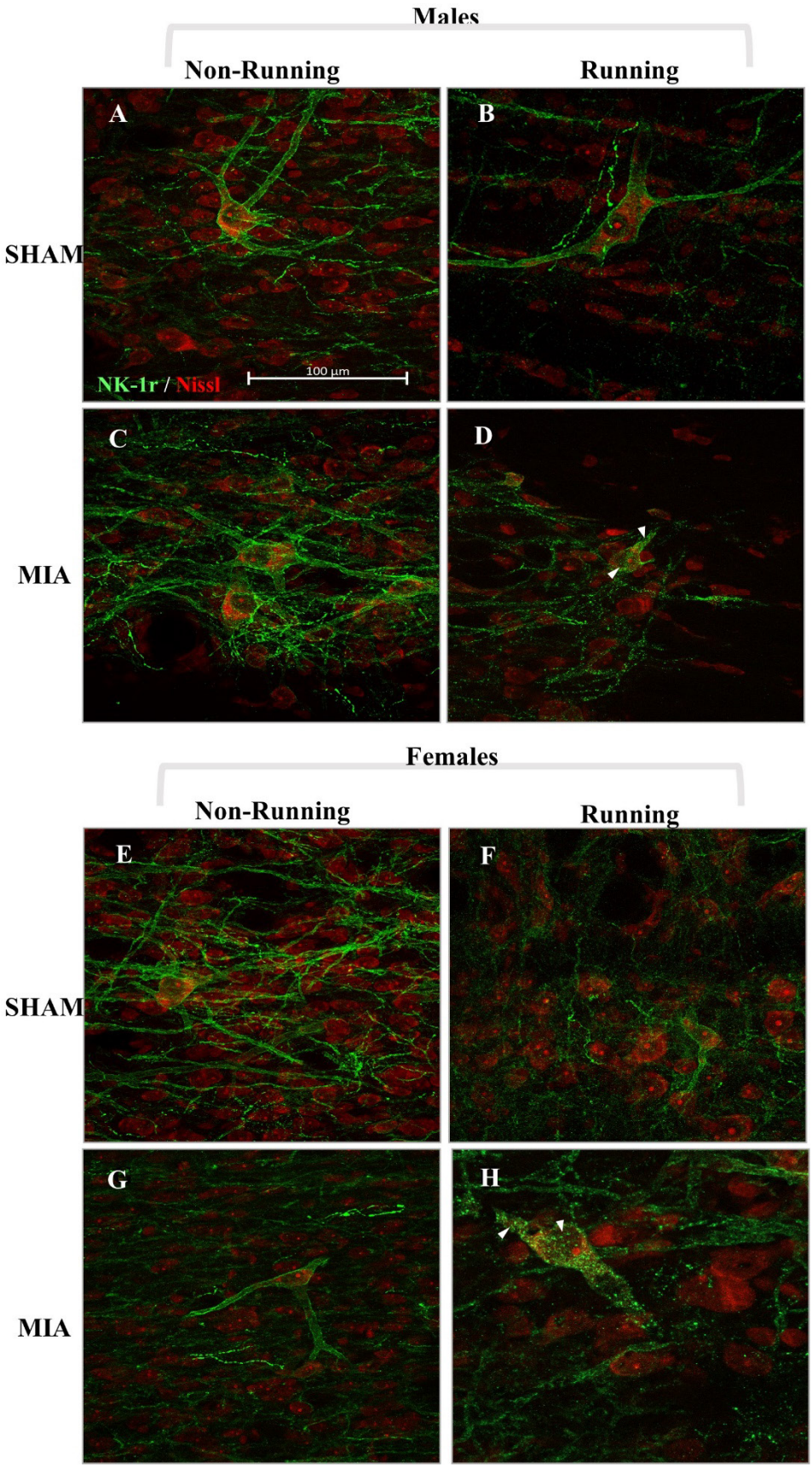
Males
Non-Running
Running
A
B
SHAM
NK-1r / Nissl
100 µm
C
D
MIA
Females
Non-Running
Running
E
F
SHAM
G
H
MIA

Chapter 5 Figure 2: Movement leads to internalization of the NK1-r.

Images A-D show NK1-r expressing neurons in males in the SHAM (A, B) and MIA (C, D) groups, where B and D were the running groups. Images E-H show NK1-r positive neurons in females in the SHAM (E, F) and MIA (G, H) group, where F and H were the running groups. Only in D and H, which were the male MIA running and female MIA running groups respectively, the presence of internalized NK1-r can be detected, characterized by large immunoreactive intracellular dots (arrows) that represent internalized NK1-r..

5.6 DISCUSSION

In this study, we detected increased numbers of lamina I NK1-r positive pyramidal neurons in the OA group. In a previous study, we found that in naïve animals only 22% of pyramidal neurons express the NK1-r [18]. As in the present study we did not use a retrograde labelling of projection neurons like we did in previous studies previously [3; 18], the increased number of pyramidal neurons expressing the NK1-r indicates that more cells of this type had upregulated the NK1-r bringing it to detection levels, so more neurons were detected. The lack of retrograde labelling to identify projection neurons is not as serious as it seems, because if only a very low percentage of lamina I project, the great majority of those expressing the NK1-r are projection neurons [21]. Therefore, we can say that the NK1-r immunopositive neurons in the current study represent projection neurons, The detection of NK1-r upregulation had not been previously described in an OA model.

We detected an internalization of NK1-r after treadmill exercise in all three types of lamina I projection neurons. This is important because it had never been detected in an OA model and such internalization a critical event in signaling cascades and has been associated with a marker of activation of pain-related pathways of the central nervous system [1; 2; 13]. We identified the presence of NK1-r internalization in both male and female MIA groups after running on the treadmill. This suggests that a movement of the OA-affected joint, in this case movement of the ankle joint via moderate running before the animals were perfused with fixatives, is sufficient to cause plasticity in pain circuitry.

Although antagonizing the NK1-r in clinical trials did not show any convincing efficacy, it was never tested as an adjuvant to novel approaches to pain treatment. Therefore, it is possible

that preventing NK1-r internalization with receptor antagonists may represent a novel target for therapeutic intervention in the management of chronic pain. By selectively modulating NK1-r receptor trafficking, it may be possible to attenuate maladaptive changes in pain processing reducing nociceptive signaling. Thus, elucidating the mechanisms underlying NK1-r internalization in the context of pain holds promise for the development of novel analgesic strategies with improved efficacy and fewer side effects.

The preliminary observations in this study have to be followed by a full study using retrograde labelling of spinal cord projection neurons, a larger number of animals, more time points and extensive behaviour testing. This should also include the effect of blocking receptor internalization on pain behaviour. However, our preliminary data looks promising.

5.7 ACKNOWLEDGEMENTS

We wish to thank Manon St. Louis for laboratory expertise. Valerie Bourassa acknowledges doctoral studentships from the Louise and Alan Edwards Foundation. Haley Deamond was a recipient of studentship from the McGill University Faculty of Medicine. This work was funded by Canadian Institutes of Health Research Operating Grant MOP-136903 and a grant from the Louise and Alan Edwards Foundation. The authors would also like to thank the McGill Advanced BioImaging Facility for the use of the LSM 710 and Zeiss AxioObserver. None of the authors have competing interests to disclose.

5.8 REFERENCES

[1] Abbadie C, Brown JL, Mantyh PW, Basbaum AI. Spinal cord substance P receptor immunoreactivity increases in both inflammatory and nerve injury models of persistent pain. Neuroscience 1996;70(1):201-209.

[2] Adelson D, Lao L, Zhang G, Kim W, Marvizón JC. Substance P release and neurokinin 1 receptor activation in the rat spinal cord increase with the firing frequency of C-fibers. Neuroscience 2009;161(2):538-553.

[3] Almarestani L, Waters SM, Krause JE, Bennett GJ, Ribeiro-da-Silva A. *De novo* expression of the neurokinin 1 receptor in spinal lamina I pyramidal neurons in polyarthritis. J Comp Neurol 2009;514(3):284-295.

[4] Bourassa V, Deamond H, Yousefpour N, Fitzcharles MA, Ribeiro-da-Silva A. Pain-related behavior is associated with increased joint innervation, ipsilateral dorsal horn gliosis, and dorsal root ganglia activating transcription factor 3 expression in a rat ankle joint model of osteoarthritis. Pain Rep 2020;5(5):e846.

[5] Carrasquillo Y, Gereau RW. Rodent models clarify the role of cells expressing the substance P receptor in pain. Drug Discovery Today: Disease Models 2004;1(2):107-113.

[6] Catherine A, Jodie T, Hantao L, Patrick WM, Allan IB. Inflammation Increases the Distribution of Dorsal Horn Neurons That Internalize the Neurokinin-1 Receptor in Response to Noxious and Non-Noxious Stimulation. The Journal of Neuroscience 1997;17(20):8049.

[7] Chen W, Marvizon JC. Neurokinin 1 receptor activation in the rat spinal cord maintains latent sensitization, a model of inflammatory and neuropathic chronic pain. Neuropharmacology 2020;177:108253.

[8] Ferguson SS, Downey WE, 3rd, Colapietro AM, Barak LS, Ménard L, Caron MG. Role of beta-arrestin in mediating agonist-promoted G protein-coupled receptor internalization. Science 1996;271(5247):363-366.

[9] Garcia M, Sakamoto K, Shigekawa M, Nakanishi S, Ito S. Multiple mechanisms of arachidonic acid release in Chinese hamster ovary cells transfected with cDNA of substance P receptor. Biochem Pharmacol 1994;48(9):1735-1741.

[10] Han ZS, Zhang ET, Craig AD. Nociceptive and thermoreceptive lamina I neurons are anatomically distinct. Nature Neurosci 1998;1(3):218-225.

[11] Hunt SP, Mantyh PW. The molecular dynamics of pain control. Nat Rev Neurosci 2001;2(2):83-91.

[12] Khasabov SG, Rogers SD, Ghilardi JR, Peters CM, Mantyh PW, Simone DA. Spinal neurons that possess the substance P receptor are required for the development of central sensitization. J Neurosci 2002;22(20):9086-9098.

[13] Mantyh PW, DeMaster E, Malhotra A, Ghilardi JR, Rogers SD, Mantyh CR, Liu H, Basbaum AI, Vigna SR, Maggio JE, et al. Receptor endocytosis and dendrite reshaping in spinal neurons after somatosensory stimulation. Science 1995;268(5217):1629-1632.

[14] Mitsuhashi M, Ohashi Y, Shichijo S, Christian C, Sudduth-Klinger J, Harrowe G, Payan DG. Multiple intracellular signaling pathways of the neuropeptide substance P receptor. J Neurosci Res 1992;32(3):437-443.

[15] Nakajima Y, Tsuchida K, Negishi M, Ito S, Nakanishi S. Direct linkage of three tachykinin receptors to stimulation of both phosphatidylinositol hydrolysis and cyclic AMP cascades in transfected Chinese hamster ovary cells. J Biol Chem 1992;267(4):2437-2442.

[16] Neogi T. The epidemiology and impact of pain in osteoarthritis. Osteoarthritis Cartilage 2013;21(9):1145-1153.

[17] Premont RT, Gainetdinov RR. Physiological roles of G protein-coupled receptor kinases and arrestins. Annu Rev Physiol 2007;69:511-534.

[18] Saeed AW, Ribeiro-da-Silva A. De novo expression of neurokinin-1 receptors by spinoparabrachial lamina I pyramidal neurons following a peripheral nerve lesion. J Comp Neurol 2013;521(8):1915-1928.

[19] Sharif Naeini R, Cahill CM, Ribeiro-da-Silva A, Ménard HA, Henry JL. Remodelling of spinal nociceptive mechanisms in an animal model of monoarthritis. Eur J Neurosci 2005;22(8):2005-2015.

[20] Todd AJ. Changes in NK1 and Glutamate Receptors in Pain. In: M Malcangio, editor. Synaptic Plasticity in Pain. New York, NY: Springer New York, 2009. pp. 3-19.

[21] Todd AJ, McGill MM, Shehab SAS. Neurokinin 1 receptor expression by neurons in laminae I, III and IV of the rat spinal dorsal horn that project to the brainstem. European Journal of Neuroscience 2000;12(2):689-700.

[22] Trafton JA, Basbaum AI. The contribution of spinal cord neurokinin-1 receptor signaling to pain. The Journal of Pain 2000;1(3, Supplement):57-65.

CHAPTER 6

General Discussion

6.1 Overview

This body of work highlights the importance of robust methodology to adequately study onset and maintenance of arthritis. For example, studies of changes in bone innervation have been few and far between in the literature, owing primarily to the difficulty and poor success of performing histological labelling on decalcified bone tissue. As a result, the pain field has suffered from a lack of understanding of pain mechanisms in arthritis, but also in diseases such as osteoporosis, and low back pain. For this thesis work, we developed a robust methodology for labelling nerve fibres in bone in various animal models of OA, osteoporosis, and bone fracture (see Chapter 2).

Additionally, we presented a fully integrated behavioral, histopathological and radiological characterization of a mono-iodoacetate (MIA) model of osteoarthritis (OA) of the rat ankle joint, which has advantages over commonly used models. We have shown that a dose of 2.4 mg of MIA in 40 µl of saline induced significant mechanical hypersensitivity and cold allodynia starting at 5 weeks post injection. Significant reduction of functional mobility, as reflected by time on treadmill, was observed in MIA animals starting at 4 weeks post MIA injection. This was likely due to pain in the affected joint, as percent ipsilateral weight-bearing decreased significantly in MIA animals after the treadmill activity.

Histological studies of decalcified joints showed significant cartilage loss correlating with the behaviour pattern and replicating known pathologic features of the human disease. X-ray microtomography (micro CT) scans of the ankle joint performed at 5 and 10 weeks post MIA injection confirmed that bone fragmentation and remodeling in our model are similar to those in human OA. Furthermore, a time course quantitative analysis performed at 1, 2, 5, and 10 weeks post MIA injection shows an increase in innervation by sympathetic and sensory nociceptive fibers

of the subchondral bone and synovial membrane, as detected by immunohistochemistry using antibodies against VMAT2 and CGRP. The suppression of sympathetic fibre activity following intra-peritoneal guanethidine also significantly, although modestly, reduced hyperalgesia in MIA animals at the 5-week time-point. These findings strongly suggest that anomalous fibre sprouting contributes to pain in OA.

In the dorsal horn, microgliosis and astrocytosis have previously been demonstrated in models of chronic pain. In this study, we provide a time course of changes in density of glial cells using antibodies against Iba1 and GFAP, markers of microglia and astrocytes respectively. We observed an increased density of both astrocyte and microglia starting at 4 weeks, which correlate with pain-related behavior in this model. Area to length ratio analysis also revealed a switch from the ramified to the amoeboid form in microglia, indicative of activation. Interestingly, the suppression of microglia activity by minocycline, and inhibition of astrocytes by fluorocitrate reduced mechanical allodynia in MIA animals at the 5-week time-point. This alleviation was not observed in cold allodynia. These findings suggest that pro-inflammatory changes caused by glial activation also contribute to chronic pain in OA.

Additionally, a time course characterization of cyclic AMP-dependent transcription factor (ATF3) expression, a marker for neuronal stress associated with axonal degeneration/regeneration, in dorsal root ganglia shows a biphasic pattern of ATF3 expression consistent with injection of MIA and occurrence of pain-related behavior. At late time-points, over 50% of large-diameter cell bodies are ATF3. Immunohistochemistry of DRGs using antibodies against CGRP, NF200, Parvalbumin (PV), and IB4 staining show that these large diameter neurons expressing ATF3 also express PV. These findings may implicate Aβ mechanoreceptors innervating the articular joint in

OA pain and drives interest in understanding the contribution of lamina III-V that receives input from these fibers, in the persistence of OA pain.

In agreement with a previous studies from our lab in neuropathic and inflammatory arthritis models [12; 178], we detected an increase of substance P receptor (NK1-r) expression in pyramidal projection neurons of lamina I, which normally only express the NK1-r in few cells. Importantly, we observed NK1 receptor internalization following treadmill exercise in lamina I projection neurons in the MIA ankle joint model of arthritis, in cohorts of male and female rats, but these whether these changes occur in lamina III-V is yet to be investigated.

This comprehensive body of work accentuates the critical significance of methodological robustness in the study of disease onset and maintenance. Our research presents a novel methodology for nerve fiber labeling in various animal models of osteoarthritis (OA), osteoporosis, and bone fracture. Our studies also introduced a novel mono-iodoacetate (MIA) model of rat ankle joint OA. This was important as previous studies wee limited to the knee joint, which makes harder the comparison of data with neuropathic pain models. We provided a fully integrated characterization of our model, encompassing behavioral, histopathological, and radiological aspects. Furthermore, our thesis explores the temporal expression of ATF3, a marker for neuronal stress, implicating Aβ mechanoreceptors in OA pain. These findings shed light on the complex mechanisms underpinning OA pain and emphasize the potential for innovative interventions and enhanced understanding of chronic pain pathways.

6.2 An evolutionary and compassionate perspective on chronic pain

As pain scientist, we spend years studying the best methods to assess pain in human patients, and to replicate pain behaviors in animal models. A lot of this time is spent commenting and providing criticism on our current methods which are simplistic and may be unreliable in regard to correlation with the clinic. Yet, we always circle back to those same old methods because they are established. Why does this happen? It is because physical pain, like psychological pain, are unique individual experiences that are hard to describe. The best written description of pain that I have ever read has come from the book Darkness Visible: A Memoir of Madness by William Styron [211]. The author describes the continuum between physical and psychological pain as he experiences, and even he, a prolific writer, is at loss for words when the pain is at its worst. This is a very moving account of the pain experience.

One of the common themes throughout the chapters of this thesis as been the ever-growing list of contributors to underlying mechanisms of chronic pain, specifically in OA. A previous version of this thesis stated that “unlike acute pain, chronic pain has no useful purpose”. I have since reflected on this statement and contemplated the following: while acute pain serves as a vital alarm system, alerting us to potential harm and promoting protective behaviors, the concept of chronic pain's "usefulness" becomes more intricate upon deeper analysis.

Advancements in comprehending pain mechanisms can be enriched through an evolutionary medicine lens, which considers how the ability to experience pain offers selective advantages, the trade-offs that have shaped these mechanisms, and the evolutionary rationale behind the system's susceptibility to prolonged and excessive pain. Instances of deficient pain syndromes tragically underscore pain's role in motivating escape from and avoidance of situations leading to tissue damage. An example of a deficient pain syndrome is congenital insensitivity to

pain (CIP), also known as congenital analgesia. This rare condition is characterized by the inability to perceive pain, leading affected individuals to not experience typical sensations of pain, even in response to injuries or harmful stimuli. This might seem like an advantage at first glance, but it can have serious consequences, as the absence of pain signals makes it difficult for individuals to recognize injuries, infections, or other health issues that usually prompt protective behaviors. As a result, individuals with CIP are at a higher risk of sustaining injuries and complications that could otherwise be avoided with normal pain perception [39].

What may appear as excessive pain often reflects a normal response, as the cost of heightened pain is frequently far lower than the consequences of diminished pain (just like the principle of having a carbon dioxide detector in your home, we would prefer to be woken up by an alarm than and be annoyed than not to). The tendency for acute pain to be adaptive by lowering pain thresholds as stimulation persists is fascinating and is contrasting to chronic pain which has been shown to involve many peripheral and central sensitization mechanisms [35; 92; 150; 223].

There is a theory that emotional states such as anxiety, guilt, and low mood might have evolved from antecedent physical pain. The brain mechanisms overseeing physical pain exhibit strong overlaps with those responsible for psychological pain [53; 134; 135]. An extensive meta-analysis of 18 studies unveiled notable diversity in the brain regions engaged in different forms of psychological pain. While no single brain region consistently activated across all studies, an intriguing pattern is that the regions that were activated are almost always those associated with pain mechanisms [135]. Genetic correlation between psychological and physical pain are yet to be described [146]. Yet, the psychological pain in the form of depression, anxiety, and insomnia is almost always associated with chronic physical pain [71].

Chronic pain, arising from conditions like osteoarthritis, can persist long after its initial trigger has subsided, leading to significant physical, emotional, and societal burdens. While chronic pain may not possess the same immediate survival-oriented purpose as acute pain, its persistence highlights the complexity of the nervous system and the intricate nature of pain processing. Moreover, chronic pain's multifaceted impacts on an individual's quality of life and overall well-being prompt a re-evaluation of its significance.

I have grown to have a better appreciation an understanding for nuanced roles that pain plays in different contexts. While acute pain is undoubtedly adaptive and protective, chronic pain challenges our understanding of pain's purpose. It serves as a reminder that pain perception is not solely a biological phenomenon; rather, it is influenced by psychological, social, and environmental factors. Chronic pain's persistence raises questions about maladaptive changes within the nervous system, emphasizing the importance of deciphering the underlying mechanisms to develop targeted interventions. Recognizing that chronic pain is not isolated to a specific body part but rather engulfs the individual's entire being, we are compelled to explore comprehensive treatment approaches that address physical, mental, and emotional aspects. For this reason, midway trough my Ph.D. degree, I enrolled in the McGill's Certificate in Chronic Pain Management offered by the Faculty of Physical and Occupational Therapy, which I completed co-currently with this degree.

My introduction to the bio-psycho-social model of chronic pain came through my participation in this certificate program. The bio-psycho-social model presents a holistic perspective on pain by recognizing the intricate interplay of biological, psychological, and social factors in shaping an individual's experience of chronic pain. Unlike the traditional biomedical approach that predominantly focuses on physiological aspects, the bio-psycho-social model

considers how biological, psychological, and social factors interact and influence each other to contribute to the development and perpetuation of chronic pain. It emphasizes that chronic pain is not solely the result of a specific injury or tissue damage but is influenced by a complex web of physical, emotional, cognitive, and social factors. Understanding this model has been transformative for the field as it underscores the need for a comprehensive and multidisciplinary approach to treating and managing chronic pain, taking into account not only the biological aspects but also the psychological and social dimensions that play a pivotal role in an individual's pain experience and overall well-being.

The very act of acknowledging the distress that individuals with chronic pain experience fosters a collective determination to alleviate their suffering. This empathy spurs innovation, propelling us to delve deeper into the intricate mechanisms of pain perception, seeking novel interventions that mitigate pain's impact on every facet of a person's life. As we bridge the gap between science and compassion, we not only advance our understanding of pain but also affirm our commitment to enhancing the quality of life for those who bear its burden. Chronic pain may not serve a positive purpose, but the courage and resilience of those suffering with chronic pain certainly does.

6.3 Osteoarthritis: a disease of the joint or the bone?

Studying chronic pain associated with osteoarthritis (OA) and studying the prevention of OA represent two distinct but interconnected areas of research within the field of musculoskeletal health. Studying the prevention of OA involves identifying risk factors, early markers, and interventions that can potentially delay or mitigate the onset of OA in individuals at risk. This research often emphasizes understanding the biomechanical, genetic, environmental, and lifestyle

factors that contribute to the development of OA. Preventive measures might include promoting healthy habits, encouraging physical activity, addressing joint biomechanics, and understanding the role of inflammation and metabolic factors. By focusing on prevention, researchers aim to reduce the overall burden of OA by slowing down or even halting the disease process before it leads to symptomatic joint degeneration and chronic pain.

On the other hand, studying chronic pain associated with OA focuses on understanding the mechanisms underlying pain perception, transmission, and modulation in individuals already experiencing the condition. This line of research delves into how changes in joint structure, neural pathways, and signaling molecules contribute to the development and persistence of pain in OA patients. This requires animal models that can quickly and consistently generate irreversible pain and established pathological markers. Although investigating onset of OA was never the focus of this work, investigating chronic pain in OA is crucial for developing effective pain management strategies and improving the quality of life for those living with this condition, and preventative measure for OA may be one of most minimally invasive and feasible measure to adopt to manage the arthritis pain epidemic.

We discussed in this work that there exists a substantiated debate regarding the direction of damage, in both OA and RA. For long, the accepted theory was that mechanical stress on the joint caused a cascade of degeneration to the cartilage and subsequently the bone that led to advanced progression of arthritis. However, invasion of synovial tissue within the joint cavity and the presence of inflammatory infiltrates from the bone marrow have been implicated in the aforementioned damage [212]. In RA, research exploring the immune modulation of osteoclasts has shaped of the creation of a research domain known as “osteoimmunology” [78]. This emerging field is dedicated to unraveling the intricate interactions between the skeletal and immune systems

at a molecular level. Mounting empirical data supports the hypothesis that the augmented osteoclast activity implicated in the bone deterioration observed in RA is a consequence of the heightened activity of osteoclasts, which is driven by the activation of a distinct subset of helper T cells, which produces IL-17 [155]. Osteoclasts are responsible for bone resorption, where bone tissue is broken down and its mineral and organic components are released into the bloodstream. Bone resorption is a natural part of bone remodeling, which helps maintain bone health and structure by replacing old bone with new bone. However, excessive or unregulated bone resorption can lead to bone loss and inflammation. More specifically, produced primarily by macrophages and dendritic cells in response to both exogenous and endogenous cues, IL-23 plays a pivotal role in driving the differentiation and activation of T helper 17 (Th17) cells. This process leads to the subsequent secretion of various cytokines, including IL-17A, IL-17F, IL-6, IL-22, and TNF-α. Antibodies directed against IL-17 or IL-23 were anticipated to confer favorable outcomes in autoimmune conditions. However, despite the compelling findings from experimental models and human in vitro and in situ studies, the therapeutic effectiveness of IL-17A inhibition in RA appears to be somewhat moderate [216].

In OA, osteoclasts have also been implicated to play a role both in animal models and human patients. In equine OA, osteoclasts are observed migrating to the subchondral bone [23]. The inhibition of subchondral bone resorption has also been favorable in animal models of OA [161; 200].

Although the work presented in this thesis did not investigate changes in osteoclast mechanisms that may contribute to OA pathology or OA pain-related behavior, the methodology presented in Chapter 2 could offer to propel our understanding forward by visualizing markers of such mechanisms in the bone using immunostaining, which is very complex to achieve. Although

Chapter 2 focused on detection of nerve fibers in bone, the same IHC protocol can help identify markers associated with disrupted bone resorption by detecting specific proteins or cell types involved in the process. For example, IHC can be used to detect markers of osteoclast activity, such as tartrate-resistant acid phosphatase (TRAP) and cathepsin K, which are enzymes involved in bone matrix degradation. Additionally, markers of bone turnover, such as receptor activator of nuclear factor kappa-B ligand (RANKL) and osteoprotegerin (OPG), can be visualized using immunostaining to understand the balance between bone resorption and formation. We propose that these experiments could be carried out in a way that can also track migration of these markers through the subchondral bone, in the hope to identify direction of damage. This information can help in the development of targeted therapies and interventions to mitigate excessive bone loss and related diseases.

In essence, although we cannot yet elucidate the origin of disease in OA, this body of work examines the dynamics of multiple pathological factors of the joint, and an investigation into bone resorption is the logical next step to explore whether osteoarthritis primarily stems from joint dysfunction or bone alterations. These methodologies have the potential to unravel the intricate relationship between nerve fibers and joint or bone pathology, ultimately advancing our comprehension of OA-related pain and contributing to more tailored pain management approaches.

6.4 Correlative studies of proprioceptive afferent contributions to chronic pain

In this body of work, we provided several pieces of evidence that proprioceptors are affected in the OA disease state. However, the evidence that we provided does not confirm that proprioceptors are actively participating in pain circuitry in the spinal cord.

Large-fiber neuropathy refers to a specific type of peripheral neuropathy that predominantly affects the larger nerve fibers responsible for transmitting sensory information related to touch, proprioception, and vibration. These nerve fibers, known as A-alpha and A-beta fibers, are crucial for relaying signals connected to position sense, coordination, and tactile sensations. It's important to note that while arthritis is generally not considered a condition arising from or sustained by large-fiber neuropathy, osteoarthritis patients often exhibit symptoms such as muscle weakness, protective movement avoidance, and joint instability [60; 157; 167; 193]. These symptoms can disrupt the normal flow of proprioceptive signals that aid the brain in comprehending joint alignment and orientation.

As OA progresses, the joint's cartilage, which plays a crucial role in transmitting sensory information, deteriorates. A proposed mechanisms is that the diminished cartilage can lead to irregular joint mechanics, altered joint positioning, and reduced proprioceptive feedback [191]. Consequently, individuals with OA might experience difficulties in accurately sensing joint position, movement, and alignment. This compromised proprioceptive function can negatively impact their ability to maintain balance, coordinate movements, and execute daily activities.

In light of these considerations, the relationship between pain and proprioception in OA remains a significant research question. Numerous studies have demonstrated a phenomenon where thick afferents undergo disinhibition, consequently permitting the transmission of touch and proprioceptive information into the pain pathway by activating nociceptive cells in lamina I [147; 241]. Initially, it was believed that following nerve lesions, these afferents would regenerate and innervate the superficial layer, but whether this contributes to the disinhibition is challenged [105]. Despite the limited current understanding, studies examining the connection between knee joint proprioception, pain, and disability in a substantial cohort of knee OA patients have yielded

intriguing results. Surprisingly, individuals with varying impairment exhibited minimal differences in pain and disability [21]. In more recent prospective and longitudinal assessments, notable although modest connections have been identified between initial proprioceptive acuity and the course of pain experienced over an extended period [60]. These contrasting findings underscore the complexity of the interplay between proprioceptive deficits and the pain experienced in osteoarthritis. To unravel this intricate relationship, further investigations are warranted to elucidate how proprioceptive impairment contributes to pain signaling pathways and overall functional limitations in OA individuals.

Proprioceptors terminate predominantly in lamina III-V of the dorsal horn of the spinal cord, where they communicate with interneurons and projection neurons. If proprioceptors are indeed affected in established OA, they may convey abnormal signalling to the CNS. These aberrant proprioceptive signals can be interpreted by the central nervous system as pain, contributing to the perception of pain in OA patients, similar to what happens in neuropathic pain [163]. What could likely be happening is that the abnormal proprioceptive signals from the joint can interact with pain-signaling pathways, leading to a complex interplay between sensory information related to joint movement and the perception of pain. This interaction can potentially contribute to the chronic pain experienced by individuals with osteoarthritis.

The investigation into proprioceptive and nociceptive mix-up has precedence. Chapter 5 of this thesis showed an increased population of pyramidal projection neurons expressing the Nk1-r, which normally does not transmit nociceptive signals [12]. The presence of Nk1-r in this cell type suggests the recruitment of innocuous circuitry into pain transmission in the pathological state. Another study that comes to mind is Yaksh et al. (1980) in the work titled “Behavioral and autonomic correlates of the tactile evoked allodynia produced by spinal glycine inhibition: effects

of modulatory receptor systems and excitatory amino acid antagonists". In this publication, the authors investigated how well described primary afferents, in this case low threshold afferents, are in reality subject to ongoing modulation. When that modulation is lost, a miscoding of the afferent stimulus occurs, and now these low thresholds primary afferents are yielding a pain relevant message [243].

For instance, wide dynamic range (WDR) neurons are an essential part of the pain processing pathway, as they contribute to the perception of both acute and chronic pain. Their ability to respond to a wide range of stimuli allows them to transmit information about the intensity and location of pain signals. In the context of chronic pain conditions, such as osteoarthritis, WDR neurons may become sensitized and contribute to the amplification of pain signals, leading to persistent pain perception. Understanding the role of WDR neurons in pain processing is important for developing effective pain management strategies.

Future studies could show incredible promise in answering the question whether proprioceptors are functionally equipped to transmit or modulate pain-related signaling. To return to Yaksh's study mentioned above, primary afferents were modulated by the intrathecal administration of glycine (strychnine) or GABA (bicuculline) to successfully inhibit that aforementioned modulation. This implies that these afferents have the "capacity" to take on another role, and that role can be activated in a specific setting. No studies have yet investigated whether this is also true for other types of primary afferents. If proprioceptors are in fact capable of yielding pain-related inputs, supressing central modulation could reveal this behavior. This would highly support our claims that proprioceptors are affected in the chronic pain state of OA.

Overall, the involvement of proprioceptors in the dorsal horn of the spinal cord suggests that altered proprioceptive signaling due to joint pathology can contribute to the pain experienced

by individuals with osteoarthritis. Understanding these mechanisms can provide insights into the complex nature of pain perception in OA and may guide the development of more targeted treatments aimed at addressing the neuropathic aspects of OA pain.

6.5 Overall summary and conclusion

We discussed the challenges and complexities of understanding and managing pain, specifically chronic pain associated with conditions like osteoarthritis (OA). We reflected on the difficulties in assessing pain and replicating pain behaviors in animal models, emphasizing the uniqueness of individual pain experiences. We explored the purpose of chronic pain, suggesting that while acute pain serves as an alarm system, the usefulness of chronic pain is more intricate and requires deeper analysis. While we can continue to reflect on the role of the scientist in the wellbeing of individuals living with chronic pain, we can also map out the complexities of pathological changes that occur in OA to identify the best directions for therapeutic strategies.

In this thesis, we presented a time-course comprehensive study in a rat ankle joint model of osteoarthritis (OA) induced by mono-iodoacetate (MIA). Our research establishes a link between pain-related behaviors and pathological transformations, encompassing cartilage and bone deterioration, nerve sprouting in the bone and synovium, as well as heightened glial cell density and activation in the dorsal horn.

Numerous clinical and pre-clinical indications point toward a neuropathic element in OA pain, evidenced by occurrences like microgliosis in the spinal cord and the modulation of nociceptors by sympathetic afferents. Yet, a plausible neuropathic pain-like component in OA entails the potential influence of primary afferent damage subsequent to joint degeneration. Our

investigation reveals the presence of Activating Transcription Factor 3 (ATF3), a marker of neuronal stress, predominantly within larger cell bodies co-located with parvalbumin (PV), a marker characteristic of proprioceptors. This suggests that Aβ mechanoreceptors innervating the articular joint are particularly influenced by joint degeneration in OA pain. This underscores the significance of understanding the role of laminae III-V, which receives input from these fibers, in the perpetuation of OA pain.

I would like to stress again that the relationship between proprioception and chronic pain in OA should be investigated further, as I sense that my exploration of this topic only covered the surface. Nonetheless, I hope that after reading this work, you too can go to bed having a better appreciation of the intricate nature of pain perception, the challenges in comprehending chronic pain, and the potential implications of altered proprioception in the context of OA-related pain.

REFERENCES (Introduction and Discussion)

[1] Aapro M, Carides A, Rapoport BL, Schmoll HJ, Zhang L, Warr D. Aprepitant and fosaprepitant: a 10-year review of efficacy and safety. The oncologist 2015;20(4):450-458.

[2] Ab Aziz CB, Ahmad AH. The role of the thalamus in modulating pain. Malays J Med Sci 2006;13(2):11-18.

[3] Abdo H, Calvo-Enrique L, Lopez JM, Song J, Zhang MD, Usoskin D, El Manira A, Adameyko I, Hjerling-Leffler J, Ernfors P. Specialized cutaneous Schwann cells initiate pain sensation. Science 2019;365(6454):695-699.

[4] Abraira VE, Ginty DD. The sensory neurons of touch. Neuron 2013;79(4):618-639.

[5] Adães S, Mendonça M, Santos TN, Castro-Lopes JM, Ferreira-Gomes J, Neto FL. Intra-articular injection of collagenase in the knee of rats as an alternative model to study nociception associated with osteoarthritis. Arthritis research & therapy 2014;16(1):R10-R10.

[6] Adams F. The genuine works of Hippocrates, Vol. 1: W. Wood, 1886.

[7] Ahmed M, Bjurholm A, Kreicbergs A, Schultzberg M. Sensory and autonomic innervation of the facet joint in the rat lumbar spine. Spine (Phila Pa 1976) 1993;18(14):2121-2126.

[8] Aho K, Koskenvuo M, Tuominen J, Kaprio J. Occurrence of rheumatoid arthritis in a nationwide series of twins. The Journal of rheumatology 1986;13(5):899-902.

[9] Aj LB. The first description of rheumatoid arthritis. Unabridged text of the doctoral dissertation presented in 1800. Joint Bone Spine 2001;68(2):130-143.

[10] Al-Saffar FJ, Ganabadi S, Yaakub H, Fakurazi S. Collagenase and Sodium Iodoacetate-Induced Experimental Osteoarthritis Model in Sprague Dawley Rats. Asian Journal of Scientific Research 2009;2(4):167-179.

[11] Almarestani L, Longo G, Ribeiro-da-Silva A. Autonomic fiber sprouting in the skin in chronic inflammation. Mol Pain 2008;4:56.

[12] Almarestani L, Waters SM, Krause JE, Bennett GJ, Ribeiro-da-Silva A. *De novo* expression of the neurokinin 1 receptor in spinal lamina I pyramidal neurons in polyarthritis. J Comp Neurol 2009;514(3):284-295.

[13] Almeida A, Lima D. Activation by Cutaneous or Visceral Noxious Stimulation of Spinal Neurons Projecting to the Medullary Dorsal Reticular Nucleus in the Rat: A c-fos Study. European Journal of Neuroscience 1997;9(4):686-695.

[14] Angum F, Khan T, Kaler J, Siddiqui L, Hussain A. The Prevalence of Autoimmune Disorders in Women: A Narrative Review. Cureus 2020;12(5):e8094-e8094.

[15] Asato F, Butler M, Blomberg H, Gordh T. Variation in rat sciatic nerve anatomy: implications for a rat model of neuropathic pain. J Peripher Nerv Syst 2000;5(1):19-21.

[16] Badley EM, Wilfong JM, Zahid S, Perruccio AV. THE STATUS OF ARTHRITIS IN CANADA: NATIONAL REPORT. Arthritis Society: Arthritis Community Research and Evaluation Unit (ACREU), 2019. p. 34.

[17] Bauer GE, Croll FJ, Goldrick RB, Jeremy D, Raftos J, Whyte HM, Young AA. Guanethidine in treatment of hypertension. Br Med J 1961;2(5249):410-415.

[18] Bautista DM, Siemens J, Glazer JM, Tsuruda PR, Basbaum AI, Stucky CL, Jordt S-E, Julius D. The menthol receptor TRPM8 is the principal detector of environmental cold. Nature 2007;448(7150):204-208.

[19] Benbouzid M, Pallage V, Rajalu M, Waltisperger E, Doridot S, Poisbeau P, Freund-Mercier MJ, Barrot M. Sciatic nerve cuffing in mice: a model of sustained neuropathic pain. Eur J Pain 2008;12(5):591-599.

[20] Benito MJ, Veale DJ, FitzGerald O, van den Berg WB, Bresnihan B. Synovial tissue inflammation in early and late osteoarthritis. Annals of the Rheumatic Diseases 2005;64(9):1263.

[21] Bennell KL, Hinman RS, Metcalf BR, Crossley KM, Buchbinder R, Smith M, McColl G. Relationship of knee joint proprioception to pain and disability in individuals with knee osteoarthritis. Journal of Orthopaedic Research 2003;21(5):792-797.

[22] Bennett GJ, Xie YK. A peripheral mononeuropathy in rat that produces disorders of pain sensation like those seen in man. Pain 1988;33(1):87-107.

[23] Bertuglia A, Lacourt M, Girard C, Beauchamp G, Richard H, Laverty S. Osteoclasts are recruited to the subchondral bone in naturally occurring post-traumatic equine carpal osteoarthritis and may contribute to cartilage degradation. Osteoarthritis and Cartilage 2016;24(3):555-566.

[24] Besson J-M, Fardin V, Olivéras J-L. Analgesia Produced by Stimulation of the Periaqueductal Gray Matter: True Antinoceptive Effects Versus Stress Effects. In: A Depaulis, R Bandler, editors. The Midbrain Periaqueductal Gray Matter: Functional, Anatomical, and Neurochemical Organization. Boston, MA: Springer US, 1991. pp. 121-138.

[25] Besson JM, Chaouch A. Peripheral and spinal mechanisms of nociception. Physiol Rev 1987;67(1):67-186.

[26] Boscan P, Pickering AE, Paton JF. The nucleus of the solitary tract: an integrating station for nociceptive and cardiorespiratory afferents. Exp Physiol 2002;87(2):259-266.

[27] Boyle KA, Gradwell MA, Yasaka T, Dickie AC, Polgár E, Ganley RP, Orr DPH, Watanabe M, Abraira VE, Kuehn ED, Zimmerman AL, Ginty DD, Callister RJ, Graham BA, Hughes DI. Defining a Spinal Microcircuit that Gates Myelinated Afferent Input: Implications for Tactile Allodynia. Cell Rep 2019;28(2):526-540.e526.

[28] Buckland-Wright C. Subchondral bone changes in hand and knee osteoarthritis detected by radiography. Osteoarthritis Cartilage 2004;12 Suppl A:S10-19.

[29] Buckwalter JA, Mankin HJ, Grodzinsky AJ. Articular cartilage and osteoarthritis. Instr Course Lect 2005;54:465-480.

[30] Caligaris M, Ateshian GA. Effects of sustained interstitial fluid pressurization under migrating contact area, and boundary lubrication by synovial fluid, on cartilage friction. Osteoarthritis Cartilage 2008;16(10):1220-1227.

[31] Cameron D, Polgár E, Gutierrez-Mecinas M, Gomez-Lima M, Watanabe M, Todd AJ. The organisation of spinoparabrachial neurons in the mouse. Pain 2015;156(10):2061-2071.

[32] Chen CG, Thuillier D, Chin EN, Alliston T. Chondrocyte-intrinsic Smad3 represses Runx2-inducible matrix metalloproteinase 13 expression to maintain articular cartilage and prevent osteoarthritis. Arthritis Rheum 2012;64(10):3278-3289.

[33] Chen M, Lichtler AC, Sheu TJ, Xie C, Zhang X, O'Keefe RJ, Chen D. Generation of a transgenic mouse model with chondrocyte-specific and tamoxifen-inducible expression of Cre recombinase. Genesis 2007;45(1):44-50.

[34] Choi B, Rowbotham MC. Effect of adrenergic receptor activation on post-herpetic neuralgia pain and sensory disturbances. Pain 1997;69(1-2):55-63.

[35] Coderre TJ, Katz J. Peripheral and central hyperexcitability: differential signs and symptoms in persistent pain. Behavioral and Brain Sciences 1997;20(3):404-419.

[36] Condemi JJ. The Autoimmune Diseases. JAMA 1992;268(20):2882-2892.

[37] Copeman WSC. A Short History of the Gout and the Rheumatic Diseases: University of California Press, 1964.

[38] Craig AD. Distribution of brainstem projections from spinal lamina I neurons in the cat and the monkey. J Comp Neurol 1995;361(2):225-248.

[39] Daneshjou K, Jafarieh H, Raaeskarami SR. Congenital Insensitivity to Pain and Anhydrosis (CIPA) Syndrome; A Report of 4 Cases. Iran J Pediatr 2012;22(3):412-416.

[40] Darian-Smith I, Johnson KO, Dykes R. "Cold" fiber population innervating palmar and digital skin of the monkey: responses to cooling pulses. J Neurophysiol 1973;36(2):325-346.

[41] De Clerck LS, De Gendt CM, Bridts CH, Van Osselaer N, Stevens WJ. Expression of neutrophil activation markers and neutrophil adhesion to chondrocytes in rheumatoid arthritis patients: relationship with disease activity. Res Immunol 1995;146(2):81-87.

[42] Decosterd I, Woolf CJ. Spared nerve injury: an animal model of persistent peripheral neuropathic pain. Pain 2000;87(2):149-158.

[43] Dequeker J. Arthritis in Flemish paintings (1400-1700). British medical journal 1977;1(6070):1203-1205.

[44] Dequeker J, Luyten FP. The history of osteoarthritis-osteoarthrosis. Ann Rheum Dis 2008;67(1):5-10.

[45] Descartes R, Hall TS. Treatise of man. Amherst, N.Y.: Prometheus Books, 2003.

[46] Descartes R, Reynolds B. Principles of philosophy. Lewiston, N.Y., USA: E. Mellen Press, 1988.

[47] Diamandopoulos AA, Rakatsanis KG, Diamantopoulos N. A neolithic case of down syndrome? Journal of the History of the Neurosciences 1997;6(1):86-89.

[48] Dimitroulas T, Duarte RV, Behura A, Kitas GD, Raphael JH. Neuropathic pain in osteoarthritis: a review of pathophysiological mechanisms and implications for treatment. Seminars in arthritis and rheumatism 2014;44(2):145-154.

[49] Ding C, Jones G, Wluka AE, Cicuttini F. What can we learn about osteoarthritis by studying a healthy person against a person with early onset of disease? Curr Opin Rheumatol 2010;22(5):520-527.

[50] Dobson GP, Letson HL, Grant A, McEwen P, Hazratwala K, Wilkinson M, Morris JL. Defining the osteoarthritis patient: back to the future. Osteoarthritis and Cartilage 2018;26(8):1003-1007.

[51] Down JL. Observations on an ethnic classification of idiots. 1866. Ment Retard 1995;33(1):54-56.

[52] Drummond PD. Noradrenaline increases hyperalgesia to heat in skin sensitized by capsaicin. Pain 1995;60(3):311-315.

[53] Eisenberger NI. The pain of social disconnection: examining the shared neural underpinnings of physical and social pain. Nat Rev Neurosci 2012;13(6):421-434.

[54] Entezami P, Fox DA, Clapham PJ, Chung KC. Historical perspective on the etiology of rheumatoid arthritis. Hand clinics 2011;27(1):1-10.

[55] Erickson JD, Schafer MK, Bonner TI, Eiden LE, Weihe E. Distinct pharmacological properties and distribution in neurons and endocrine cells of two isoforms of the human vesicular monoamine transporter. Proc Natl Acad Sci U S A 1996;93(10):5166-5171.

[56] Feldman DE, Brecht M. Map plasticity in somatosensory cortex. Science 2005;310(5749):810-815.

[57] Fell HB, Jubb RW. The Effect of Synovial Tissue on the Breakdown of Articular Cartilage in Organ Culture. Arthritis & Rheumatism 1977;20(7):1359-1371.

[58] Felson DT. Clinical practice. Osteoarthritis of the knee. N Engl J Med 2006;354(8):841-848.

[59] Felson DT, Couropmitree NN, Chaisson CE, Hannan MT, Zhang Y, McAlindon TE, LaValley M, Levy D, Myers RH. Evidence for a Mendelian gene in a segregation analysis of generalized radiographic osteoarthritis: the Framingham Study. Arthritis Rheum 1998;41(6):1064-1071.

[60] Felson DT, Gross KD, Nevitt MC, Yang M, Lane NE, Torner JC, Lewis CE, Hurley MV. The effects of impaired joint position sense on the development and progression of pain and structural damage in knee osteoarthritis. Arthritis Rheum 2009;61(8):1070-1076.

[61] Feng X, McDonald JM. Disorders of bone remodeling. Annu Rev Pathol 2011;6:121-145.

[62] Finerman G, Noyes FR. Biology and Biomechanics of The traumatized synovial joint: the knee as a model: Amer Academy of Orthopaedic, 1992.

[63] Fiorito S, Magrini L, Adrey J, Mailhé D, Brouty-Boyé D. Inflammatory status and cartilage regenerative potential of synovial fibroblasts from patients with osteoarthristis and chondropathy. Rheumatology 2005;44(2):164-171.

[64] Forster H, Fisher J. The influence of continuous sliding and subsequent surface wear on the friction of articular cartilage. Proc Inst Mech Eng H 1999;213(4):329-345.

[65] Frank EH, Grodzinsky AJ. Cartilage electromechanics—I. Electrokinetic transduction and the effects of electrolyte pH and ionic strength. Journal of biomechanics 1987;20(6):615-627.

[66] Fulwiler CE, Saper CB. Subnuclear organization of the efferent connections of the parabrachial nucleus in the rat. Brain Res 1984;319(3):229-259.

[67] Galen. Claudii Galeni opera omnia: Cambridge University Press, 1822.

[68] García-García MJ. A History of Mouse Genetics: From Fancy Mice to Mutations in Every Gene. In: A Liu, editor. Animal Models of Human Birth Defects. Singapore: Springer Singapore, 2020. pp. 1-38.

[69] Gardner E. The innervation of the knee joint. The Anatomical Record 1948;101(1):109-130.

[70] Gardner E, Gray DJ. The innervation of the joints of the foot. The Anatomical Record 1968;161(2):141-148.

[71] Gatchel RJ. Comorbidity of Chronic Pain and Mental Health Disorders: The Biopsychosocial Perspective: American Psychological Association, 2004. pp. 795-805.

[72] Gibbs RA, Weinstock GM, Metzker ML, Muzny DM, Sodergren EJ, Scherer S, Scott G, Steffen D, Worley KC, Burch PE, Okwuonu G, Hines S, Lewis L, DeRamo C, Delgado O, Dugan-Rocha S, Miner G, Morgan M, Hawes A, Gill R, Celera, Holt RA, Adams MD, Amanatides PG, Baden-Tillson H, Barnstead M, Chin S, Evans CA, Ferriera S, Fosler C, Glodek A, Gu Z, Jennings D, Kraft CL, Nguyen T, Pfannkoch CM, Sitter C, Sutton GG, Venter JC, Woodage T, Smith D, Lee HM, Gustafson E, Cahill P, Kana A, Doucette-Stamm L, Weinstock K, Fechtel K, Weiss RB, Dunn DM, Green ED, Blakesley RW,

Bouffard GG, De Jong PJ, Osoegawa K, Zhu B, Marra M, Schein J, Bosdet I, Fjell C, Jones S, Krzywinski M, Mathewson C, Siddiqui A, Wye N, McPherson J, Zhao S, Fraser CM, Shetty J, Shatsman S, Geer K, Chen Y, Abramzon S, Nierman WC, Havlak PH, Chen R, Durbin KJ, Egan A, Ren Y, Song XZ, Li B, Liu Y, Qin X, Cawley S, Worley KC, Cooney AJ, D'Souza LM, Martin K, Wu JQ, Gonzalez-Garay ML, Jackson AR, Kalafus KJ, McLeod MP, Milosavljevic A, Virk D, Volkov A, Wheeler DA, Zhang Z, Bailey JA, Eichler EE, Tuzun E, Birney E, Mongin E, Ureta-Vidal A, Woodwark C, Zdobnov E, Bork P, Suyama M, Torrents D, Alexandersson M, Trask BJ, Young JM, Huang H, Wang H, Xing H, Daniels S, Gietzen D, Schmidt J, Stevens K, Vitt U, Wingrove J, Camara F, Mar Albà M, Abril JF, Guigo R, Smit A, Dubchak I, Rubin EM, Couronne O, Poliakov A, Hübner N, Ganten D, Goesele C, Hummel O, Kreitler T, Lee YA, Monti J, Schulz H, Zimdahl H, Himmelbauer H, Lehrach H, Jacob HJ, Bromberg S, Gullings-Handley J, Jensen-Seaman MI, Kwitek AE, Lazar J, Pasko D, Tonellato PJ, Twigger S, Ponting CP, Duarte JM, Rice S, Goodstadt L, Beatson SA, Emes RD, Winter EE, Webber C, Brandt P, Nyakatura G, Adetobi M, Chiaromonte F, Elnitski L, Eswara P, Hardison RC, Hou M, Kolbe D, Makova K, Miller W, Nekrutenko A, Riemer C, Schwartz S, Taylor J, Yang S, Zhang Y, Lindpaintner K, Andrews TD, Caccamo M, Clamp M, Clarke L, Curwen V, Durbin R, Eyras E, Searle SM, Cooper GM, Batzoglou S, Brudno M, Sidow A, Stone EA, Venter JC, Payseur BA, Bourque G, López-Otín C, Puente XS, Chakrabarti K, Chatterji S, Dewey C, Pachter L, Bray N, Yap VB, Caspi A, Tesler G, Pevzner PA, Haussler D, Roskin KM, Baertsch R, Clawson H, Furey TS, Hinrichs AS, Karolchik D, Kent WJ, Rosenbloom KR, Trumbower H, Weirauch M, Cooper DN, Stenson PD, Ma B, Brent M, Arumugam M, Shteynberg D, Copley RR,

Taylor MS, Riethman H, Mudunuri U, Peterson J, Guyer M, Felsenfeld A, Old S, Mockrin S, Collins F. Genome sequence of the Brown Norway rat yields insights into mammalian evolution. Nature 2004;428(6982):493-521.

[73] Glasson SS, Askew R, Sheppard B, Carito B, Blanchet T, Ma HL, Flannery CR, Peluso D, Kanki K, Yang Z, Majumdar MK, Morris EA. Deletion of active ADAMTS5 prevents cartilage degradation in a murine model of osteoarthritis. Nature 2005;434(7033):644-648.

[74] Glasson SS, Askew R, Sheppard B, Carito BA, Blanchet T, Ma HL, Flannery CR, Kanki K, Wang E, Peluso D, Yang Z, Majumdar MK, Morris EA. Characterization of and osteoarthritis susceptibility in ADAMTS-4-knockout mice. Arthritis Rheum 2004;50(8):2547-2558.

[75] Goldring MB, Goldring SR. Articular cartilage and subchondral bone in the pathogenesis of osteoarthritis. Ann N Y Acad Sci 2010;1192:230-237.

[76] Grelik C, Bennett GJ, Ribeiro-da-Silva A. Autonomic fibre sprouting and changes in nociceptive sensory innervation in the rat lower lip skin following chronic constriction injury. Eur J Neurosci 2005;21(9):2475-2487.

[77] Griffin TM, Huebner JL, Kraus VB, Yan Z, Guilak F. Induction of osteoarthritis and metabolic inflammation by a very high-fat diet in mice: effects of short-term exercise. Arthritis Rheum 2012;64(2):443-453.

[78] Guder C, Gravius S, Burger C, Wirtz DC, Schildberg FA. Osteoimmunology: A Current Update of the Interplay Between Bone and the Immune System. Frontiers in Immunology 2020;11.

[79] Guzman RE, Evans MG, Bove S, Morenko B, Kilgore K. Mono-iodoacetate-induced histologic changes in subchondral bone and articular cartilage of rat femorotibial joints: an animal model of osteoarthritis. Toxicologic pathology 2003;31(6):619-624.

[80] Hammergren L. The Power of Classification. In: SL Foster, editor. Worlding Dance. London: Palgrave Macmillan UK, 2009. pp. 14-31.

[81] Han ZS, Zhang ET, Craig AD. Nociceptive and thermoreceptive lamina I neurons are anatomically distinct. Nat Neurosci 1998;1(3):218-225.

[82] Hartt F. E. H. Ramsden, The Letters of Michelangelo. Art Journal 1965;25(1):100-102.

[83] Heijink A, Gomoll AH, Madry H, Drobnič M, Filardo G, Espregueira-Mendes J, Van Dijk CN. Biomechanical considerations in the pathogenesis of osteoarthritis of the knee. Knee Surg Sports Traumatol Arthrosc 2012;20(3):423-435.

[84] Heneka MT, Kummer MP, Latz E. Innate immune activation in neurodegenerative disease. Nat Rev Immunol 2014;14(7):463-477.

[85] Henry SP, Jang CW, Deng JM, Zhang Z, Behringer RR, de Crombrugghe B. Generation of aggrecan-CreERT2 knockin mice for inducible Cre activity in adult cartilage. Genesis 2009;47(12):805-814.

[86] Hirata M, Kugimiya F, Fukai A, Saito T, Yano F, Ikeda T, Mabuchi A, Sapkota BR, Akune T, Nishida N, Yoshimura N, Nakagawa T, Tokunaga K, Nakamura K, Chung UI, Kawaguchi H. C/EBPβ and RUNX2 cooperate to degrade cartilage with MMP-13 as the target and HIF-2α as the inducer in chondrocytes. Hum Mol Genet 2012;21(5):1111-1123.

[87] Ho Kim S, Mo Chung J. An experimental model for peripheral neuropathy produced by segmental spinal nerve ligation in the rat. Pain 1992;50(3):355-363.

[88] Hofer A-S, Scheuber MI, Sartori AM, Good N, Stalder SA, Hammer N, Fricke K, Schalbetter SM, Engmann AK, Weber RZ, Rust R, Schneider MP, Russi N, Favre G, Schwab ME. Stimulation of the cuneiform nucleus enables training and boosts recovery after spinal cord injury. Brain 2022;145(10):3681-3697.

[89] Hosobuchi Y, Rossier J, Bloom FE, Guillemin R. Stimulation of human periaqueductal gray for pain relief increases immunoreactive beta-endorphin in ventricular fluid. Science 1979;203(4377):279-281.

[90] Hylden JL, Hayashi H, Bennett GJ, Dubner R. Spinal lamina I neurons projecting to the parabrachial area of the cat midbrain. Brain Res 1985;336(1):195-198.

[91] Jacobs KM. Somatosensory System. In: JS Kreutzer, J DeLuca, B Caplan, editors. Encyclopedia of Clinical Neuropsychology. New York, NY: Springer New York, 2011. pp. 2320-2324.

[92] Ji R-R, Nackley A, Huh Y, Terrando N, Maixner W. Neuroinflammation and central sensitization in chronic and widespread pain. Anesthesiology 2018;129(2):343-366.

[93] Jimenez PA, Glasson SS, Trubetskoy OV, Haimes HB. Spontaneous osteoarthritis in Dunkin Hartley guinea pigs: histologic, radiologic, and biochemical changes. Lab Anim Sci 1997;47(6):598-601.

[94] Jordt SE, Julius D. Molecular basis for species-specific sensitivity to "hot" chili peppers. Cell 2002;108(3):421-430.

[95] Kaiser H, Keitel W. [Guillaume de Baillou (1538-1616)--the father of "rheumatism"?]. Z Rheumatol 2006;65(8):743-746.

[96] Kamekura S, Kawasaki Y, Hoshi K, Shimoaka T, Chikuda H, Maruyama Z, Komori T, Sato S, Takeda S, Karsenty G, Nakamura K, Chung UI, Kawaguchi H. Contribution of runt-

related transcription factor 2 to the pathogenesis of osteoarthritis in mice after induction of knee joint instability. Arthritis Rheum 2006;54(8):2462-2470.

[97] Kellgren JH, Moore R. Generalized Osteoarthritis And Heberden's Nodes. The British Medical Journal 1952;1(4751):181-187.

[98] Kikuchi T, Sakuta T, Yamaguchi T. Intra-articular injection of collagenase induces experimental osteoarthritis in mature rabbits. Osteoarthritis Cartilage 1998;6(3):177-186.

[99] Kim YS, Anderson M, Park K, Zheng Q, Agarwal A, Gong C, Saijilafu, Young L, He S, LaVinka PC, Zhou F, Bergles D, Hanani M, Guan Y, Spray DC, Dong X. Coupled Activation of Primary Sensory Neurons Contributes to Chronic Pain. Neuron 2016;91(5):1085-1096.

[100] Kobayashi K, Imaizumi R, Sumichika H, Tanaka H, Goda M, Fukunari A, Komatsu H. Sodium iodoacetate-induced experimental osteoarthritis and associated pain model in rats. The Journal of veterinary medical science 2003;65(11):1195-1199.

[101] Kozhemyakina E, Zhang M, Ionescu A, Ayturk UM, Ono N, Kobayashi A, Kronenberg H, Warman ML, Lassar AB. Identification of a Prg4-expressing articular cartilage progenitor cell population in mice. Arthritis Rheumatol 2015;67(5):1261-1273.

[102] Kraus VB, Blanco FJ, Englund M, Karsdal MA, Lohmander LS. Call for standardized definitions of osteoarthritis and risk stratification for clinical trials and clinical use. Osteoarthritis Cartilage 2015;23(8):1233-1241.

[103] Lander ES, Linton LM, Birren B, Nusbaum C, Zody MC, Baldwin J, Devon K, Dewar K, Doyle M, FitzHugh W, Funke R, Gage D, Harris K, Heaford A, Howland J, Kann L, Lehoczky J, LeVine R, McEwan P, McKernan K, Meldrim J, Mesirov JP, Miranda C, Morris W, Naylor J, Raymond C, Rosetti M, Santos R, Sheridan A, Sougnez C, Stange-

Thomann Y, Stojanovic N, Subramanian A, Wyman D, Rogers J, Sulston J, Ainscough R, Beck S, Bentley D, Burton J, Clee C, Carter N, Coulson A, Deadman R, Deloukas P, Dunham A, Dunham I, Durbin R, French L, Grafham D, Gregory S, Hubbard T, Humphray S, Hunt A, Jones M, Lloyd C, McMurray A, Matthews L, Mercer S, Milne S, Mullikin JC, Mungall A, Plumb R, Ross M, Shownkeen R, Sims S, Waterston RH, Wilson RK, Hillier LW, McPherson JD, Marra MA, Mardis ER, Fulton LA, Chinwalla AT, Pepin KH, Gish WR, Chissoe SL, Wendl MC, Delehaunty KD, Miner TL, Delehaunty A, Kramer JB, Cook LL, Fulton RS, Johnson DL, Minx PJ, Clifton SW, Hawkins T, Branscomb E, Predki P, Richardson P, Wenning S, Slezak T, Doggett N, Cheng JF, Olsen A, Lucas S, Elkin C, Uberbacher E, Frazier M, Gibbs RA, Muzny DM, Scherer SE, Bouck JB, Sodergren EJ, Worley KC, Rives CM, Gorrell JH, Metzker ML, Naylor SL, Kucherlapati RS, Nelson DL, Weinstock GM, Sakaki Y, Fujiyama A, Hattori M, Yada T, Toyoda A, Itoh T, Kawagoe C, Watanabe H, Totoki Y, Taylor T, Weissenbach J, Heilig R, Saurin W, Artiguenave F, Brottier P, Bruls T, Pelletier E, Robert C, Wincker P, Smith DR, Doucette-Stamm L, Rubenfield M, Weinstock K, Lee HM, Dubois J, Rosenthal A, Platzer M, Nyakatura G, Taudien S, Rump A, Yang H, Yu J, Wang J, Huang G, Gu J, Hood L, Rowen L, Madan A, Qin S, Davis RW, Federspiel NA, Abola AP, Proctor MJ, Myers RM, Schmutz J, Dickson M, Grimwood J, Cox DR, Olson MV, Kaul R, Raymond C, Shimizu N, Kawasaki K, Minoshima S, Evans GA, Athanasiou M, Schultz R, Roe BA, Chen F, Pan H, Ramser J, Lehrach H, Reinhardt R, McCombie WR, de la Bastide M, Dedhia N, Blöcker H, Hornischer K, Nordsiek G, Agarwala R, Aravind L, Bailey JA, Bateman A, Batzoglou S, Birney E, Bork P, Brown DG, Burge CB, Cerutti L, Chen HC, Church D, Clamp M, Copley RR, Doerks T, Eddy

SR, Eichler EE, Furey TS, Galagan J, Gilbert JG, Harmon C, Hayashizaki Y, Haussler D, Hermjakob H, Hokamp K, Jang W, Johnson LS, Jones TA, Kasif S, Kaspryzk A, Kennedy S, Kent WJ, Kitts P, Koonin EV, Korf I, Kulp D, Lancet D, Lowe TM, McLysaght A, Mikkelsen T, Moran JV, Mulder N, Pollara VJ, Ponting CP, Schuler G, Schultz J, Slater G, Smit AF, Stupka E, Szustakowki J, Thierry-Mieg D, Thierry-Mieg J, Wagner L, Wallis J, Wheeler R, Williams A, Wolf YI, Wolfe KH, Yang SP, Yeh RF, Collins F, Guyer MS, Peterson J, Felsenfeld A, Wetterstrand KA, Patrinos A, Morgan MJ, de Jong P, Catanese JJ, Osoegawa K, Shizuya H, Choi S, Chen YJ, Szustakowki J. Initial sequencing and analysis of the human genome. Nature 2001;409(6822):860-921.

[104] Langford LA, Schmidt RF. Afferent and efferent axons in the medial and posterior articular nerves of the cat. The Anatomical Record 1983;206(1):71-78.

[105] Lavertu G, Cote SL, De Koninck Y. Enhancing K-Cl co-transport restores normal spinothalamic sensory coding in a neuropathic pain model. Brain 2014;137(Pt 3):724-738.

[106] Lawson SN, Waddell PJ. Soma neurofilament immunoreactivity is related to cell size and fibre conduction velocity in rat primary sensory neurons. J Physiol 1991;435:41-63.

[107] Lazzeri D, Castello MF, Matucci-Cerinic M, Lippi D, Weisz GM. Osteoarthritis in the hands of Michelangelo Buonarroti. J R Soc Med 2016;109(5):180-183.

[108] Lazzeri D, Xi W, Zhang YX, Persichetti P. A systematic reappraisal of the fifth finger in Renaissance paintings. Journal of the Royal Society of Medicine 2014;107(12):474-479.

[109] Lejeune J. Etude des chromosomes somatiques de neuf enfants mongoliens. C R Acad Sci (Paris) 1959;248:1721-1722.

[110] Li F-X-Z, Xu F, Lin X, Wu F, Zhong J-Y, Wang Y, Guo B, Zheng M-H, Shan S-K, Yuan L-Q. The Role of Substance P in the Regulation of Bone and Cartilage Metabolic Activity. Frontiers in Endocrinology 2020;11.

[111] Light A, Perl E. Spinal termination of functionally identified primary afferent neurons with slowly conducting myelinated fibers. Journal of Comparative Neurology 1979;186(2):133-150.

[112] Lima D, Almeida A. The medullary dorsal reticular nucleus as a pronociceptive centre of the pain control system. Prog Neurobiol 2002;66(2):81-108.

[113] Lin AC, Seeto BL, Bartoszko JM, Khoury MA, Whetstone H, Ho L, Hsu C, Ali SA, Alman BA. Modulating hedgehog signaling can attenuate the severity of osteoarthritis. Nat Med 2009;15(12):1421-1425.

[114] Little CB, Hunter DJ. Post-traumatic osteoarthritis: from mouse models to clinical trials. Nature Reviews Rheumatology 2013;9(8):485-497.

[115] Little CB, Smith MM. Animal models of osteoarthritis. Current Rheumatology Reviews 2008;4(3):175-182.

[116] Llewellyn J. Arthritis Deformans. Archives of The Roentgen Ray 1909;14(5):159-160.

[117] Locke S, Yousefpour N, Mannarino M, Xing S, Yashmin F, Bourassa V, Ribeiro-da-Silva A. Peripheral and central nervous system alterations in a rat model of inflammatory arthritis. Pain 2020;161(7):1483-1496.

[118] Loughlin J, Mustafa Z, Smith A, Irven C, Carr AJ, Clipsham K, Chitnavis J, Bloomfield VA, McCartney M, Cox O, Sinsheimer JS, Sykes B, Chapman KE. Linkage analysis of chromosome 2q in osteoarthritis. Rheumatology (Oxford) 2000;39(4):377-381.

[119] Loyd DR, Murphy AZ. The role of the periaqueductal gray in the modulation of pain in males and females: are the anatomy and physiology really that different? Neural Plast 2009;2009:462879.

[120] Lu HJ, Gao YJ. Astrocytes in Chronic Pain: Cellular and Molecular Mechanisms. Neurosci Bull 2023;39(3):425-439.

[121] Lundblad H, Kreicbergs A, Jansson KA. Prediction of persistent pain after total knee replacement for osteoarthritis. J Bone Joint Surg Br 2008;90(2):166-171.

[122] Ma HL, Blanchet TJ, Peluso D, Hopkins B, Morris EA, Glasson SS. Osteoarthritis severity is sex dependent in a surgical mouse model. Osteoarthritis Cartilage 2007;15(6):695-700.

[123] MacGregor AJ, Snieder H, Rigby AS, Koskenvuo M, Kaprio J, Aho K, Silman AJ. Characterizing the quantitative genetic contribution to rheumatoid arthritis using data from twins. Arthritis & Rheumatism: Official Journal of the American College of Rheumatology 2000;43(1):30-37.

[124] Madden JF, Davis OC, Boyle KA, Iredale JA, Browne TJ, Callister RJ, Smith DW, Jobling P, Hughes DI, Graham BA. Functional and Molecular Analysis of Proprioceptive Sensory Neuron Excitability in Mice. Frontiers in Molecular Neuroscience 2020;13.

[125] Mapp PI, Kidd BL, Gibson SJ, Terry JM, Revell PA, Ibrahim NB, Blake DR, Polak JM. Substance P-, calcitonin gene-related peptide- and C-flanking peptide of neuropeptide Y-immunoreactive fibres are present in normal synovium but depleted in patients with rheumatoid arthritis. Neuroscience 1990;37(1):143-153.

[126] Maroudas A. In Freeman, MAR (Ed.), Adult Articular Cartilage. London, Pitman 1979:215-290.

[127] Martel-Pelletier J, Pelletier JP. Is osteoarthritis a disease involving only cartilage or other articular tissues? Eklem Hastalik Cerrahisi 2010;21(1):2-14.

[128] Masuda T, Prinz M. Microglia: A Unique Versatile Cell in the Central Nervous System. ACS Chem Neurosci 2016;7(4):428-434.

[129] Masuda T, Tsuda M, Yoshinaga R, Tozaki-Saitoh H, Ozato K, Tamura T, Inoue K. IRF8 is a critical transcription factor for transforming microglia into a reactive phenotype. Cell Rep 2012;1(4):334-340.

[130] McCutchen CW. The frictional properties of animal joints. Wear 1962;5(1):1-17.

[131] McGonagle D, Conaghan PG, O'Connor P, Gibbon W, Green M, Wakefield R, Ridgway J, Emery P. The relationship between synovitis and bone changes in early untreated rheumatoid arthritis: a controlled magnetic resonance imaging study. Arthritis & Rheumatism: Official Journal of the American College of Rheumatology 1999;42(8):1706-1711.

[132] McKemy DD, Neuhausser WM, Julius D. Identification of a cold receptor reveals a general role for TRP channels in thermosensation. Nature 2002;416(6876):52-58.

[133] McQueen FM, Stewart N, Crabbe J, Robinson E, Yeoman S, Tan PLJ, McLean L. Magnetic resonance imaging of the wrist in early rheumatoid arthritis reveals a high prevalence of erosions at four months after symptom onset. Annals of the Rheumatic Diseases 1998;57(6):350.

[134] Mee S, Bunney BG, Reist C, Potkin SG, Bunney WE. Psychological pain: a review of evidence. J Psychiatr Res 2006;40(8):680-690.

[135] Meerwijk EL, Ford JM, Weiss SJ. Brain regions associated with psychological pain: implications for a neural network and its relationship to physical pain. Brain Imaging Behav 2013;7(1):1-14.

[136] Millan MJ. Descending control of pain. Progress in neurobiology 2002;66(6):355-474.

[137] Mills EP, Keay KA, Henderson LA. Brainstem Pain-Modulation Circuitry and Its Plasticity in Neuropathic Pain: Insights From Human Brain Imaging Investigations. Frontiers in Pain Research 2021;2.

[138] Mirando AJ, Liu Z, Moore T, Lang A, Kohn A, Osinski AM, O'Keefe RJ, Mooney RA, Zuscik MJ, Hilton MJ. RBP-Jκ-dependent Notch signaling is required for murine articular cartilage and joint maintenance. Arthritis Rheum 2013;65(10):2623-2633.

[139] Mogil JS. The translatability of pain across species. Philosophical transactions of the Royal Society of London Series B, Biological sciences 2019;374(1785):20190286-20190286.

[140] Molander C, Xu Q, Grant G. The cytoarchitectonic organization of the spinal cord in the rat. I. The lower thoracic and lumbosacral cord. Journal of Comparative Neurology 1984;230(1):133-141.

[141] Morrison SF, Nakamura K. Central Mechanisms for Thermoregulation. Annu Rev Physiol 2019;81:285-308.

[142] Morton CR, Hutchison WD, Hendry IA, Duggan AW. Somatostatin: evidence for a role in thermal nociception. Brain Res 1989;488(1-2):89-96.

[143] Mosconi T, Kruger L. Fixed-diameter polyethylene cuffs applied to the rat sciatic nerve induce a painful neuropathy: Ultrastructural morphometric analysis of axonal alterations. Pain 1996;64(1):37-57.

[144] Mow V, Gu W, Chen F. Structure and function of articular cartilage. Basic orthopedic biomechanics and mechano-biology 2005;3:181-258.

[145] Nelson RJ. The somatosensory system: Deciphering the brain's own body image: CRC Press, 2001.

[146] Nesse RM, Schulkin J. An evolutionary medicine perspective on pain and its disorders. Philos Trans R Soc Lond B Biol Sci 2019;374(1785):20190288.

[147] Neumann S, Doubell TP, Leslie T, Woolf CJ. Inflammatory pain hypersensitivity mediated by phenotypic switch in myelinated primary sensory neurons. Nature 1996;384(6607):360-364.

[148] Nicholas M, Vlaeyen JWS, Rief W, Barke A, Aziz Q, Benoliel R, Cohen M, Evers S, Giamberardino MA, Goebel A, Korwisi B, Perrot S, Svensson P, Wang S-J, Treede R-D, The ITftCoCP. The IASP classification of chronic pain for ICD-11: chronic primary pain. PAIN 2019;160(1).

[149] Niedermair T, Schirner S, Seebröker R, Straub RH, Grässel S. Substance P modulates bone remodeling properties of murine osteoblasts and osteoclasts. Sci Rep 2018;8(1):9199.

[150] Nijs J, George SZ, Clauw DJ, Fernández-de-las-Peñas C, Kosek E, Ickmans K, Fernández-Carnero J, Polli A, Kapreli E, Huysmans E. Central sensitisation in chronic pain conditions: latest discoveries and their potential for precision medicine. The Lancet Rheumatology 2021;3(5):e383-e392.

[151] Nijs J, Lahousse A, Kapreli E, Bilika P, Saraçoğlu İ, Malfliet A, Coppieters I, De Baets L, Leysen L, Roose E, Clark J, Voogt L, Huysmans E. Nociplastic Pain Criteria or Recognition of Central Sensitization? Pain Phenotyping in the Past, Present and Future. J Clin Med 2021;10(15).

[152] Nijs J, Leysen L, Vanlauwe J, Logghe T, Ickmans K, Polli A, Malfliet A, Coppieters I, Huysmans E. Treatment of central sensitization in patients with chronic pain: time for change? Expert Opinion on Pharmacotherapy 2019;20(16):1961-1970.

[153] Normandin A, Luccarini P, Molat JL, Gendron L, Dallel R. Spinal μ and δ opioids inhibit both thermal and mechanical pain in rats. J Neurosci 2013;33(28):11703-11714.

[154] Nuki G, Simkin PA. A concise history of gout and hyperuricemia and their treatment. Arthritis Research & Therapy 2006;8(1):S1.

[155] Okamoto K, Takayanagi H. Regulation of bone by the adaptive immune system in arthritis. Arthritis Research & Therapy 2011;13(3):219.

[156] Orita S, Ishikawa T, Miyagi M, Ochiai N, Inoue G, Eguchi Y, Kamoda H, Arai G, Toyone T, Aoki Y, Kubo T, Takahashi K, Ohtori S. Pain-related sensory innervation in monoiodoacetate-induced osteoarthritis in rat knees that gradually develops neuronal injury in addition to inflammatory pain. BMC musculoskeletal disorders 2011;12:134.

[157] Pai YC, Rymer WZ, Chang RW, Sharma L. Effect of age and osteoarthritis on knee proprioception. Arthritis & Rheumatism: Official Journal of the American College of Rheumatology 1997;40(12):2260-2265.

[158] Parish LC. An historical approach to the nomenclature of rheumatoid arthritis. Arthritis & Rheumatism 1963;6(2):138-158.

[159] Park J, Lee J, Kim K-I, Lee J, Jang S, Choi HT, Son Y, Kim HJ, Woo EJ, Lee E, Oh TI. A Pathophysiological Validation of Collagenase II-Induced Biochemical Osteoarthritis Animal Model in Rabbit. Tissue engineering and regenerative medicine 2018;15(4):437-444.

[160] Pearle AD, Scanzello CR, George S, Mandl LA, DiCarlo EF, Peterson M, Sculco TP, Crow MK. Elevated high-sensitivity C-reactive protein levels are associated with local inflammatory findings in patients with osteoarthritis. Osteoarthritis and Cartilage 2007;15(5):516-523.

[161] Pelletier J-P, Boileau C, Brunet J, Boily M, Lajeunesse D, Reboul P, Laufer S, Martel-Pelletier J. The inhibition of subchondral bone resorption in the early phase of experimental dog osteoarthritis by licofelone is associated with a reduction in the synthesis of MMP-13 and cathepsin K. Bone 2004;34(3):527-538.

[162] Perl E. Myelinated afferent fibres innervating the primate skin and their response to noxious stimuli. The Journal of physiology 1968;197(3):593-615.

[163] Petitjean H, Pawlowski SA, Fraine SL, Sharif B, Hamad D, Fatima T, Berg J, Brown CM, Jan LY, Ribeiro-da-Silva A, Braz JM, Basbaum AI, Sharif-Naeini R. Dorsal Horn Parvalbumin Neurons Are Gate-Keepers of Touch-Evoked Pain after Nerve Injury. Cell Rep 2015;13(6):1246-1257.

[164] Pitcher GM, Henry JL. Nociceptive response to innocuous mechanical stimulation is mediated via myelinated afferents and NK-1 receptor activation in a rat model of neuropathic pain. Exp Neurol 2004;186(2):173-197.

[165] Pollard TC, Gwilym SE, Carr AJ. The assessment of early osteoarthritis. J Bone Joint Surg Br 2008;90(4):411-421.

[166] Pritchett JW. Substance P level in synovial fluid may predict pain relief after knee replacement. J Bone Joint Surg Br 1997;79(1):114-116.

[167] Proske U, Gandevia SC. The Proprioceptive Senses: Their Roles in Signaling Body Shape, Body Position and Movement, and Muscle Force. Physiological Reviews 2012;92(4):1651-1697.

[168] Ralston Iii HJ. The fine structure of laminae I, II and III of the macaque spinal cord. Journal of Comparative Neurology 1979;184(4):619-641.

[169] Ramien M, Ruocco I, Cuello AC, St-Louis M, Ribeiro-Da-Silva A. Parasympathetic nerve fibers invade the upper dermis following sensory denervation of the rat lower lip skin. J Comp Neurol 2004;469(1):83-95.

[170] Rexed B. The cytoarchitectonic organization of the spinal cord in the cat. Journal of Comparative Neurology 1952;96(3):415-495.

[171] Ribeiro-da-Silva A, Cuello AC. Organization of peptidergic neurons in the dorsal horn of the spinal cord: anatomical and functional correlates. Progress in brain research 1995;104:41-59.

[172] Rigaud M, Gemes G, Barabas M-E, Chernoff DI, Abram SE, Stucky CL, Hogan QH. Species and strain differences in rodent sciatic nerve anatomy: Implications for studies of neuropathic pain. PAIN 2008;136(1).

[173] Roberts WJ, Elardo SM. Sympathetic activation of unmyelinated mechanoreceptors in cat skin. Brain Res 1985;339(1):123-125.

[174] Rothwell J. Proprioceptors in muscles, joints and skin. In: J Rothwell, editor. Control of Human Voluntary Movement. Dordrecht: Springer Netherlands, 1994. pp. 86-126.

[175] Ruffolo RR, Jr., Hieble JP. Alpha-adrenoceptors. Pharmacol Ther 1994;61(1-2):1-64.

[176] Ruocco I, Cuello AC, Parent A, Ribeiro-da-Silva A. Skin blood vessels are simultaneously innervated by sensory, sympathetic, and parasympathetic fibers. J Comp Neurol 2002;448(4):323-336.

[177] Säämänen AM, Hyttinen M, Vuorio E. Analysis of arthritic lesions in the Del1 mouse: a model for osteoarthritis. Methods Mol Med 2007;136:283-302.

[178] Saeed AW, Ribeiro-da-Silva A. De novo expression of neurokinin-1 receptors by spinoparabrachial lamina I pyramidal neurons following a peripheral nerve lesion. J Comp Neurol 2013;521(8):1915-1928.

[179] Saito T, Fukai A, Mabuchi A, Ikeda T, Yano F, Ohba S, Nishida N, Akune T, Yoshimura N, Nakagawa T, Nakamura K, Tokunaga K, Chung UI, Kawaguchi H. Transcriptional regulation of endochondral ossification by HIF-2alpha during skeletal growth and osteoarthritis development. Nat Med 2010;16(6):678-686.

[180] Saito T, Koshino T. Distribution of neuropeptides in synovium of the knee with osteoarthritis. Clin Orthop Relat Res 2000(376):172-182.

[181] Sakao K, Takahashi KA, Arai Y, Saito M, Honjo K, Hiraoka N, Asada H, Shin-Ya M, Imanishi J, Mazda O, Kubo T. Osteoblasts derived from osteophytes produce interleukin-6, interleukin-8, and matrix metalloproteinase-13 in osteoarthritis. J Bone Miner Metab 2009;27(4):412-423.

[182] Santos S, Emery N, Neu CP, Pierce DM. Propagation of microcracks in collagen networks of cartilage under mechanical loads. Osteoarthritis and Cartilage 2019;27(9):1392-1402.

[183] Sassi N, Laadhar L, Allouche M, Achek A, Kallel-Sellami M, Makni S, Sellami S. WNT signaling and chondrocytes: from cell fate determination to osteoarthritis physiopathology. J Recept Signal Transduct Res 2014;34(2):73-80.

[184] Schepers RJ, Ringkamp M. Thermoreceptors and thermosensitive afferents. Neurosci Biobehav Rev 2010;34(2):177-184.

[185] Schlesinger N. Diagnosis of gout. Minerva Med 2007;98(6):759-767.

[186] Scholz J, Finnerup NB, Attal N, Aziz Q, Baron R, Bennett MI, Benoliel R, Cohen M, Cruccu G, Davis KD. The IASP classification of chronic pain for ICD-11: chronic neuropathic pain. Pain 2019;160(1):53-59.

[187] Schulte E, Fisseler-Eckhoff A, Müller KM. [Differential diagnosis of synovitis. Correlation of arthroscopic-biopsy to clinical findings]. Pathologe 1994;15(1):22-27.

[188] Schwartz SA. Disease of Distinction. EXPLORE 2006;2(6):515-519.

[189] Seltzer Z, Dubner R, Shir Y. A novel behavioral model of neuropathic pain disorders produced in rats by partial sciatic nerve injury. Pain 1990;43(2):205-218.

[190] Serra R, Johnson M, Filvaroff EH, LaBorde J, Sheehan DM, Derynck R, Moses HL. Expression of a truncated, kinase-defective TGF-beta type II receptor in mouse skeletal tissue promotes terminal chondrocyte differentiation and osteoarthritis. J Cell Biol 1997;139(2):541-552.

[191] Shakoor N, Moisio K. A biomechanical approach to musculoskeletal disease. Best Practice & Research Clinical Rheumatology 2004;18(2):173-186.

[192] Sharif Naeini R, Cahill CM, Ribeiro-da-Silva A, Ménard HA, Henry JL. Remodelling of spinal nociceptive mechanisms in an animal model of monoarthritis. Eur J Neurosci 2005;22(8):2005-2015.

[193] Sharma L, Pai Y-C. Impaired proprioception and osteoarthritis. Current opinion in rheumatology 1997;9(3):253-258.

[194] Sharpless S. The effects of intravenous epinephrine and norepinephrine on a conditioned response in the cat. Psychopharmacologia 1959;1(2):140-149.

[195] Shen J, Li J, Wang B, Jin H, Wang M, Zhang Y, Yang Y, Im HJ, O'Keefe R, Chen D. Deletion of the transforming growth factor β receptor type II gene in articular chondrocytes leads to a progressive osteoarthritis-like phenotype in mice. Arthritis Rheum 2013;65(12):3107-3119.

[196] Sherrington CS. Qualitative difference of spinal reflex corresponding with qualitative difference of cutaneous stimulus. J Physiol 1903;30(1):39-46.

[197] Sherrington CS. On the proprio-ceptive system, especially in its reflex aspect. Brain 1907;29(4):467-482.

[198] Sherrington CSS. The integrative action of the nervous system. New Haven: Yale University Press, 1961.

[199] Shi T-JS, Xiang Q, Zhang M-D, Tortoriello G, Hammarberg H, Mulder J, Fried K, Wagner L, Josephson A, Uhlén M, Harkany T, Hökfelt T. Secretagogin is expressed in sensory CGRP neurons and in spinal cord of mouse and complements other calcium-binding proteins, with a note on rat and human. Molecular pain 2012;8:80-80.

[200] Siebelt M, Waarsing JH, Groen HC, Müller C, Koelewijn SJ, de Blois E, Verhaar JAN, de Jong M, Weinans H. Inhibited osteoclastic bone resorption through alendronate treatment in rats reduces severe osteoarthritis progression. Bone 2014;66:163-170.

[201] Silman A, MacGregor A, Thomson W, Holligan S, Carthy D, Farhan A, Ollier W. Twin concordance rates for rheumatoid arthritis: results from a nationwide study. Rheumatology 1993;32(10):903-907.

[202] Simone DA, Kajander KC. Responses of cutaneous A-fiber nociceptors to noxious cold. J Neurophysiol 1997;77(4):2049-2060.

[203] Skou ST, Roos EM, Laursen MB, Rathleff MS, Arendt-Nielsen L, Simonsen O, Rasmussen S. A Randomized, Controlled Trial of Total Knee Replacement. N Engl J Med 2015;373(17):1597-1606.

[204] Smith MD, Triantafillou S, Parker A, Youssef PP, Coleman M. Synovial membrane inflammation and cytokine production in patients with early osteoarthritis. The Journal of rheumatology 1997;24(2):365-371.

[205] Sofat N, Ejindu V, Kiely P. What makes osteoarthritis painful? The evidence for local and central pain processing. Rheumatology (Oxford) 2011;50(12):2157-2165.

[206] Sophia Fox AJ, Bedi A, Rodeo SA. The basic science of articular cartilage: structure, composition, and function. Sports health 2009;1(6):461-468.

[207] Spector TD, Cicuttini F, Baker J, Loughlin J, Hart D. Genetic influences on osteoarthritis in women: a twin study. Bmj 1996;312(7036):940-943.

[208] Stahl A, Tourame P. La trisomie 21 dans les arts visuels. Archives de Pédiatrie 2013;20(12):1342-1351.

[209] Stannus O, Jones G, Cicuttini F, Parameswaran V, Quinn S, Burgess J, Ding C. Circulating levels of IL-6 and TNF-α are associated with knee radiographic osteoarthritis and knee cartilage loss in older adults. Osteoarthritis Cartilage 2010;18(11):1441-1447.

[210] Stecher RM. Heberden's nodes; a clinical description of osteo-arthritis of the finger joints. Ann Rheum Dis 1955;14(1):1-10.

[211] Styron W. Darkness Visible : a Memoir of Madness. New York: Vintage Books, 1992.

[212] Sudoł-Szopińska I, Kontny E, Maśliński W, Prochorec-Sobieszek M, Kwiatkowska B, Zaniewicz-Kaniewska K, Warczyńska A. The pathogenesis of rheumatoid arthritis in radiological studies. Part I: Formation of inflammatory infiltrates within the synovial membrane. Journal of ultrasonography 2012;12(49):202-213.

[213] Sun G, McCartin M, Liu W, Zhang Q, Kenefati G, Chen ZS, Wang J. Temporal pain processing in the primary somatosensory cortex and anterior cingulate cortex. Molecular Brain 2023;16(1):3.

[214] Suri S, Gill SE, Massena de Camin S, Wilson D, McWilliams DF, Walsh DA. Neurovascular invasion at the osteochondral junction and in osteophytes in osteoarthritis. Annals of the rheumatic diseases 2007;66(11):1423-1428.

[215] Swett JE, Torigoe Y, Elie VR, Bourassa CM, Miller PG. Sensory neurons of the rat sciatic nerve. Experimental Neurology 1991;114(1):82-103.

[216] Taams LS. Interleukin-17 in rheumatoid arthritis: Trials and tribulations. Journal of Experimental Medicine 2020;217(3).

[217] Tan CH, McNaughton PA. The TRPM2 ion channel is required for sensitivity to warmth. Nature 2016;536(7617):460-463.

[218] Tavares I, Lima D. The caudal ventrolateral medulla as an important inhibitory modulator of pain transmission in the spinal cord. J Pain 2002;3(5):337-346.

[219] Taylor AM, Peleshok JC, Ribeiro-da-Silva A. Distribution of P2X(3)-immunoreactive fibers in hairy and glabrous skin of the rat. J Comp Neurol 2009;514(6):555-566.

[220] Thambyah A, Broom N. On new bone formation in the pre-osteoarthritic joint. Osteoarthritis Cartilage 2009;17(4):456-463.

[221] Thomas KR, Capecchi MR. Site-directed mutagenesis by gene targeting in mouse embryo-derived stem cells. Cell 1987;51(3):503-512.

[222] Todd AJ. Neuronal circuitry for pain processing in the dorsal horn. Nat Rev Neurosci 2010;11(12):823-836.

[223] Toth C. Peripheral and Central sensitization. Neuropathic Pain: Causes, Management, and Understanding Cory Toth, DE Moulin, Eds Cambridge University Press—2013—P 2013:51-64.

[224] Usoskin D, Furlan A, Islam S, Abdo H, Lönnerberg P, Lou D, Hjerling-Leffler J, Haeggström J, Kharchenko O, Kharchenko PV, Linnarsson S, Ernfors P. Unbiased classification of sensory neuron types by large-scale single-cell RNA sequencing. Nature Neuroscience 2015;18(1):145-153.

[225] van der Kraan PM, Vitters EL, van Beuningen HM, van de Putte LB, van den Berg WB. Degenerative knee joint lesions in mice after a single intra-articular collagenase injection. A new model of osteoarthritis. J Exp Pathol (Oxford) 1990;71(1):19-31.

[226] van der Kraan PM, Vitters EL, van de Putte LB, van den Berg WB. Development of osteoarthritic lesions in mice by "metabolic" and "mechanical" alterations in the knee joints. Am J Pathol 1989;135(6):1001-1014.

[227] Venter JC, Adams MD, Myers EW, Li PW, Mural RJ, Sutton GG, Smith HO, Yandell M, Evans CA, Holt RA, Gocayne JD, Amanatides P, Ballew RM, Huson DH, Wortman JR, Zhang Q, Kodira CD, Zheng XH, Chen L, Skupski M, Subramanian G, Thomas PD, Zhang J, Gabor Miklos GL, Nelson C, Broder S, Clark AG, Nadeau J, McKusick VA, Zinder N, Levine AJ, Roberts RJ, Simon M, Slayman C, Hunkapiller M, Bolanos R, Delcher A, Dew I, Fasulo D, Flanigan M, Florea L, Halpern A, Hannenhalli S, Kravitz S,

Levy S, Mobarry C, Reinert K, Remington K, Abu-Threideh J, Beasley E, Biddick K, Bonazzi V, Brandon R, Cargill M, Chandramouliswaran I, Charlab R, Chaturvedi K, Deng Z, Di Francesco V, Dunn P, Eilbeck K, Evangelista C, Gabrielian AE, Gan W, Ge W, Gong F, Gu Z, Guan P, Heiman TJ, Higgins ME, Ji RR, Ke Z, Ketchum KA, Lai Z, Lei Y, Li Z, Li J, Liang Y, Lin X, Lu F, Merkulov GV, Milshina N, Moore HM, Naik AK, Narayan VA, Neelam B, Nusskern D, Rusch DB, Salzberg S, Shao W, Shue B, Sun J, Wang Z, Wang A, Wang X, Wang J, Wei M, Wides R, Xiao C, Yan C, Yao A, Ye J, Zhan M, Zhang W, Zhang H, Zhao Q, Zheng L, Zhong F, Zhong W, Zhu S, Zhao S, Gilbert D, Baumhueter S, Spier G, Carter C, Cravchik A, Woodage T, Ali F, An H, Awe A, Baldwin D, Baden H, Barnstead M, Barrow I, Beeson K, Busam D, Carver A, Center A, Cheng ML, Curry L, Danaher S, Davenport L, Desilets R, Dietz S, Dodson K, Doup L, Ferriera S, Garg N, Gluecksmann A, Hart B, Haynes J, Haynes C, Heiner C, Hladun S, Hostin D, Houck J, Howland T, Ibegwam C, Johnson J, Kalush F, Kline L, Koduru S, Love A, Mann F, May D, McCawley S, McIntosh T, McMullen I, Moy M, Moy L, Murphy B, Nelson K, Pfannkoch C, Pratts E, Puri V, Qureshi H, Reardon M, Rodriguez R, Rogers YH, Romblad D, Ruhfel B, Scott R, Sitter C, Smallwood M, Stewart E, Strong R, Suh E, Thomas R, Tint NN, Tse S, Vech C, Wang G, Wetter J, Williams S, Williams M, Windsor S, Winn-Deen E, Wolfe K, Zaveri J, Zaveri K, Abril JF, Guigó R, Campbell MJ, Sjolander KV, Karlak B, Kejariwal A, Mi H, Lazareva B, Hatton T, Narechania A, Diemer K, Muruganujan A, Guo N, Sato S, Bafna V, Istrail S, Lippert R, Schwartz R, Walenz B, Yooseph S, Allen D, Basu A, Baxendale J, Blick L, Caminha M, Carnes-Stine J, Caulk P, Chiang YH, Coyne M, Dahlke C, Mays A, Dombroski M, Donnelly M, Ely D, Esparham S, Fosler C, Gire H, Glanowski S, Glasser K, Glodek A, Gorokhov M,

Graham K, Gropman B, Harris M, Heil J, Henderson S, Hoover J, Jennings D, Jordan C, Jordan J, Kasha J, Kagan L, Kraft C, Levitsky A, Lewis M, Liu X, Lopez J, Ma D, Majoros W, McDaniel J, Murphy S, Newman M, Nguyen T, Nguyen N, Nodell M, Pan S, Peck J, Peterson M, Rowe W, Sanders R, Scott J, Simpson M, Smith T, Sprague A, Stockwell T, Turner R, Venter E, Wang M, Wen M, Wu D, Wu M, Xia A, Zandieh A, Zhu X. The sequence of the human genome. Science 2001;291(5507):1304-1351.

[228] Wall PD, Devor M, Inbal R, Scadding JW, Schonfeld D, Seltzer Z, Tomkiewicz MM. Autotomy following peripheral nerve lesions: experimental anaesthesia dolorosa. Pain 1979;7(2):103-113.

[229] Wall PD, Dubner R. Somatosensory pathways. Annu Rev Physiol 1972;34:315-336.

[230] Wang L, Zhao R, Shi X, Wei T, Halloran BP, Clark DJ, Jacobs CR, Kingery WS. Substance P stimulates bone marrow stromal cell osteogenic activity, osteoclast differentiation, and resorption activity in vitro. Bone 2009;45(2):309-320.

[231] Wang M, Tang D, Shu B, Wang B, Jin H, Hao S, Dresser KA, Shen J, Im HJ, Sampson ER, Rubery PT, Zuscik MJ, Schwarz EM, O'Keefe RJ, Wang Y, Chen D. Conditional activation of β-catenin signaling in mice leads to severe defects in intervertebral disc tissue. Arthritis Rheum 2012;64(8):2611-2623.

[232] Wang Z, Tran MC, Bhatia NJ, Hsing AW, Chen C, LaRussa MF, Fattakhov E, Rashidi V, Jang KY, Choo KJ, Nie X, Mathy JA, Longaker MT, Dauskardt RH, Helms JA, Yang GP. Del1 Knockout Mice Developed More Severe Osteoarthritis Associated with Increased Susceptibility of Chondrocytes to Apoptosis. PLoS One 2016;11(8):e0160684.

[233] Waterston RH, Lindblad-Toh K, Birney E, Rogers J, Abril JF, Agarwal P, Agarwala R, Ainscough R, Alexandersson M, An P, Antonarakis SE, Attwood J, Baertsch R, Bailey J,

Barlow K, Beck S, Berry E, Birren B, Bloom T, Bork P, Botcherby M, Bray N, Brent MR, Brown DG, Brown SD, Bult C, Burton J, Butler J, Campbell RD, Carninci P, Cawley S, Chiaromonte F, Chinwalla AT, Church DM, Clamp M, Clee C, Collins FS, Cook LL, Copley RR, Coulson A, Couronne O, Cuff J, Curwen V, Cutts T, Daly M, David R, Davies J, Delehaunty KD, Deri J, Dermitzakis ET, Dewey C, Dickens NJ, Diekhans M, Dodge S, Dubchak I, Dunn DM, Eddy SR, Elnitski L, Emes RD, Eswara P, Eyras E, Felsenfeld A, Fewell GA, Flicek P, Foley K, Frankel WN, Fulton LA, Fulton RS, Furey TS, Gage D, Gibbs RA, Glusman G, Gnerre S, Goldman N, Goodstadt L, Grafham D, Graves TA, Green ED, Gregory S, Guigó R, Guyer M, Hardison RC, Haussler D, Hayashizaki Y, Hillier LW, Hinrichs A, Hlavina W, Holzer T, Hsu F, Hua A, Hubbard T, Hunt A, Jackson I, Jaffe DB, Johnson LS, Jones M, Jones TA, Joy A, Kamal M, Karlsson EK, Karolchik D, Kasprzyk A, Kawai J, Keibler E, Kells C, Kent WJ, Kirby A, Kolbe DL, Korf I, Kucherlapati RS, Kulbokas EJ, Kulp D, Landers T, Leger JP, Leonard S, Letunic I, Levine R, Li J, Li M, Lloyd C, Lucas S, Ma B, Maglott DR, Mardis ER, Matthews L, Mauceli E, Mayer JH, McCarthy M, McCombie WR, McLaren S, McLay K, McPherson JD, Meldrim J, Meredith B, Mesirov JP, Miller W, Miner TL, Mongin E, Montgomery KT, Morgan M, Mott R, Mullikin JC, Muzny DM, Nash WE, Nelson JO, Nhan MN, Nicol R, Ning Z, Nusbaum C, O'Connor MJ, Okazaki Y, Oliver K, Overton-Larty E, Pachter L, Parra G, Pepin KH, Peterson J, Pevzner P, Plumb R, Pohl CS, Poliakov A, Ponce TC, Ponting CP, Potter S, Quail M, Reymond A, Roe BA, Roskin KM, Rubin EM, Rust AG, Santos R, Sapojnikov V, Schultz B, Schultz J, Schwartz MS, Schwartz S, Scott C, Seaman S, Searle S, Sharpe T, Sheridan A, Shownkeen R, Sims S, Singer JB, Slater G, Smit A, Smith DR, Spencer B, Stabenau A, Stange-Thomann N,

Sugnet C, Suyama M, Tesler G, Thompson J, Torrents D, Trevaskis E, Tromp J, Ucla C, Ureta-Vidal A, Vinson JP, Von Niederhausern AC, Wade CM, Wall M, Weber RJ, Weiss RB, Wendl MC, West AP, Wetterstrand K, Wheeler R, Whelan S, Wierzbowski J, Willey D, Williams S, Wilson RK, Winter E, Worley KC, Wyman D, Yang S, Yang SP, Zdobnov EM, Zody MC, Lander ES. Initial sequencing and comparative analysis of the mouse genome. Nature 2002;420(6915):520-562.

[234] Weisz GM. Arthritis in the Durer family. Wien Klin Wochenschr 2007;119(17-18):553-556.

[235] Welch ID, Cowan MF, Beier F, Underhill TM. The retinoic acid binding protein CRABP2 is increased in murine models of degenerative joint disease. Arthritis Res Ther 2009;11(1):R14.

[236] Wilhelmi G, Faust R. Suitability of the C57 black mouse as an experimental animal for the study of skeletal changes due to ageing, with special reference to osteo-arthrosis and its response to tribenoside. Pharmacology 1976;14(4):289-296.

[237] Willis WD, Westlund KN. Neuroanatomy of the pain system and of the pathways that modulate pain. J Clin Neurophysiol 1997;14(1):2-31.

[238] Willy C, Schneider P, Engelhardt M, Hargens AR, Mubarak SJ. Richard von Volkmann. Clinical Orthopaedics and Related Research 2008;466(2):500-506.

[239] Woo SH, Ranade S, Weyer AD, Dubin AE, Baba Y, Qiu Z, Petrus M, Miyamoto T, Reddy K, Lumpkin EA, Stucky CL, Patapoutian A. Piezo2 is required for Merkel-cell mechanotransduction. Nature 2014;509(7502):622-626.

[240] Woolf CJ. Central sensitization: implications for the diagnosis and treatment of pain. Pain 2011;152(3 Suppl):S2-s15.

[241] Woolf CJ, Shortland P, Coggeshall RE. Peripheral nerve injury triggers central sprouting of myelinated afferents. Nature 1992;355(6355):75-78.

[242] Xie J, Ho Lee Y, Wang C, Mo Chung J, Chung K. Differential expression of alpha1-adrenoceptor subtype mRNAs in the dorsal root ganglion after spinal nerve ligation. Molecular Brain Research 2001;93(2):164-172.

[243] Yaksh TL. Behavioral and autonomic correlates of the tactile evoked allodynia produced by spinal glycine inhibition: effects of modulatory receptor systems and excitatory amino acid antagonists. Pain 1989;37(1):111-123.

[244] Yang S, Kim J, Ryu JH, Oh H, Chun CH, Kim BJ, Min BH, Chun JS. Hypoxia-inducible factor-2alpha is a catabolic regulator of osteoarthritic cartilage destruction. Nat Med 2010;16(6):687-693.

[245] Yang X, Chen L, Xu X, Li C, Huang C, Deng CX. TGF-beta/Smad3 signals repress chondrocyte hypertrophic differentiation and are required for maintaining articular cartilage. J Cell Biol 2001;153(1):35-46.

[246] Yen LD, Bennett GJ, Ribeiro-da-Silva A. Sympathetic sprouting and changes in nociceptive sensory innervation in the glabrous skin of the rat hind paw following partial peripheral nerve injury. J Comp Neurol 2006;495(6):679-690.

[247] Yu XH, Ribeiro-da-Silva A, De Koninck Y. Morphology and neurokinin 1 receptor expression of spinothalamic lamina I neurons in the rat spinal cord. J Comp Neurol 2005;491(1):56-68.

[248] Yu XH, Zhang ET, Craig AD, Shigemoto R, Ribeiro-da-Silva A, De Koninck Y. NK-1 receptor immunoreactivity in distinct morphological types of lamina I neurons of the primate spinal cord. J Neurosci 1999;19(9):3545-3555.

[249] Zan Y, Haag JD, Chen K-S, Shepel LA, Wigington D, Wang Y-R, Hu R, Lopez-Guajardo CC, Brose HL, Porter KI. Production of knockout rats using ENU mutagenesis and a yeast-based screening assay. Nature biotechnology 2003;21(6):645-651.

[250] Zeisel A, Hochgerner H, Lönnerberg P, Johnsson A, Memic F, van der Zwan J, Häring M, Braun E, Borm LE, La Manno G, Codeluppi S, Furlan A, Lee K, Skene N, Harris KD, Hjerling-Leffler J, Arenas E, Ernfors P, Marklund U, Linnarsson S. Molecular Architecture of the Mouse Nervous System. Cell 2018;174(4):999-1014.e1022.

[251] Zhang ET, Craig AD. Morphology and distribution of spinothalamic lamina I neurons in the monkey. J Neurosci 1997;17(9):3274-3284.

[252] Zhang ET, Han ZS, Craig AD. Morphological classes of spinothalamic lamina I neurons in the cat. J Comp Neurol 1996;367(4):537-549.

[253] Zhang RX, Ren K, Dubner R. Osteoarthritis pain mechanisms: basic studies in animal models. Osteoarthritis and Cartilage 2013;21(9):1308-1315.

[254] Zhu M, Tang D, Wu Q, Hao S, Chen M, Xie C, Rosier RN, O'Keefe RJ, Zuscik M, Chen D. Activation of beta-catenin signaling in articular chondrocytes leads to osteoarthritis-like phenotype in adult beta-catenin conditional activation mice. J Bone Miner Res 2009;24(1):12-21.